Improvement of crashworthiness of Bishoftu pickup for frontal and side collision using Finite Element analyses

Adane Gashu Zerga

A Thesis Submitted to

The Department of Mechanical Engineering

School of Mechanical, Chemical and Materials Engineering

Presented in Partial Fulfilment of the Requirement for Master of Science in Automotive Engineering

Office of Graduate Studies

Adama Science and Technology University

June, 2022

Adama, Ethiopia

Improvement of crashworthiness of Bishoftu pickup for frontal and side collision using Finite Element analyses

Adane Gashu Zerga

Advisor: Dr. N. Ramesh Babu

A Thesis Submitted to

The Department of Mechanical Engineering
School of Mechanical, Chemical and Materials Engineering

Presented in Partial Fulfilment of the Requirement for Master of Science in Automotive Engineering

Office of Graduate Studies

Adama Science and Technology University

June, 2022

Adama, Ethiopia

DECLARATION

I hereby declare that this master's thesis entitled “Improvement of crashworthiness of Bishoftu pickup for frontal and side collision using Finite Element analyses " partially fulfills the requirements for the award of the Master of Science degree in Automotive Engineering. It is an authentic record of my original work. That is, it has not been submitted to any other university for a degree, diploma, or diploma award. All sources of material used in this thesis have been acknowledged by citation.

Adane Gashu Zerga	________________________	________________
Name of student	Signature	Date

RECOMMENDATION

I, the major advisor of this thesis, hereby certify that I have read the revised version of the thesis entitled "Improvement of crashworthiness of Bishoftu pickup for frontal and side collision using Finite Element analyses" prepared under my guidance by Adane Gashu submitted in partial fulfilment of the requirements for Master of Science in automotive engineering. Therefore, I recommend the submission of the revised version of the thesis to the department following the applicable procedures.

Dr. Ramesh Babu Nallamothu	______________________	_______________
Advisor	Signature	Date
________________________	______________________	_______________
Co-advisor	Signature	Date

APPROVAL SHEET

I, the advisors of the thesis entitled "Improvement of crashworthiness of Bishoftu pickup for frontal and side collision using Finite Element analyses" developed by Adane Gashu, hereby certify that the recommendation and suggestions made by the board of examiners are appropriately incorporated into the final version of the thesis.

Dr. Ramesh Babu Nallamothu	________________________	________________
Advisor	Signature	Date

APPROVAL OF BOARD EXAMINERS

We, the undersigned, members of the Board of Examiners of the thesis by Adane Gashu have read and evaluated the thesis entitled "Improvement of crashworthiness of Bishoftu pickup for frontal and side collision using Finite Element analyses" and examined the candidate during the open defence. This is, therefore, to certify that the thesis is accepted for partial fulfilment of the requirement of Master of Science in Automotive Engineering.

______________________	______________________	______________________
Chairperson	Signature	Date
______________________	______________________	______________________
Internal Examiner	Signature	Date
______________________	______________________	______________________
External Examiner	Signature	Date

Finally, approval and acceptance of the thesis is contingent upon submission of its final copy to the Office of Postgraduate Studies (OPGS) through the Department Graduate Council (DGC) and School Graduate Committee (SGC).

______________________	______________________	______________________
Department Head	Signature	Date
______________________	______________________	______________________
School Dean	Signature	Date
______________________	______________________	______________________
Office of Postgraduate Studies, Dean	Signature	Date

ACKNOWLEDGMENT

First of all, I would like to thank almighty God for giving me everything. Next, I would like to express my sincere gratitude to my teacher and advisor Dr. Ramesh Babu Nallamothu for his guidance and golden advice to complete this thesis. He is always happy and willing to help me to solve confusion, patient to help me out with questions, and direct me to the final result of the thesis. On top of that, he is an easy-going and open-minded person. Without his encouragement, and guidance this project would not have materialized and finished. Next, I would like to express my special gratitude to my family for their support and guidance throughout my life. I am here because of their support. Finally, I would like to thank my friends for their support throughout the process.

TABLE OF CONTENTS

Contents page

LIST OF FIGURES

LIST OF TABLES

LIST OF ACRONYMS

BPV	Bishoftu Pickup vehicle
CATIA	computer-aided three-dimensional interactive application
ECE	Economic commission of Europe
FEA	Finite element analysis
FMVSS	Federal motor vehicle safety standard
FUPD	Front underride protective device
IIHS	Insurance institute for highway safety
MASH	Manual for assessment program
MDB	Moving deformable barrier
NCAC	National crash analysis center
NCAP	New car assessment program
NHTSA	National Highway Traffic Safety Administration
NSGA	Non – dominated sorting genetic algorithm
CFRP	Carbon fiber reinforced plastic
GERP	Glass fiber reinforced plastic

ABSTRACT

Pickup truck, usually named as Bishoftu pickup, are gaining popularity in our country Ethiopia due to the assembling company is found around central Ethiopia, Bishoftu. They are typically used for means of transportation in Ethiopia for construction companies, governmental sectors and so on. Now a day's, vehicle accident is becoming a critical issue all over the world specially in Ethiopia that demands engineers endeavor to find ways to minimize the injury occurrence. So, preservation of occupant compartment space during vehicle collision is the most significant thing. These vehicles haven't checked of any crash safety test specifications and are not evaluated for crashworthiness. So, it is now time to consider safety features (modification) of Bishoftu pickup vehicles to reduce the grave consequences of its users. Improvements should be made on the structure of BPV in order to improve the structure strength, crashworthiness and also safety. This thesis aimed to solve and improve the crashworthiness of the existing Bishoftu pickup vehicle by remodeling in such way that crash injuries are minimized. The structural response for frontal and side impact collision of the existing BPV is analyzed. Based on the results obtained from the existing model then modifications are made by means of energy absorbing components, stable frame structure and better crash performance. Then the modified BPV was analyzed under the same condition as the existing one. For doing the analysis Software like that of CATIA is used for 3d modeling and LS-DYNA for FEM analysis. The results shows that by applying the modification, 39 KN (7.82%) reduction of impact force, and 5 kJ (3.52%) of additional energy is absorbed during frontal collision. The side structure of the modified model also provided additional 162 mm space (30.05% more protection for the occupant, a reduction of 12.2 KN in impact force (14.4% improvement) and absorb additional 2.9 KJ energy (7.6% improvement). Finally it can be concluded that with the modified model, the safety and crashworthiness of BPV was greatly improved without affecting the appearance and weight of the existing one. So, that the existing model of BPV should be fitted with the designed crashworthiness futures implemented on this thesis work.

***Keywords**: Bishoftu pickup, Crashworthiness, Collision, LS-DYNA, Validation*

CHAPTER ONE

INTRODUCTION

1.1 Background of the study

Transportation industry plays a major role in the economic development of many nations. The automotive or vehicle industry is facing tremendous engineering challenges over several years to meet the requirements generated by the fuel shortage, stability, crashworthiness, fuel cost, pollution control, raw material cost, customer safety and weight. In meeting these challenges a wide variety of new models has been emerged or entered into the market in search for better strength and safety and fuel efficiency.

Bishoftu Automotive Engineering Industry (BAEI) is an automotive industry which is exerting its effort in assembling many varieties of vehicles in Ethiopia. BAEI is built the vehicle body, the same shape with the China manufactures, there has been limited in performing detail aerodynamic analysis yet. Some of the vehicles that are assembled in BAEI are pickups, transit buses, school buses, trucks and so on.

Plutus double cabin with model number DD1022TA is one of the vehicles that are assembled in BAEI. Chassis, power transmission and related materials (electronics material such as head light, radio…etc.) is imported from Chinese company, some of the vehicle (vehicle body) is welded at Bishoftu. Most of the time they use sheet metal for manufacturing the body part by using different welding techniques (types) like Gas Metal Arc Welding (MIG), Gas Tungsten Arc Welding (TIG) …etc.

Plutus Pickup truck, usually named as Bishoftu pickup, are gaining popularity in our country Ethiopia due to the assembling company is found around central Ethiopia, Bishoftu**.** They are typically used in Ethiopia. They are front wheel steering similar to those of other pickup trucks and the two rear wheels are driving wheels with a differential and suspension, front engine rear wheel drive. They are popular means of transportation in Ethiopia for construction companies, governmental sectors like Telecommunication, Ethiopian electric utility and other business owners.

They are generally characterized by Body on frame and have two wheels in front and two wheels in their rear in which the engine is found on the front and the driving axel is the rear. A frontal frame geometry consisting of a front bumper, grille, fenders, hood, windscreen, cabin and so on. It has gross weight of 2.5 ton (2495 kg) with 1.2ton / 1.3ton axel load distribution and a maximum velocity of 120 km/h, the driver is placed in the left front of the vehicle cabin and other 3 up to 4 passengers sit in the front right and rear part of the cabin.

The body structure is mostly made with carbon steel and has a carbon range of 0.31–0.6% and a manganese range of 0.6–1.65%. This steel can be heat treated and quenched to further adjust the microstructure and mechanical properties. This makes it hard for maintenance specially for normal arc welding because it needs special treatment with heat in order to do welding process during body maintenance. And also, the carbon content of the steel gives strength but this minimizes deformation this lead to decrease in energy absorption and increase in impact force. So, this thesis gives that an improvement on both energy absorption and impact energy.

Road safety report describes an occupant cell as a 'survival box' and suggests that the survival of occupants involved in the circumstance of an accident depend highly on the strength of the cell which is a fundamental pre-requisite for vehicle safety design. Other factors such as bad design, wrong communication, wrong decision, risk taken etc. can equally lead to road accident (A. E. Ikpe1*, 2017).

In Ethiopia, a country with a small vehicle population ratio, 95 deaths per 10, 000 vehicles were registered between 2007 and 2008. While this is the highest road traffic collision (RTC) rate among African countries, little research has been carried out on the causes of collisions in the country. Among these accidents, Collisions in the Addis Ababa and Oromia Regions account for 58% of all fatal collisions and two-thirds of all the injuries in Ethiopia (Asefa et al., 2014).

Data from police-reported traffic crashes in Ethiopia and characteristics of the existing state of road safety examines, six years (July 2005 - June 2011) of police reported crash data were analyzed, consisting of 12,140 fatal and 29,454 injury crashes on the country's road network. The 12,140 fatal crashes involved 1,070 drivers, 5,702 passengers, and 7,770 pedestrians, total of 14,542 fatalities, an average of 1.2 road user fatalities per crash. An important and glaring trend that emerges is that more than half of the fatalities in Ethiopia involve pedestrians(Tulu et al., 2013). Figure 1.1 shows frontal collision and side collision which causes rollover. So, it is a time to consider safety features modification of Bishoftu pickups to reduce the grave consequences of its users.

Figure1.1: (a) side collision which causes rollover (b) Front collision of pickup vehicle

Experimental Crashworthiness is very expensive but, with the advancement of computer hardware and software, several analytical design capabilities have evolved, providing engineers with a variety of tools to design modern vehicle structures that can meet the growing Customer demands for better crashworthiness performance (Srikanth & Prakash, 2009).

This Research paper aimed to solve and improve the crashworthiness of the existing Bishoftu pickup vehicle by remodeling in such way that crash injuries are minimized. Therefore, the first task carried out in this paper was modeling and analysis of the existing Bishoftu pickup vehicle structure. After that the result will be interpreted and then depending on the results, the new model is created to avoid the shortcomings of the existing Bishoftu pickup vehicle. To do so, different software's like that of CATIA, for 3D modeling and LS-DYNA, for FEM analysis are used.

1.2 Crashworthiness

Vehicle accidents have become one of the major causes for increasing death rates of humans worldwide. Hence, stringent norms on vehicle safety have been imposed on automobile industries. In various incidents, the accidents of the vehicles on the road, front and side impact have highest contribution to mortality. In both impacts, the occupants inside the vehicle or near side of the vehicle and the occupants on the opposite of the vehicle are at risk of injury.

Protecting passengers in vehicle collisions was an essential consideration since automobile industry was developed. In recent years, due to an increase in awareness on occupant safety and necessity of energy-efficient engineering, manufacturers are proceeding toward an optimal design of the occupant space using the high strength structures for better crashworthiness without significant increase in total mass(Zahedan et al., 2022; Liu, 2013; Marzougui et al., 2014).

Information about structural reactions to various transport hazards can be determined by many different systems. Advanced crash simulation techniques allow for improvements to vehicle structure (crashworthiness) to improve passenger safety, yet to reconstruct the capacity of road accidents (Vangi et al., 2018; Huh et al., 2003). Structural optimization is very important in engineering designs. It is an important tool used to remove unnecessary features and improve the function of a component or system (Ikpe et al., 2017).

Vehicle Crashworthiness is the ability of the vehicle to protect the occupant during an impact. At present, most of the vehicle bodies are built primarily with stamped steel panels and joined by welding and fastening techniques. Vehicle structures, other than providing protection to the occupants, also control the crash deceleration pulse to level below the upper limit of human tolerance. A crash deceleration pulse (Energy absorption) with an early peak in time and a gradual decay is more beneficial for defense of a restrained occupant. Generally, vehicle collisions are classified as frontal, side and rear impact, with majority of injuries because of frontal impact, followed by rear impact and side impact (Srikanth & Prakash, 2009; Mahajan & Kamble, 2016; Ibrahim et al., 2014)**.**

Vehicular lightweight and structural crashworthiness have been the main concerns in automotive industry for higher and higher requirements in fuel conservation and crash safety as shown in figure 1.2. Like, cars are designed to have high speed and light weight; Road accidents and injuries are increasing dramatically on a very principal factors in the testing is vehicle safety (Lebaal et al., 2022). However, these two criteria usually compete with each other and a tradeoff must be made so that vehicle structure allows absorbing the maximum crashing energy via structural deformation and maintaining the structural integrity of the passenger compartment for the occupant safety in the event of the crash (Gu et al., 2013; Yu et al., 2021; Abdulqadir & Tarlochan, 2022; Zhu et al., 2013).

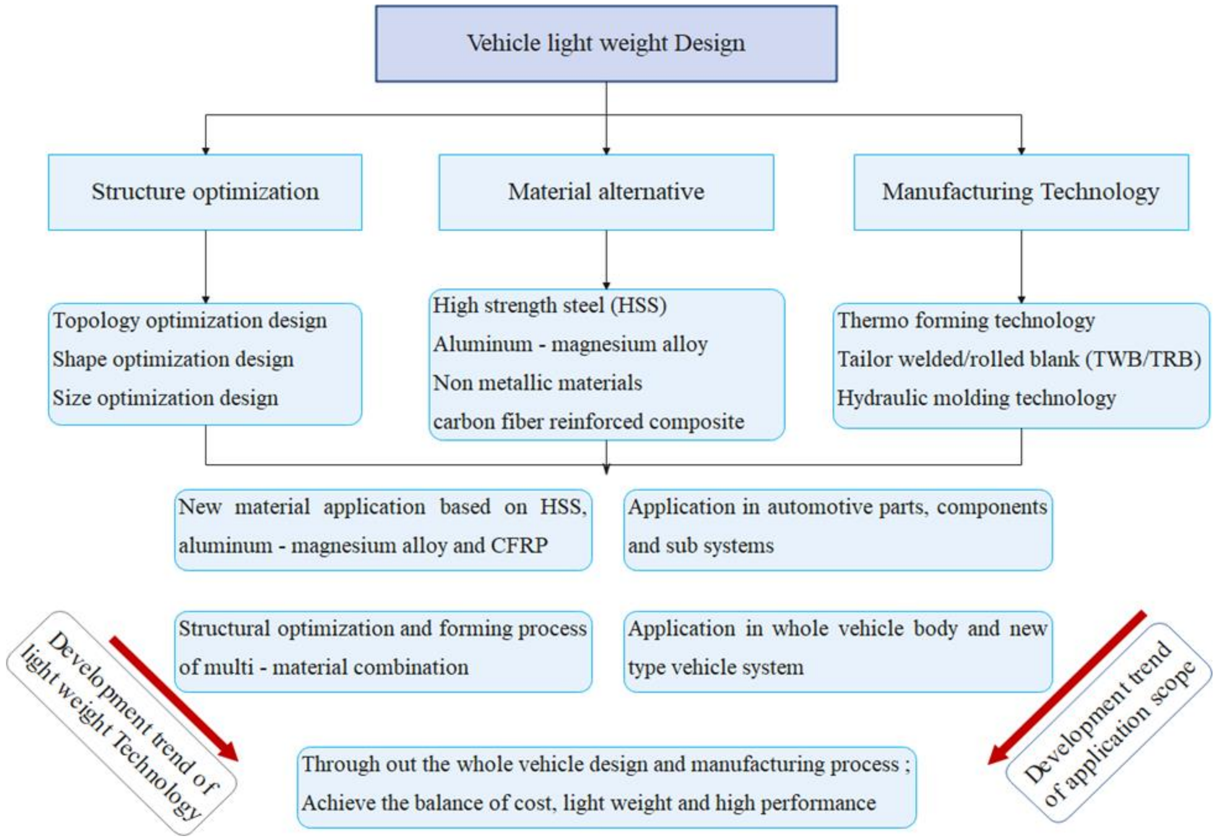

Figure1.2: Design method and technical route of vehicle lightweight design (Yu et al., 2021)

In reality, vehicle collisions are unique dynamic events where the vehicle may collide with another vehicle of similar or different shape, stiffness and mass; or it may collide with another stationary object. Some of the pickup vehicle collisions are classified and shown below.

Frontal Collision: A frontal collision is one where the front ends of two vehicles hit each other or a vehicle hit with stationary object. This has the potential for the highest crash energy. In the case shown in Figure 1.3, the vehicle is hit through its front wheel body structure.

Figure1.3: Frontal impact (Frontal Crash Test with Limo, 2022)

Side Impact: Side impact mechanisms come into play when the vehicle is involved in an intersection collision or when the vehicle veers off the road and impacts sideways utility pole, tree or another obstacle on the roadside. In side impact of a car, the impacting vehicle slows down due to the reaction force generated by different structural members like car doors, side impact beams, roof bow, B-Pillar etc. As these structural members plastically deform and absorb energy, the impacting vehicle decelerates (Mahajan & Kamble, 2016). Figure 1.4 shows side collision which hits the driver compartment.

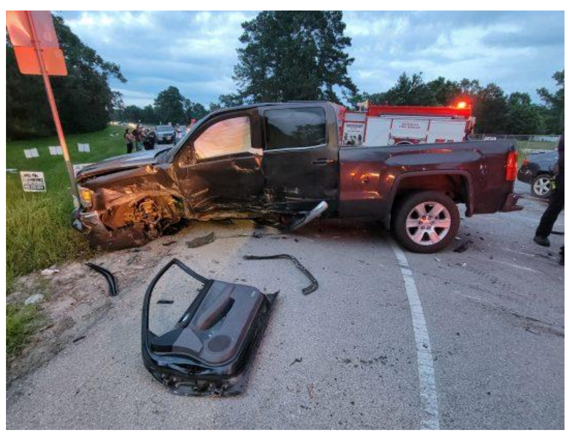

Figure1.4: Side impact (Side Crash in NE Harris County - Free Texas Accident Report, 2022)

Rear impact collisions: Occur when a slower moving or stationary vehicle is struck from behind by a vehicle moving at a faster rate of speed. For cases of rear impact, the seats should be designed with high back rests and integrated head rests to help keep the head, neck and upper torso in safe alignment during the dynamics of a crash.

Rollover Impact Analysis: It is a type of vehicle crash during which a vehicle tips over on to its side or roof. Rollovers have more mortality than other kinds of vehicle collisions Vehicle rollovers are divided into two categories: tripped and un-tripped. Tripped rollovers are caused by forces from an external object, like a curb or a collision with another vehicle. Un-tripped crashes are the results of steering input, speed and friction with the ground (Seyedi et al., 2020).

Many crash analysis however, have been neglected with the result of the formation created by stamping and performing procedures to measure the accuracy of the automatic body crash, which gives erroneous results in crash mode and crash rate. The traditional way to optimize vehicle components for better lightweight or crashworthiness is to use high strength steel (HSS) and advanced high strength steel (AHSS) or some composite materials such as glass fiber polyester composite (GFRP) and carbon fiber reinforced composite (CFRP)(Yu et al., 2021). Recently, crash analysis for spontaneous body parts is considered for functionality such as rigidity and abnormal thickness distribution, deformation and so on. Figure 1.5 shows the Critical components that are affected during frontal crash.

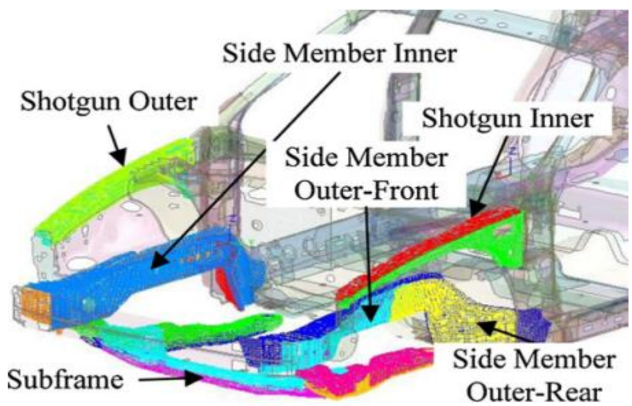

Figure1.5: Critical components in the case of frontal crash (P. Zhu et al., 2013)

Crash simulation is a real time test of a car crash test using computer simulation to assess the safety level of a car and its occupants. The data obtained from the crash test show the body's ability to protect the occupants of the vehicle in the event of a collision. These simulation technologies have greatly increased the protection, reliability and production capacity of modern cars(Yadav & Pradhan, 2014).

1.3 Statement of the Problem

Vehicle collision can cause mild to severe injuries and even fatality. Statistically, frontal collisions are the main cause and side collision is the second cause of fatality during motor vehicle accidents. Common injuries that can be caused by frontal collision are head injuries, thoracic injuries, and internal injuries (Mihradi et al., 2017). The worsening situations in the rate of car crash calls for hand-to-hand efforts of all concerned bodies and the society in general. It is a well-known fact that the socio economic, physical and psychological crisis caused by vehicle accidents need to be dealt with seriously. Various studies have indicated that Ethiopia has one of the highest rates of fatality per vehicle in Africa. Studies have been made on Adama locally named around mebrat and wonji mazoriya node, and Addiss Ababa on kolfe Keranio sub city locally named 18 node, and asked some questions to traffic polices. From this study around 57.14% of the pickup collisions are frontal which causes the highest fatality and property damage, and around 28.57% are side collisions. So, this research is attempting a different approach to this problem particularly front-end and side-end collision by modifying frontal and side frame structure for the self-protection of bishoftu pickups in frontal and side vehicle crash, which is assembled in Bishoftu Automotive engineering industry by analyzing the existing one and improving it by making modification with the help of proper software and using material more stiffer, less deformed ,less weight and can absorb more energy during impact which improve the self and partner protection for frontal as well as side collision which happened due to driver failure, road condition or other . As a result, especially Ethiopia is facing a challenge not only due to increased number of death but also economic damage. The system intended to be innovative, this thesis work will save the life and property damage during frontal and side car crash.

1.4 Objectives

1.4.1 General objective

The general objective of this thesis work is to Improve the crashworthiness of Bishoftu pickup for frontal and side collision using Finite Element analyses

1.4.2 Specific objectives

The main objective of this thesis was achieved through the following specific objectives:-

- To model the existing structure of Bishoftu pickup to simulate the crashworthiness using CATIA V5.
- To analyze the existing frame structural responses for different speed ranges of the pickup using nonlinear FEM during frontal and side collision.
- To identify the weak & strong structural parts of the pickup which play important role in frontal and side collision.
- To make modification (improvement) on existing frame structure
- To analyze its improvement on crashworthiness for the average speed ranges of frontal as well as side collision using FEM
- To compare and validate the improvement of the crashworthiness of the pickup.

1.5 Significance of study

Vehicle crash is becoming the major cause of death. Ethiopia has one of Africa's fastest growing non-oils producing economies and an increasing level of motorization. This rapidly increasing mobility has created some unique road safety concerns. Since Sufficient studies have not been conducted to alleviate the negative impacts of vehicle crash in Ethiopia. So, the outcome of this study would give input for car manufacturers especially during assembling process. Therefore, this study will help our country at large and the public in particular when the outcome from the study becomes evaluated and implemented. After finishing, this thesis work is expected to give:

- Economic benefit
  - ✓ Optimization of Bishoftu Automotive Engineering Industry usage, and
  - ✓ Improving market share of the experiment vehicle type.
- Social benefits
  - ✓ Improve safety of the society and minimization of death rate
- Environmental benefits
  - ✓ Safe and convenient living environment

Beneficiaries of the study: -The researcher, higher institutes, BAEI industry and their customers in general, the public and the country as a whole.

1.6 Scope of this thesis

This thesis work is aimed to cover the improvement and analysis of the existing Bishoftu pickup by remodeling in such a way that crash injuries are minimized. Here the intention was achieved by the means of a light weight frame structure and energy-absorbing components. The frontal and side impact collision of Bishoftu pickup was analyzed. It also includes the modification of the body structure to improve crashworthiness. To accomplish these goals CATIA V5 software is used for modeling, simulation and stress analysis is done by FEA (Finite element analysis) and LS-DYNA. The dynamic analysis of Bishoftu pickup using LS-DYNA software is covered on this paper, based on the obtained values some alternative modifications were proposed in order to increase the collision behavior and toughness of the body structure without affecting the total weight and stability and then, comparison of existing with the new front and side frame structure is done in order to get the material which best met the design criteria of vehicle frontal and side structure. The scope of this work includes only Bishoftu pickup (double cab) structures. Other pickup vehicles were not included. In addition to this, the injuries to occupants were not analyzed.

1.7 Limitation

Some of the limitations of this thessis work are as follows;

- Due to high cost of experimental crashworthiness test, this thessis work focus on the numerical (FEM) aspects of Bishoftu pickup crashworthiness improvement.
- The usage of numerical method also required a high-performance computer. Since it was very challenging to get such kind of machines, so with the use of medium performance computer the required results were obtained by waiting for more than 5 days for one simulation.

1.8 Organization of the thessis

This thessis is organized with the following chapters. **Chapter one**: Introduction part which includes background, statement of the problem, objectives, scope, limitation and the significance of the study. **Chapter two**: Literature review that deals with concepts and past studies which have information pertinent to the study. **Chapter three**: Materials and methods deals with the methodology to be followed to accomplish the thesis work. **Chapter four**: the detail of the modeling and analysis procedures used for analyzing the existing and modified BPV. It also described the methods and material used for developing the BPV safety. **Chapter five**: the result of different computational simulation were imported and discussed. It shows the result and discussion of the modifications, existing and modified model of Bishoftu pickup. **Chapter six**: presents the summary and conclusions of the work conducted in this thesis, highlighting the findings and concluding with recommendations for further work.

CHAPTER TWO

LITERATURE REVIEW

In order to have deep understanding on the problem of this study, it is vital to review several literatures and exercising different software that have been used in the field so far. For this reason, related literature such as books, accident data, articles, proceeding papers and some other sources that are retrieved from the internet are consulted so as to understand the domain knowledge, concepts, principles and methods that are important for developing knowledge-based systems.

2.1 Vehicle structural response

The crash relevant components are designed to absorb the kinetic energy of the vehicle by plastic deformation. These components usually form several parallel load paths going through the front structure of the vehicle in driving direction. During the deformation of the load paths, the acceleration at the pillars (A-pillar, B-pillar) must not exceed the critical value. The acceleration of the B-pillar correlates with the dummy acceleration constrained by the injury criteria. In addition, deformation of the compartment is restricted to prevent injuries caused by crushing or penetrating to the occupants. Firewall intrusion is used as a measure of the severity of the compartment deformation during a head-on collision. In addition to the dummy protection, the number of the affected components depending on the crash velocity is considered due to the structural reparability and reusability (Song et al., 2015).

Collision energy is absorbed by the vehicle structure with multi-level EA (energy absorbing) system to control the load path into the vehicle structure. The specific requirements of CEM (crash energy management) are: under the first speed limit, the coupler works; under the second speed limit, the coupler shear device is damaged, the anti-climber of the vehicle in collision engages and absorbs the energy; under the third speed limit, the first two parts of the EA reach the limit, and the remaining energy is absorbed by high energy crash zone (HE-zone) at the end of the car body so as to ensure the integrity of the passenger living space of the car body (T. Zhu et al., 2021).

The front-end structures of a vehicle, including front members, bumper assembly and front longitude beam, are the most important components in absorbing crash energy when a vehicle collision happened. These components are designed in such a way that, after involving in an impact they absorb the impending kinetic energy and deforms to dissipate it such that the effect of the collisions does not transcend to the passengers (Yu et al., 2021; Lebaal et al., 2022; Duan et al., 2016). The multi-objective optimization method is used to find the optimal thickness distribution and structure combination of tailor rolled blank (TRB) structures (Yu et al., 2021). Figure 2.1 shows the percentage of fatality at different collision parts.

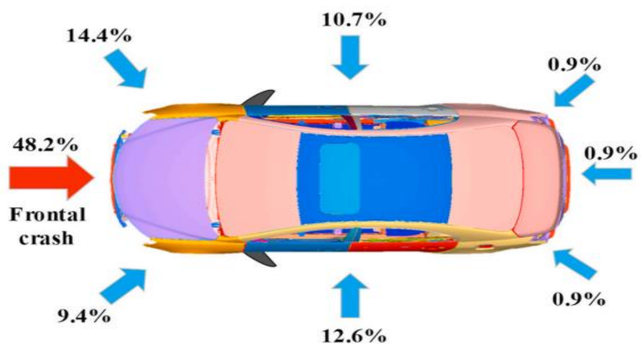

Figure 2.1: Proportion of fatalities at different collision positions (Yu et al., 2021)

2.1.2 Vehicle Architectures

In order to minimize the development cost of the vehicle, the concept of the vehicle platform is introduced. A platform denotes a technical basis, on which various vehicle models can be constructed. The platform is also called vehicle architecture. The common parts that make up an automotive platform are: chassis, suspension, steering mechanism and drive train components. Analogously the platform concept is also applied for the corresponding components in Crash. The vehicles, which share the common components in the passive safety design, are grouped in one cluster (Song et al., 2015).

The Vehicle Cluster within Architecture

For economic reasons, the vehicles are desired to share as many components as possible. The vehicles are grouped into one cluster if they are coupled in the following ways:

Direct coupling: When several vehicles share common components, they are directly coupled. (Shown in Figure 2.2)

Indirect coupling: The indirect coupling denotes the situation, in which several vehicles don’t have common components. Nevertheless, they have common components with the same vehicle(s) as shown in Figure 2.2.

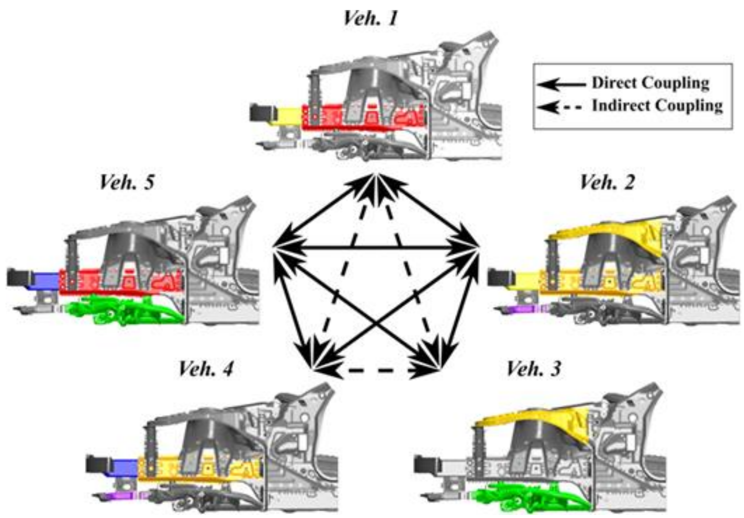

Figure 2.2: The coupling relation of a cluster with five vehicles (Song et al., 2015)

2.2 Crashworthiness parameters

Collision performance requirements focus on occupant injury parameters and structural deformation measurements such as penetration, acceleration, and velocity of deforming structures (Zahedan et al., 2022). To assess the quality and performance of the crash parts, certain key parameters have to be quantified to relate to the crashworthiness of those structures. Parameters include energy absorption, mean crash force, specific energy absorption, and crash force efficiencies. To obtain the solution towards these crashworthiness constants, certain empirical relations have been derived to aid the analyses (Lebaal et al., 2022). The basic requirements that help achieve this goal are limiting vehicle impact acceleration and minimizing firewall penetration through effective deformation and energy absorption in the process (T. Zhu et al., 2021).

To explain the basic principle of frontal impact, it includes 100% front rigid barrier (FRB) impact, 40% offset deformation barrier (ODB) impact and 25% overlap (small overlap) impact are the most accident types and may result in remarkable deformation to the body. Crash evaluation rating protocols use those impact types to improve crashworthiness of the vehicles (Liu et al., 2021).

Besides frontal collisions, other collisions, such as rear and side impacts, have received less attention compared to frontal collisions. Transverse impacts are a major cause of vehicle accident-related deaths and injuries. The bending deformation of the B-pillars and door intrusion beams and their energy-absorption behavior are major factors that affect the safety of passengers. As reported by the European New Car Assessment Program (Euro NCAP), side impacts or lateral impacts account for approximately 25% of all crashes. Almost 50% of the occupants injured due to lateral/side impacts are on the opposite side of the one that is struck, giving rise to serious injuries (Abdulqadir & Tarlochan, 2022).

2.2.1 Crashworthiness requirements

The vehicle structure must have sufficient flexural and torsional rigidity to allow for proper ride quality and handling. It is necessary to minimize the high frequency back and forth vibration that causes roughness. In addition, this structure must provide deceleration pulse that meet the following requirements for different occupant sizes, ages, and impact velocities for men and women (Ibrahim, T. M. H. T., Hafeez, 2014; KiranKumar et al., 2019):

- Deformable, yet stiff, front structure with crumple zones to absorb the crash kinetic energy resulting from frontal collisions by plastic deformation and prevents intrusion into the occupant compartment, especially in case of offset crashes and collisions with narrow objects such as trees. Short vehicle front ends, driven by styling considerations, present a challenging task to the crashworthiness engineer.
- Deformable rear structure to maintain integrity of the rear passenger compartment and protect the fuel tank.
- Well-designed side structures and doors to minimize intrusion into side collisions and prevent doors from opening due to impact loads.
- Strong roof structure for rollover protection.
- A well-designed restraint system that works in harmony with the vehicle structure provides optimal ride down and protection for the occupants in a variety of interior spaces and trims.
- Accommodate various chassis designs for different power train locations and drive configurations.

The need for increased crashworthiness, and lighter compact design, demands the development of more efficient body-in-white, chassis, suspension and power train components. Sub-frame and underbody cross-members provide significant rigidity to the vehicle front-end allowing longitudinal member to crash efficiently. Crashworthiness (ES) is the ratio of the mean crash stress (S) to the density of the material (D).

$$ES = \text{Mean Crash Stress/ Density of the material} = S/D$$

Design Engineers of the vehicles should keep in mind while designing the structures in the vehicles should absorb the maximum energy during the impact. In the force Vs deflection curve, the area under the curve shows the energy absorption. The structure should be designed in such way that the area under the curve should be maximum during the vehicle impact which in turn reduces the injury of the occupants. In the present-day accidents happen every hour around the world and most of these are very dangerous. Frontal-Impact crash is the one of the most severe crash scenarios. Figure 2.3 shows the comparison of different crash scenarios involved. It can be observed that the frontal impact is higher than all other impacts (Kumar Nijagal Honnagangaiah, 2016).

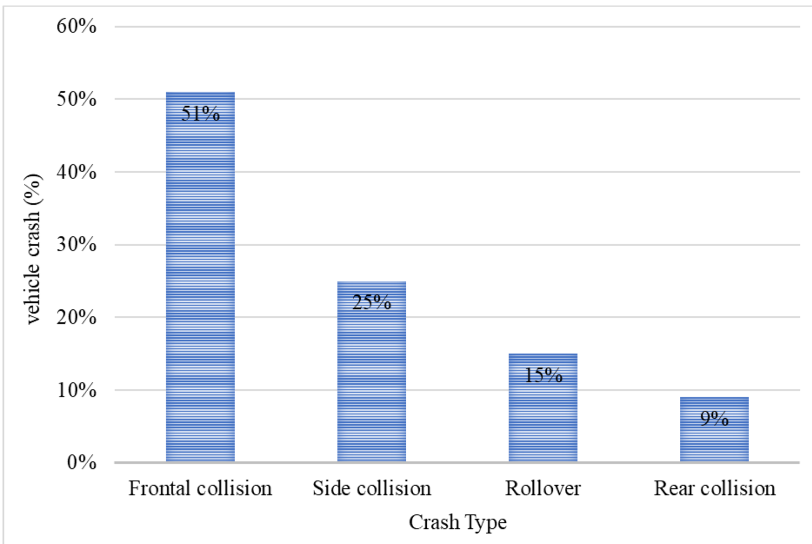

Figure 2.3: Vehicle crashes by crash type (Kumar Nijagal Honnagangaiah, 2016)

Crashworthiness mainly depends on the position, cross-section and material of the intrusion barrier, so the novel design has to cope with the following crashworthiness problems:

- Crash position: in the case of a full overlap crash (both longitudinal and engine involved) as in the case of an offset or oblique crash (at 40 per cent overlap only one longitudinal directly involved) a similar amount of energy must be absorbed by the front structure.
- Crash velocity: With a not much longer deformation length, much more energy must be absorbed at high crash velocities (resulting in less fatal injuries) and a lower injury level must be obtained at lower crash velocities.
- Crash pulse: A deceleration pulse must be obtained which is optimal (lowest injury level) for the concerning relative collision speed and the chosen dummy restraint parameters.

- Crash compatibility: The structure stiffness must also be optimized for the mass and stiffness of the struck object.
- Mean crashing load: This is the average force or load at which the energy absorber deforms in stable manner and is obtained for a particular deflection by dividing the absorbed energy by the impact distance.
- Peak force: It is the force at which first fold starts. It is higher than the mean load.
- Crash Force Efficiency: It is the mean crashing force divided by the peak crashing force (Tuljapure, 2015).

2.2.2 Crash tests and test standards

A crash-test is a form of destructive testing usually performed in order to ensure safe design standards in crash-worthiness and crash compatibility for automobiles or related components. To test the safety performance of a vehicle under different conditions and in different types of accidents, automakers use different angles, different sides, and different objects, including other vehicles, to crash the car and Carry out the test (Yadav & Pradhan, 2014; AMBATI et al., 2012). It will be performed either by numerical simulations or experimentally. Some of the general crash tests are as follows.

Frontal Impact Test- In this test the completely front structure of the car collides with something like another car, solid wall etc. On another hand, In Offset Test, only a part of front portion of the vehicle strikes on some barrier usually a Vehicle at a given speed (Yadav & Pradhan, 2014; Rajappan & Vivekanandhan, 2013). It was shown that the FUPD (front underrun protection device) compliant with ECE-R93 (Economic Commission of Europe - Regulation No. 93) was insufficient to prevent overruns in all expected real crash situations. Despite the fact that the contrast between the FUPD of the vehicle and the car longitudinal was good in all revised conditions, vehicle overriding was not prevented (Krusper & Thomson, 2010). The load (energy) distribution during frontal collision is shown in the figure 2.4 below.

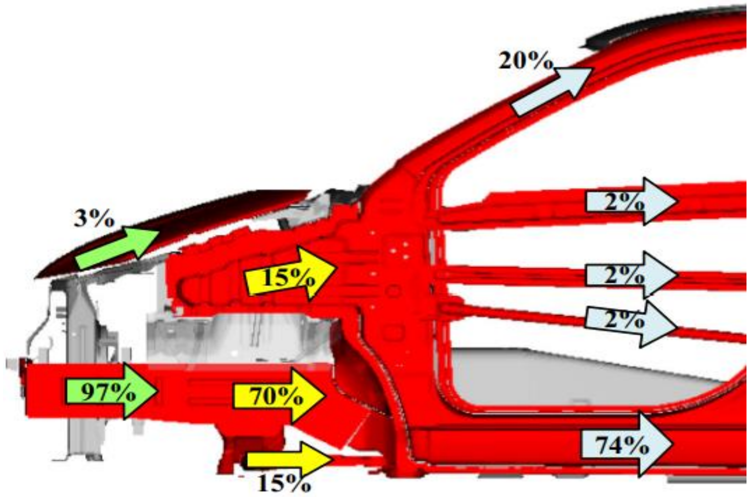

Figure 2.4: Load path distribution for frontal impact crash (Duan et al., 2016)

Side impact test – it is one of the most hazardous types of impact, Test protocols are generated and standardized for two types of side impact. It may be either a vehicle impacting a non-deformable fixed body such as the pole or colliding laterally into another vehicle as a moving deformable body. In both cases, the kinetic energy of the impact car is dispersed by the deterioration of its structure and the body of the crash partner. The kinetic energy is then converted into internal deformation of the structure and pressure on the body of the occupant. Eventually, the remaining kinetic energy is wasted as the occupant descends with the vehicle. European legislation relating to side impact assessment [ECE R 11, 1985, ECE R 95, 2005], EURONCAP [2013] pole side impact test protocol, and FMVSS (Federal Motor Vehicle Safety Standards) standard 214 [2008] in the USA are the most common sources of information. As well as side effects test procedures (Kocabas & Modelling, 2019; Teng et al., 2008).

Roll-Over Test- In this test the car is in a rolling position with a certain angle at which it tests the ability (especially the pillars holding the roof) to support it with a flexible impact. It is also performed in the case of a fixed crash test (Yadav & Pradhan, 2014). The figure 2.5 below shows the different types of crash tests that are commonly used.

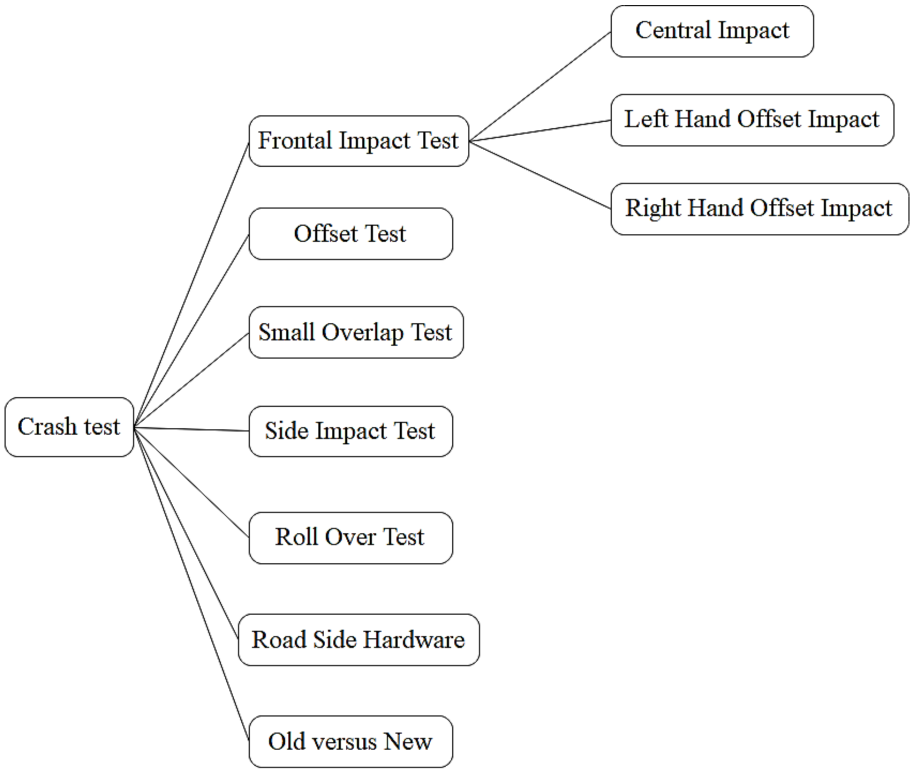

Figure 2.5: Classification of various crash test used in testing (Yadav & Pradhan, 2014)

Frontal collision test standard

NHTSA's front-end crash test accelerates the vehicle at 35 mph and collides it directly into a rigid barrier, where the entire width of the vehicle's front end collides with the barrier. Instrument-bearing, seat-belted crash-test dummies in the two front seats record the level of crash forces on the head, neck, chest, and legs. Although these measurements correlate with injury, previously only head and chest results formed the basis for star rating. Drivers and passengers are assigned individual star ratings. Some automotive experts have criticized NHTSA's full-scale stiffness barrier test as unrealistic. This is because such head-on collisions against flat, sturdy walls are relatively rare. Others argue that real-world or not, flat-barrier testing is a good way to gauge the effectiveness of the restraint systems, primarily the safety belts and air bags (“NHTSA Crash Test - Consumer Reports,” 2014).

The Insurance Institute for Highway Safety (IIHS) front-crash tests are quite different from NHTSA's in that they’re designed to highlight the vehicle's structural integrity, as well as restraint performance. Vehicles are rated as Good, Acceptable, Marginal, or Poor based on what happens to vehicle structure, as well as forces on the dummies. IIHS now conducts two series of front crash tests, one that engages 40 percent of a vehicle’s front and a newer test, inaugurated in 2012, that uses a smaller overlap, engaging just 25 percent of the car’s front. Both simulate what would happen if two cars of the same weight and type crashed head-on, partially overlapping. The older test, with the 40-percent offset, engages the portion straight ahead of the driver. The newer test is more like a head-on crash where two cars hit left-headlight to left-headlight or a single-vehicle crash into a fixed object like a utility pole or tree. These are very different from the full-width crash NHTSA uses.

Both the IIHS front-crash scenarios use an impact speed of 40 mph instead of 35 mph; and only the left front of the car hits the barrier. The 40-percent overlap test uses a deformable barrier while the 25-percent overlap test uses a rigid barrier (“NHTSA Crash Test - Consumer Reports,” 2014) as shown in figure 2.6.

Figure 2.6: The IIHS tests a Chevrolet Spark (“NHTSA Crash Test - Consumer Reports,” 2014)

The NCAP frontal test is a full-width impact to the front of the vehicle. Crash test dummies are seated in the location of the driver and the right front passenger. The vehicle crashes head-on into a rigid concrete barrier at nominally 56 kph (35 mph). During the collision, instruments in the dummies measure the severity of the impact to the body of the occupant. As compared to the Insurance Institute for Highway Safety (IIHS) frontal test, the NCAP frontal test has shorter pulse time width and lower occupant compartment intrusion. Figure 2.7 shows the test set up and the post-crash vehicle for the NCAP frontal test. In this thesis work by keeping the standards and regulation in mind, it has been decided to investigate car crashing into the rigid wall.

Figure 2.7: Test set up and the post-crash vehicle of the NCAP frontal crash (Singh, 2012)

Side impact test standard

Side impact crashes are the second most common reason for vehicle passenger deaths after frontal crashes. To reduce the number of passenger deaths occurring in accidents, several crash Tests have been established to ensure safety standards of cars and encourage automobile manufacturers to make safety improvements. The Federal Motor Vehicle Safety Standard (FMVSS) 214 Side Impact Protection was enhanced in 1990. In 1997, the National Highway Traffic Safety Administration (NHTSA) introduced a side impact crash test with a Moving Deformable Barrier (MDB), representing the front end of a car from the early 1980s, within the New Car Assessment Program (NCAP).

FMVSS 214 specifies performance requirements for protection of occupants in side impact crashes. The aim of this standard is to reduce the risk of serious and fatal injury to occupants of motor vehicles in side impact crashes by setting vehicle crashworthiness requirements in terms of accelerations measured on anthropomorphic dummies in test crashes. For the physical test, the procedure was simplified with the struck vehicle stationary and the moving deformable barrier (MDB) striking the target vehicle. The wheels of the deformable barrier were crabbed at an angle of 27 degrees from the longitudinal direction of the barrier. Figure 2.8 shows the test setup. Dummies in vehicle must satisfy requirements of FMVSS 214 when stationary vehicle is impacted by MDB at 54 km/h (33.5 mph). This test was intended to simulate an intersection crash involving two moving vehicles. Dummy injuries to the thorax and pelvic area were assessed along with vehicle structural damage (Teng et al., 2008).

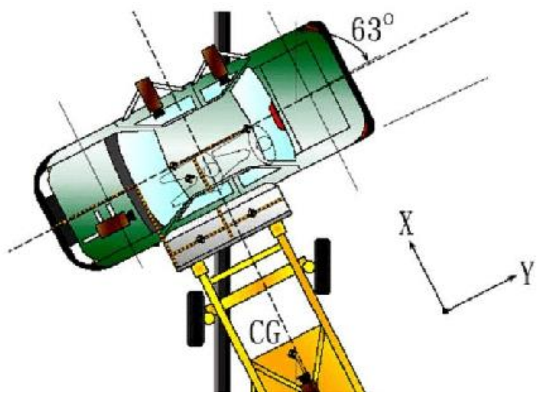

Figure 2.8: The test setup of FMVSS 214 (Teng et al., 2008)

In this test, a MDB with a mass of 1,368 kg hits a stationary vehicle at a 90° angle with a crabbed wheel angle of 27°. The velocity of the MDB is 54 km/h, see Figure 2.8. The deformable part of the barrier is 838 mm high, measured from the ground. Such a scenario mimics what could happen if you were hit on the side at an intersection. Individual side-impact star rating scores are assigned to the driver and left-rear passenger. For pre-2011 models, only a chest injury measure dictated the score. For 2011 and later models, the score factors in head, chest, abdomen, and pelvis data for the driver and injury to the head and pelvis for the rear-seat passenger ("NHTSA Crash Test - Consumer Reports," 2014).

As there is a much greater risk of head injuries from impacts with taller bullet vehicles, the Insurance Institute for Highway Safety (IIHS) decided to start its own side impact crash test in 2003 with a modified MDB as show on Figure 2.9. In the IIHS side impact crash test, the modified MDB hits the driver side of a stationary target vehicle at 50 km/h. The IIHS MDB has the geometry, shape, and height of a typical midsize SUV. The mass of the IIHS MDB (1,500 kg) is comparable to a small SUV or midsize car. The deformable part of the barrier is 1,138 mm high, measured from the ground. The IIHS side impact rating is based on different aspects, including injury risk assessment, restraint system, and structural performance (Reichert et al., 2018).

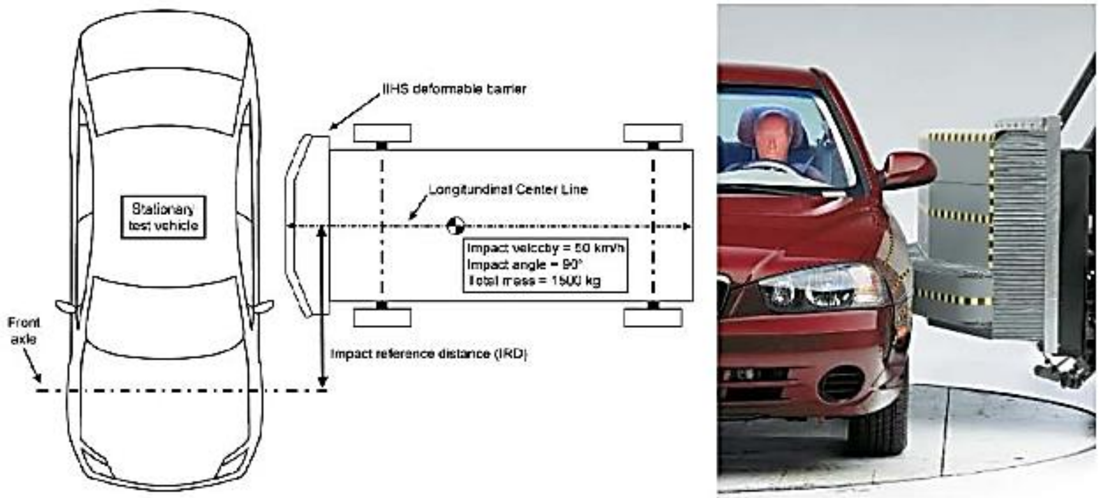

Figure 2.9: IIHS side impact configuration (Reichert et al., 2018)

Lateral NCAP Pole Test

Side Pole impact is one of the most hazardous types of impact. In pole side impact crash tests, a vehicle in motion impacts a target pole from the locations of one or more of its pillars during which the kinetic energy is transformed into deformation mainly on the impacting vehicle. This test is done to simulate what happens if a driver slides off a road and crashes into an object such as a utility pole. NHTSA and IIHS Crash Test Safety Ratings Explained A vehicle in the NCAP side pole test is sent into a fixed, rigid pole 254 mm (10 inches) in diameter, at a speed of 32 km/h (20 mph). In this thesis work by keeping the standards and regulation in mind, it has been decided to investigate car crashing into the rigid pole. Figure 2.10 (a) shows the Fixed, rigid pole (Singh, 2012; Kocabas & Modelling, 2019) and (b) The complete experimental test set-up is illustrated, Whereas Figure 2.11 show the FEA method for NACP side pole test with isometric and top view.

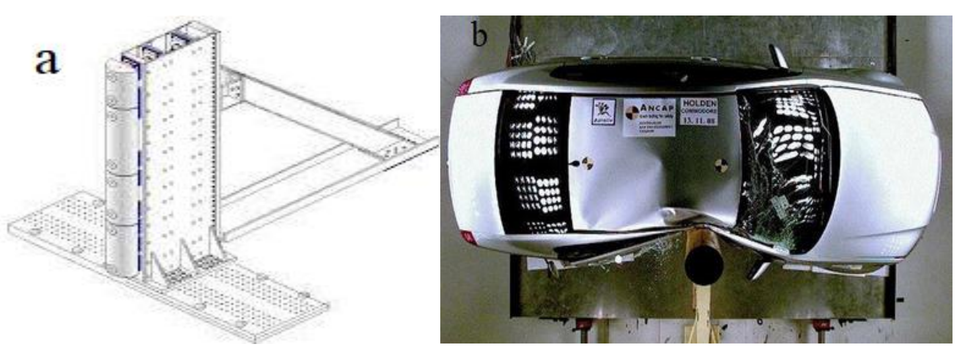

Figure 2.10: (a) Fixed, rigid pole, used for NCAP pole test (b) NCAP experimental test (Kocabas & Modelling, 2019)

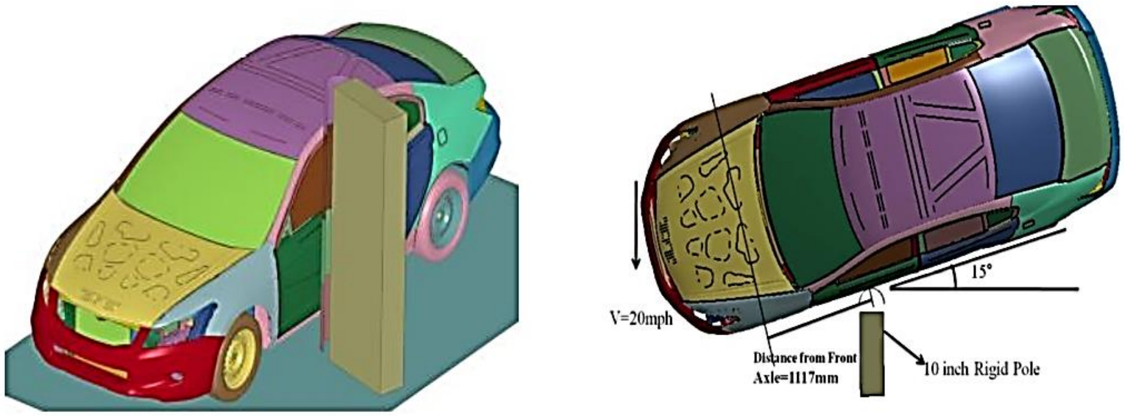

(a) (b)

Figure 2.11: The isometric and top view of the NCAP FEA method used for side pole test

Procedure

In this test the LWV (low weight vehicle) impacts the rigid pole laterally at a speed of 32 km/h such that its line of forward motion forms an angle of 75 degrees with the vehicle's longitudinal axis, simulating areal-world crash in which the vehicle hits a tree while sliding on the road. The rigid pole is vertically oriented metal structure with:

- Diameter of 254 mm.
- Beginning no more than 102 mm above the lowest point of the tires on the struck side of the fully loaded test vehicle.
- Extending at least 150 mm above the highest point of the roof of the test vehicle.
- The direction of vehicle motion is such that the pole is always aligned with the CG of the head of the driver (Singh, 2012).

Rear end collision

A rear-end collision, or simply a rear-end is a car crash scenario in which a vehicle collides with another vehicle in front of it. Rear crashes are the third most frequent type of accidents Standing behind the front and side collisions in the United States. Though common, not many rear-impact crashes are fatal. But they do cause many injuries, especially whiplash trauma to the neck injuries is the most common type of injuries to the occupants in rear-end collision. Thoracic injuries are far less common in rear-end collisions, and so are lumbar injuries. Rear-end collisions can occur in four types as shown in Figure 2.12. It can be observed that the most occurred rear-end crash is the rear offset collision. Coincidentally, The FMVSS 301R regulation also uses a similar scenario for the test where the occupant's response can be studied (Vedantam, 2018).

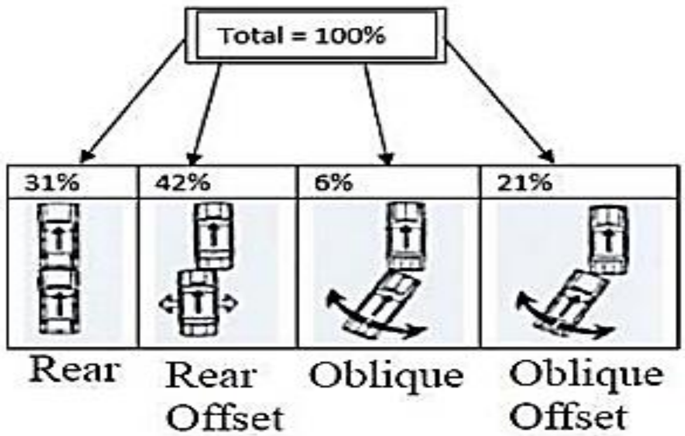

Figure 2.12: Rear crash distribution (Vedantam, 2018)

Federal Motor Vehicle Safety Standard (FMVSS) No. 301 specifies a rear-impact test. The rear impact test is designed to promote the crashworthiness of the body structure and fuel tank. In this test a moveable deformable barrier (MDB) impacts at 80 km/h (50 mph) into the rear of a stationary vehicle with an overlap of 70% as shown in Figure 2.13. The MDB used in the rear impact test weighs 1380 kg (Singh, 2012).

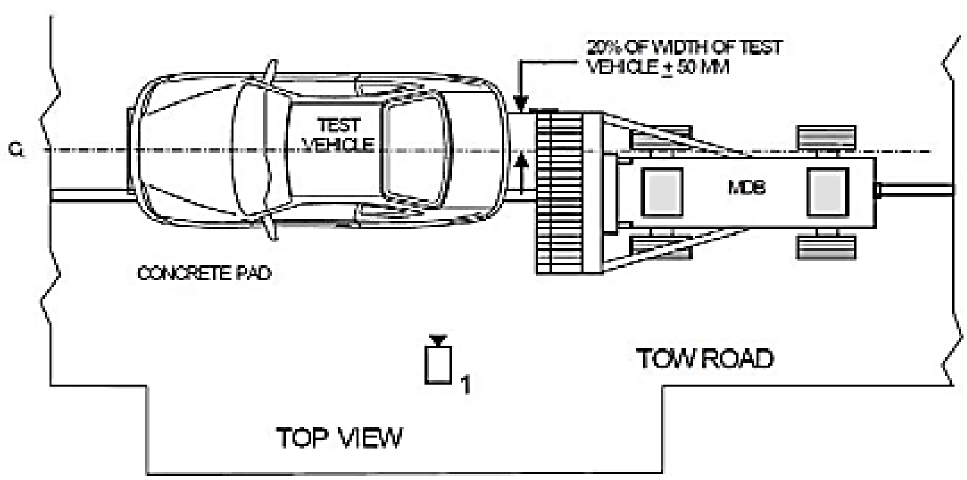

Figure 2.13: FMVSS 301R New Regulation (Vedantam, 2018)

The IIHS evaluates rear impacts with physical inspections and crash testing. The crash test, which is conducted with the vehicle seat attached to a moving sled, simulates a rear-end crash about equivalent to a stationary vehicle being struck at 20 mph by a vehicle of the same weight. The key to rear-impact protection is head-restraint design. Restraints need to be high enough and positioned close enough to the back of the head to cradle an occupant's head in a rear collision. Those restraints that are clearly too low or ill-designed automatically receive a poor rating from IIHS, while those with a chance of providing decent protection are crash-tested (Singh, 2012).

2.3 Finite element analysis (FEA)

Currently, automotive industry relies on finite element analysis (FEA) in development of product. Analyzing the energy absorption in real impact is quite complicated and depends on different parameters. The effect of design parameters on the weight, cost or functional properties of new car models can be determined using FEA. FEA is an effective way to analyze the absorption of energy during an impact to determine the probability of deviation from the effect of impact (Muhammad et al., 2017; Marzougui et al., 2014). Examples of FEM trading software are LS-DYNA ©, MADYMO, ANSYS ©, ABAQUS© …etc.

Simulation using finite element method (AMBATI et al., 2012; Yadav & Pradhan, 2014) comprises of three major phases: (1) pre-processing, in which the analyst develops a finite element mesh to divide the subject geometry into sub-domains for mathematical analysis, and applies material properties and boundary conditions, (2) solution, during which the program derives the governing matrix equations from the model and solves for the primary quantities, and (3) post-processing, in which the analyst checks the validity of the solution, examines the values of primary quantities (such as stresses and deformation), and derives and examines additional quantities (such as specialized stresses and error indicators).

The governing equations of transient dynamics are written below as follows (Yadav & Pradhan, 2014):

$$[\mathrm{M}]\left\{\frac{\mathrm{d}^2\mathrm{u}}{\mathrm{dt}^2}\right\} + \mathrm{c}\left\{\frac{\mathrm{du}}{\mathrm{dt}}\right\} + \mathrm{K}\{\mathrm{u}\} = \{\mathrm{F}_{\mathrm{ext}}(\mathrm{t})\} \qquad (2.1)$$

Where M= Mass matrix, C= Damping matrix, K= Stiffness matrix, $\mathrm{F}_{\mathrm{ext}}$ = External force, t = Time

In Explicit time integration schemes above equation can be written as:

$$[\mathrm{M}]\left\{\frac{\mathrm{d}^2\mathrm{u}}{\mathrm{dt}^2}\right\}_{\mathrm{n}} + \mathrm{c}\left\{\frac{\mathrm{du}}{\mathrm{dt}}\right\}_{\mathrm{n}} + \mathrm{K}\{\mathrm{u}\}_{\mathrm{n}} = \{\mathrm{F}_{\mathrm{ext}}\}_{\mathrm{n}} \ldots\ldots\ldots\ldots\ldots\ldots\ldots\ldots\ldots\ldots\ldots\ldots\ldots \quad (2.2)$$

Where n = time level index

Physically it refers to

Inertial force + Damping force + Stiffness force = External force……………………….. (2.3)

Typically, the finite element method and multibody dynamics are jointly used. First, the force-crush characteristic is obtained through finite element analysis. It is used as the input to the dynamic model. The gross motion and crash acceleration obtained through multibody dynamics can be used as input for models of the occupant environment. Then the forces and decelerations that will be experienced by occupants are evaluated using occupant dynamics. Finally, the likelihood of injury and fatality can be evaluated from these forces and decelerations (Gao & Wang, 2019).

Finite Element Impact Test Model

Finite Element (FEM) models require a car to be discretized by a very large number of elements. Due to the high flexibility and displacement implied in the crash, the governing equation estimates are made with many non-linear terms and the method is called Non-Linear FEM. The method is accurate, but the calculation times are high, so the method is usually used in the final phase of a new car design phase (Vangi et al., 2018; Teng et al., 2008). Figure 2.14 shows finite element model of pickup vehicle.

Figure 2.14: FE model of pickup (Park et al., 2013)

The dummy finite element model, which was used for simulation, is based entirely on the testing of the 50th percentile Hybrid dummy, as shown in Figure 2.15. Key parts, such as the chest and neck, are fitted with quality flexibility, to judge post-traumatic injury (Teng et al., 2008; Liu, 2013b). The main purpose of crash test dummy used as a substitute for human in car collisions is to determine the injury severity to human body caused by the accident. Thus, understanding how the mechanical properties of dummy meet injury mechanism of human and correspond to the harm standard is absolutely essential (Xu et al., 2018).

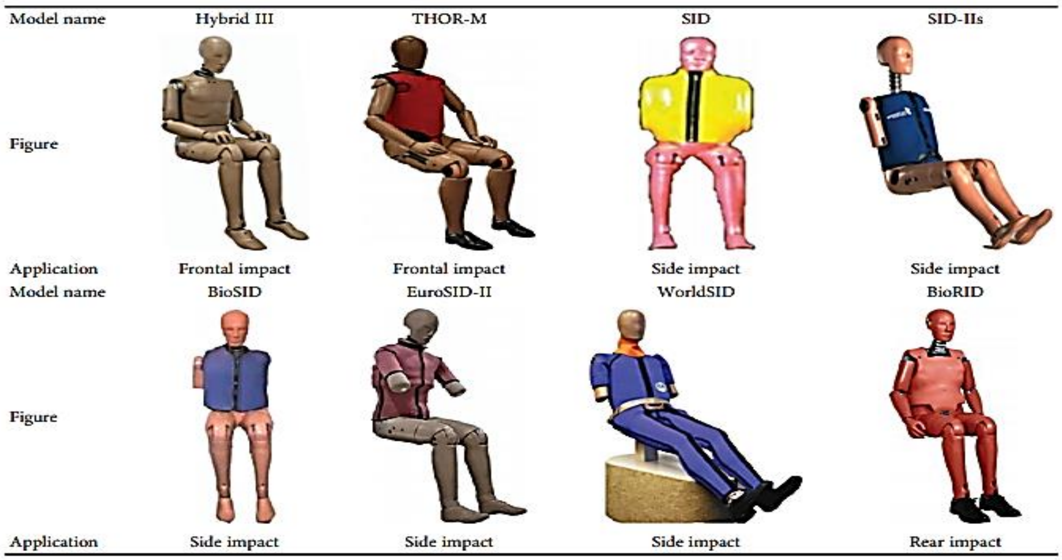

Figure 2.15: Dummies and their application (Xu et al., 2018)

The dummy is tied to a three-spot style seatbelt, as shown in Figure 2.16. Types of seat belt FEM include belt, slip ring, pre tensioner, retractor and sensor element that can make the pre-tensioner and retractor work. The seat belt model in front of the chest is modeled on a two-sided shell object (Liu, 2013b).

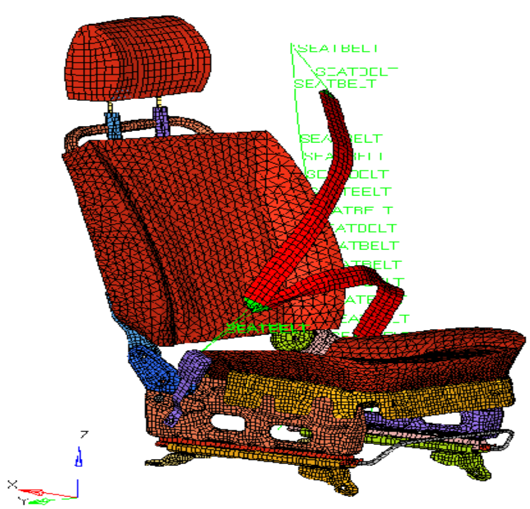

Figure 2.16: seat with seatbelt model (Yang et al., 2014)

2.4 Previous research works on crashworthiness

Many Researchers has done on crashworthiness, a special purpose vehicle model for time-efficient crash stage simulation of vehicle-to-vehicle impact and introduces the equations which rule over the model first. The Finite Element Method (FEM) represents the basis for the problem's analytical formulation (Vangi et al., 2018), Based on the obtained stiffness value then perform a simulation. The theoretical possibilities for energy-absorbing FUPDs are understudied and the analysis of the simulation results showed that a properly activated FUPD with energy-absorbing elements can decrease the severity of the crash by absorbing more than 30% of the total kinetic energy (Krusper & Thomson, 2010). Studying the effects of crash parameters on the dynamic response of automobile component through finite element approach path and presents an investigation of development done in the crash simulation of automobile components and the related process parameters through finite element approach (Yadav & Pradhan, 2014).

A complete finite element models of a passenger car and the occupant restraint system including a 50th percentile Hybrid dummy and the seatbelt subsystem III are made according to the CMVDR 294. The frontal crash into a rigid wall of the car at about 48.3 km/h is simulated in LS-DYNA (Liu, 2013a). And, an investigation on the use of deployable front-end airbags is evaluated in terms of the potential effects on passenger vehicles when they are struck in the front or rear by the front of a heavy truck. A virtual testing methodology for the evaluation of various designs under impact conditions is described. The study reports on the potential effects of radar-activated, heavy-truck, front-end airbag systems on crash mitigation in front- and rear-end impacts (Friedman et al., 2018).

Modification and analysis of frame structure for the front end of Haunghai Sports Utility Vehicle (SUV) expected to achieve a previously unavailable level of efficiency of energy absorption, strength and weight reduction in order to reduce front SUV component and passenger compartment intrusion during crash by focusing on analyzing the dynamic behavior of the frontal upper cross beam with the help of CATIA V5 for geometric modeling and ANSYS 14.5 for analysis. Depend on the analysis, thus results can be effectively utilized and the frontal frame structure behavior for crash loads and successfully identify the safe performance (Zegeye, 2020).

A mixed meta-modeling-based optimization method has been proposed and applied to a commercial vehicle for crashworthiness design subjected to the frontal crash. A full-scale finite element model of the commercial vehicle has been built and validated by a crash test. The front frame parts have been separated to build a sub-model for crashworthiness optimization. The normalized optimal solution from the front has resulted in 11.15% increase in specific energy absorption and 13.2% decrease in peak crush force for the frame and has led to an obvious improvement in occupant protection and energy absorption for the whole vehicle, verifying that the proposed method is effective for vehicle crashworthiness optimization (Tao Wang et al., 2018).

Detailed finite element (FE) models of a 2270 kg Chevrolet Silverado and 1100 kg Toyota Yaris are used as surrogates for barrier crashworthiness under the new Manual for Assessment of Safety Hardware (MASH). MASH requires assessment of barriers for both large and small vehicles, hence the use of 2270P and 1100P test vehicles and achieved two objectives, includes (1) demonstrating the viability of the FE models for the new MASH crashworthiness evaluation, and (2) describing the application of the newly developed roadside verification and validation (V&V) procedures to compare simulation results and crash test data (Marzougui et al., 2014).

Study is made to evaluate the safety of ITB's formula SAE race car and to analyze possible head injuries due to frontal collision was conducted. A reconstruction of frontal collision with an impact speed of 7 m/s to 15 m/s was made by developing a finite element model of the race car, a rigid wall, a dummy, a seatbelt, and numerical studies of guardrail systems (Soltani et al., 2017). On the other hand, a full-frontal barrier test only the race car and rigid wall were modeled and analyzed by LS-DYNA, without incorporating the dummy inside the car. The effect of impact speed on car deceleration was analyzed (Mihradi et al., 2017).

A new full vehicle-lumped proposed model is created for frontal crash. It has 12 degrees of freedom (DOF) involves all important structural parts. The study follows a new algorithm related to system identification including problem-solving and genetic algorithm (GA) to find the unknown lumped parameters. In addition, GA was used for calculating the optimized parameters of 12-DOF model for two vehicle types (a sedan and a pick-up) in two different frontal crashes (Pahlavani & Marzbanrad, 2015).

A finite element (FE) model is developed utilizing a previously generated mesh of a vehicle. The FE model is employed to simulate pole side crash test scenarios on the whole body of the vehicle (M. Ozan KOCABAŞ, Eren ÜNSAL, 2014). A systematic evaluation of two different criteria for vehicular crashworthiness designs for a side impact: energy absorption by structural components and injury to the dummy. With the objective of minimizing weight and a constraint on the lateral intrusion distance, the designs based on both criteria were evaluated under the same side-impact scenarios. The optimization in the study used the structural components of side-door as design variables and thus is a size optimization solved by two different multi-objective optimization problems: one that employed an injury-based metric and the other on that employed an energy absorption metric (Horstemeyer et al., 2009). The capability of impact energy absorption of side-door beams is discussed based on FMVSS-214 (Teng et al., 2008). Crash analysis of a front side member in an auto-body considering the effect of fabrication. The front side member is fabricated with sheet metal forming processes that induce forming histories such as plastic work hardening and non-uniform thickness distribution (Huh et al., 2003).

Analysis the worst-case scenario in which the B-Pillar after side impact that is subjected to bending, buckling, and possible breakage depending on the severity of the impact. A force of 140kN evenly distributed across the B-Pillar was considered. The crash impact can be analyzed using Hyper Works, FEA software or software add-in software for FEA in CATIA as well as ANSYS. The analysis was done using the best mesh size in order to increase the accuracy of the results obtained. From the analysis, a suitable understanding of the optimized design was then deduced indicating which areas are the most important for the structure and which parts can be simplified, allowing for several design recommendations to be made (Ikpe et al., 2017).

Crash simulation of structural components 2007 model of Chevrolet Silverado by using LS DYNA in frontal (AMBATI et al., 2012) and side crash test is investigated. In addition, the safety benefits of composites applications in future lighter vehicles are studied. The methodology of the research includes two steps: (1) developing a light-weight vehicle based on a current finite element (FE) vehicle using advanced plastics and composites, and (2) evaluating the crashworthiness of the light-weighted vehicle by frontal and side New Car Assessment Program (NCAP) test simulations (Park et al., 2013).

The structural responses of a ladder frame pickup chassis during full frontal and pole side impacts subjected to several modifications in the chassis such as the cross-sectional area geometry, reinforcements and thickness. The 1992 model Chevrolet C1500 pickup was used for investigation, and the result realized that the chassis had capable of absorbing around 50% of the crash energy at different severities (Dagdeviren et al., 2016). Reinforcement of the side door beam geometrically and materially, and evaluate the energy absorption distinctiveness of it achieving improved crash behavior compared to the current structure, and uses software's like computer aided design (CAD) for the model and is imported to LS-DYNA explicit finite element (Ghadianlou & Abdullah, 2013).

A reliable finite element model of a light truck is built by using its CAD model. The finite element model is verified against cab modal test and frontal impact test. To enhance the crashworthiness of the truck, some structural improvements are designed such as filling structural foam in the A-pillars and the side panels, adding a roof crossbeam, and reinforcing the rear wall of cab. The simulation uses RADIOSS software and Batch Mesher® to batch mesh the cab by setting fine grid standards, and results of the improved cab structure show that the cab stiffness is improved, the energy absorption is more homogeneous and there is no penetration into the survival space (Chen et al., 2015).

An Empirical analysis of real-world crashes has been made on the relationship between vehicle type and safety may be confounded by other factors, such as driver behavior and crash circumstances, and the study compared different vehicle types with respect to their crashworthiness (self-protection) and aggressiveness (risk to others) in crashes between two passenger vehicles. The result showed that the factors such as crash severity confounded the relationship between severe injury risk and vehicle body type. Results that do not account for confounding factors was cautiously interpreted (Toy & Hammitt, 2003).

An analytical description of the design space of the vehicle architecture is derived to define the component-wise force-deformation requirements of vehicle architectures for front crash structure design. The optimal orthogonal solution space within this design space is identified via optimization process. This results in maximal intervals for variations of the component forces over their deformations under the given boundary conditions. The validity of the solution space is proven through explicit FE simulation (Song et al., 2015).

A comparative study to show the response surface methodology (RSM) was first used to formulate the objective function of the weight and the radial basis function (RBF) was adopted to formulate the energy absorption and other crashworthiness criteria. The Monte Carlo Simulation (MCS) technique is then applied to enable reliable and robust analyses. After validating the surrogate models, the multi objective Non-dominated Sorting Genetic Algorithm II (NSGA-II) was applied to seek optimal solutions. As a result, different Pareto optimums were generated for deterministic and nondeterministic (reliable and robust) designs, respectively. These different Pareto optimums were finally compared in a quantitative fashion to provide some insights into the use of these different optimization schemes (Gu et al., 2013).

A traditional crashworthiness optimization problem with its augmented by inclusion of additional design criterion associated with vehicle vibration characteristics is made, Then the problem was solved by using a surrogate-based optimization technique and considering different optimization algorithms like Artificial Bee Colony (ABC), Differential Evolution (DE), Genetic Algorithm (GA), Particle Swarm Optimization (PSO), and Simulated Annealing (SA). Algorithm formulations were critically revised and the performance of DE algorithm in automotive design applications was discussed (Kiani & Yildiz, 2016).

A suitable structure for lightweight vehicle applications an investigation has been done under axial and oblique impact loadings is investigated, and study was taken out on homogeneous and heterogeneous ply orientation modeled structure of different CFRP (carbon fiber reinforced plastic) and GFRP (glass fiber reinforced plastic) materials to enhance the efficiency of crashworthiness parameters. The study encompassed the effects of various design variables involved in the crushing analysis such as ply orientations, angle, loading conditions and area of contact under impacts (Patel et al., 2019).

Experimental design and FEA have been done using LSDYNA, and the response of surface models (RSMs) of the three front rails were constructed. Based on multi-objective artificial tree (MOAT) algorithm, these three front rails were optimized with the goals of minimize structural mass (SM) and maximize mean crushing force (MCF). The optimal design schemes of these models were obtained. These optimal front rails were applied to the full-frontal barrier impact analysis of a sport utility vehicle (SUV) model, and the crashworthiness was improved significantly (Li et al., 2021).

A cutting-style energy absorbing structure to improve the crashing performance of subway vehicles through experiment and numerical simulations. The structure consists of an anti-creeper device, energy absorption tube, cutting knife and clamp. A finite element (FE) model of a cutting-style energy absorbing structure was created and validated by full-scale experimental data. The response surface method (RSM) was adopted to achieve maximum energy absorption (EA) and minimum peak cutting force (Fp) simultaneously. The optimized results showed that the objectives compete with each other, and the weighting factors are of considerable significance to the most satisfactory Pareto fronts solutions (Peng et al., 2017).

2.5 Literature summary and Research Gap

Literature summary

From the above literature reviews, it can be observed that most of the study focuses on the analysis of the structure of pickup vehicles emphasizing on their strength, stability issues, and biometrics problem and modifying the shape aerodynamically. Analyzing the crash performance of vehicle parts like bumper, crash box and cross member for self-protection is done. Most of the research work uses implicit dynamic numerical approach throughout the process for comparing the output results, and different software's are used for the analysis like MADYMO, ANSYS, PALMCRASH and so on. Ans also, different approaches are used for optimization like Artificial Bee Colony (ABC), Differential Evolution (DE), Genetic Algorithm (GA), Particle Swarm Optimization (PSO), and Simulated Annealing (SA).

Research gap

From the above reviews it can be observed that most of the study focuses on the analysis of the structure of the existing pickup rather than Bishoftu pickup. No research has been done on the full crashworthiness of this vehicle unless checking of the parts, so this will make this thesis work unique and also this thesis work uses explicit dynamic numerical approach throughout the process for comparing the results on the output of the dynamic response. Furthermore, this thesis is aimed to find solution by modifying and analyzing front and side frame structure which protect life and apart from injuries during frontal and side collision of Bishoftu pickup by using light weight - good crash performance materials for comparison in order to get lower in weight, higher energy absorbing capability and lower in deformation material. A 3D model of frontal as well as side frame structure is created in CATIA V5 and LS DYNA is used for the analysis.

CHAPTER THREE

MATERIALS AND METHODS

3.1 Introduction

A moving vehicle has a massive amount of kinetic energy and momentum force and if these occur in a crash, this massive amount of momentum force needs to be absorbed, which can be very deadly and causes a lot of damages. The amount can vary based on the speed and mass of the car and the speed and mass of whatever it hits. The heavier the vehicle, the faster the speed and the greater the amount of momentum energy that needs to be absorbed in case of a crash. Another major consideration on the amount of the momentum force and impact of the crash is whether the car comes to a sudden stop or comes to stop gradually (driverseducationusa.com, 2021). This chapter gives the details about the materials used and methodology followed during this thesis work.

3.1.1 Passenger car safety design

From the first car models, car design has evolved a lot. These evolutions were concerning aerodynamic, external design, production methods and safety. The safety part is probably one of the most important, because it is directly linked to the occupant protection. This is why a lot of efforts are made to try to increase the car occupant protection while designing a new car model.

For years now, the car safety has become more and more important in the car development and the number of safety devices in cars hasn't stop increasing. Seatbelts, airbags, or other active safety systems have been integrated in cars to protect their occupants for different crash configurations as frontal impact, side impact, and rear impact or from rollover. To achieve this goal, the car body structure is also designed to be as safe as possible with some crushing zones to absorb energy but also a stiff protective cell for the occupants so called safety cage, see Figure 3.1.

The main energy-absorbing zones are situated in the front and rear parts of the cars, they are designed in order to have a controlled deformation. This deformation is used to absorb the maximum kinetic energy during a crash. The absorbed energy can be quantified using the equation (3.6) (Lefer & Rebolloso, 2012).

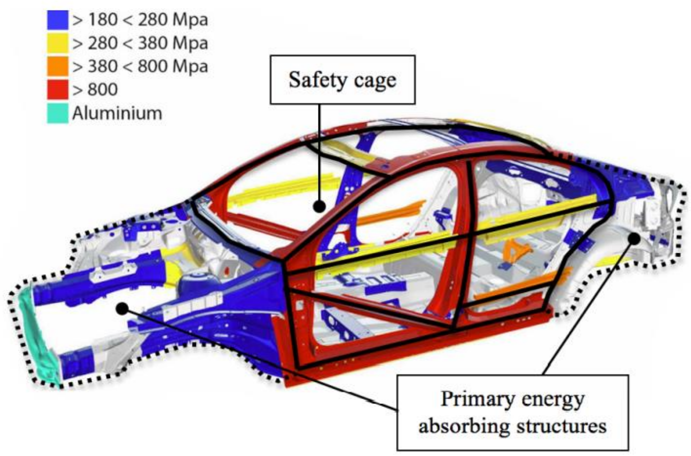

Figure 3.1: Example of a state-of-the art vehicle structure (Lefer & Rebolloso, 2012)

Simplified Modeling

The most common modelling methodologies for crashworthiness vehicle design used across the virtual product development cycle can be split into four categories, namely, (1) lumped mass-spring (LMS) systems and equivalent mechanisms, (2) collapsible beams, (3) multi-body systems (with rigid and flexible bodies) and (4) finite element models (hybrid, reduced-order, sub models and detailed) (Georgiou & Zeguer, 2018).

In the BVO system, the barrier, vehicle, and occupant are simplified to the constant masses, energy absorption of structures and restraint system are simplified to springs, as shown in Figure 3.2. The rotations of vehicle and barrier and the rebound of energy-absorbing structures are not considered in the modeling process(Tao Wang et al., 2018).

In the Figure 3.2,M_B, M, and m are the masses of barrier, vehicle, and occupant, respectively;X_B,X_V, and X_O are the displacements of barrier, vehicle, and occupant respectively; V_O is the initial velocity of three masses; K_B is the equivalent stiffness of barrier; K is the equivalent stiffness of the frontal end structures of vehicle; k is the occupant restraint stiffness (the linear system stiffness).

The input of the model is the stiffness of vehicle front-end structures. The outputs of the model are the dynamic responses of barrier, vehicle, and occupant, and the evaluation indexes of the impact system.

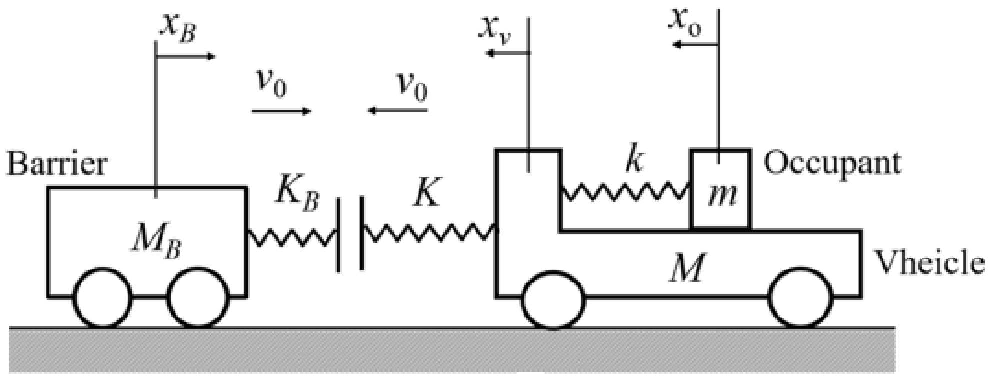

Figure 3.2: The analytic model of BVO system (D. Wang et al., 2021).

If the initial movement direction of MPDB is positive, the initial movement direction of vehicle 1 is negative. After neglecting the rotation, the momentum conservation equation between the barrier and the vehicle is:

$$(M_B - \mathrm{M}).\ V_O = (M_B * V_1) - (\mathrm{M} * V_2) \quad (3.1)$$

At the end of impact, vehicle or MPDB slow down to zero. The momentum conversion between vehicle and MPDB is divided into three cases, ignored elastic deformations, as follows:

- For large vehicle, the mass of vehicle is more than MPDB, M $>M_B$, the left side of (eq. 3.1) is less than zero. At the end of impact process, at least one of V_1 and V_2 has a speed equal to zero. Only V_1 equals zero to make (eq. 3.1) hold.
- For medium vehicle, M $=M_B$, the left side of (eq. 3.1) equals zero. So V_1 and V_2 all equal zero.
- For small vehicle, M $<M_B$, the left side of (eq. 3.1) is greater than zero. So V_2 equals zero.

Crash theory

In a head-on collision involving two vehicles, the total initial kinetic energy ($E_{k,i}$) can be determined (Lefer & Rebolloso, 2012). The mass and speed of the vehicle 1 and 2 are respectively calledm_1, V_1 andm_2, V_2.Then the initial kinetic energy is given by:

$$E_{k,i} = 0,5 \cdot (m_1 \cdot V_{12} + m_2 \cdot V_{22}) \quad (3.2)$$

From the conservation of momentum principle and assuming that after crashing the two vehicles are moving together with the same residual speed V_3 , the following equation can be written(Dange et al., 2015):

$$m_1 \cdot V_1 - m_2 \cdot V_2 = (m_1 + m_2) \cdot V_3 \Rightarrow V_3 = \frac{m_1 \cdot V_1 - m_2 \cdot V_2}{m_1 + m_2} \quad \text{……………………………} (3.3)$$

This residual speed is due to the residual kinetic energy that is equal to

$$E_{k,r} = 0,5 \cdot (m_1 + m_2) \cdot V^2{}_3 \quad \text{…………………………………………………} (3.4)$$

From these three equations, the dissipated energy used to deform both vehicles can be calculated. It is equal to the difference between the initial and residual energy.

$$E_d = E_{k,i} - E_{k,r} \Rightarrow \frac{1}{2} \cdot \frac{(m_1 \cdot m_2)}{(m_1 + m_2)} \cdot (V_1 + V_2)^2 \quad \text{……………………………………} (3.5)$$

In this study, one of the vehicles is assumed to be stationary therefore the energy that needs to be absorbed is depending on the car speed before impact (v) and the mass of both vehicles:

$$E_d = \frac{1}{2} \cdot \frac{(m_1 \cdot m_2)}{(m_1 + m_2)} \cdot (V)^2 \quad \text{…………………………………………………..} (3.6)$$

This energy is dissipated by both the deformation of the cars. The area under the force-displacement curve gives the absorbed energy of the car front structure. These curves can be extracted either from crash tests or also from the simulations. Typical force-displacement curves are shown on Figure 3.3.

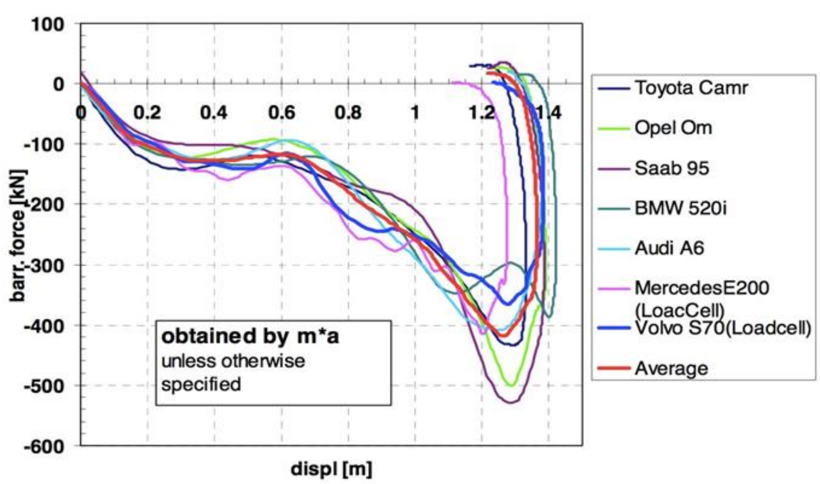

Figure 3.3: Force-displacement curves of different vehicle at 64 km/h (Lefer & Rebolloso, 2012)

Since these curves are quite complex, the car deformation can be approximated as a linear force/displacement relationship (Lefer & Rebolloso, 2012). The force reaches a maximum value, F_{max} while the displacement increases to a maximum deflection, d_{max} the energy dissipated by the car deformation can be estimated to be

$$E_{d,car\ 1} = 0.5 \cdot (F_{max}).\ d_{max} \qquad (3.7)$$

Assuming that the car 2 front structure is collapsing at a constant force level in respect to the deflection, the energy that would be absorbed by its deformation can be calculated from the equation (3.8).

$$E_{d,car\ 2} = (F_d).\ d_{\max 2} \qquad (3.8)$$

Where F_d is the constant deformation force level of the front structure and $d_{\max 2}$ the maximum deformation of car 2 front structure.

The velocities after impact may be determined with the coefficient of restitution (e). The coefficient of restitution (COR) is the ratio of speed of separation to speed of approach in a collision.

$$e = \frac{(V_2 - V_1)\ after}{(V_1 - V_2)\ before} \qquad (3.9)$$

An object with a COR equal to 1 collides elastically, while an object with a COR of 0 will collide plastically, effectively sticking to the object it collides with, not bouncing at all. The coefficient of restitution is a number which indicates how much kinetic energy (energy of motion), remains after a collision of two objects. If the coefficient is high (very close to 1), it means that very little kinetic energy was lost during the collision. If the coefficient is low (close to 0), it suggests that a large fraction of the kinetic energy was converted into the heat or was otherwise absorbed through deformation (Dange et al., 2015).

3.2 Materials

The Materials required for execution of this thesis work are given in table 3.1.

Table 3.1: Specification of Bishoftu pickup vehicle

Overview	
Model	DD1022TA
Bulletin	#240
Type of vehicle	Cargo truck
Chassis	DD1022TA
Technical Specification	
Engine model	4JB1TI
Engine power	102 hp
Engine manufacturer	Chengdu Automotive Engine Co., Ltd
Performance	
Maximum speed	120 km/hr
Capacity	
Rated load capacity	430 kg
Weight and ground pressure	
Curb weight	1740 kg
Gross vehicle weight rating	2495 kg
Axel load distribution	1190 kg / 1305 kg
Dimension	
Overall length	5350 mm
Overall width	1725 mm
Overall height	1690 mm
Cargo body length	1715 mm
Cargo body width	475 mm
Cargo body height	1455 mm
Ground clearance	200 mm
Undercarriage and suspension	
Wheel base	3380 mm
Front track	1479 mm
Rear track	1487 mm
Front overhanging	785 mm
Rear overhanging	1185 mm
Tyres and wheels	
Tyres dimension	P215/75R15, P215/75R15, P225/75R15, P225/75R15

3.2.1 Tools

Various software's are used as a tool for designing, modeling and analysis are also given here.

CATIA

CATIA (Computer-Aided Three-dimensional Interactive Application) software is a complete multi-platform solution for computer-aided design (CAD), computer-aided manufacturing (CAM), computer-aided engineering (CAE), PLM and 3D. Developed by the French company Dassault Systems, the software is ideal for creating solids, surfaces, assemblies, drawings, fabrication and analysis. platform software suite for computer-aided design, besides being used in a wide range of industries from aerospace and defence to packaging design (Aysha, 2020).

LS DYNA

LS-DYNA is an advanced general-purpose multi-physics simulation software package developed by the former Livermore Software Technology Corporation (LSTC), which was acquired by ANSYS in 2019. LS-DYNA is a general purpose transient dynamic finite element program capable of simulating complex real-world problems. It is optimized for shared and distributed memory UNIX, Linux, and Windows based, platforms. It is an explicit 3-D finite element program for analyzing the large deformation dynamic response of the elastic and inelastic solids and structures. The program is extensively used by many top automobile, aerospace and research organizations. A wide range of material types and interfaces enable the efficient mathematical modeling of many engineering problems(Livermore Software Technology Corporation, 2003).

It contains more than one hundred and fifty material models including metallic, non-metallic and composite models which enable to define any material in the real world. The contact capabilities such as contact between deformable bodies, between deformable and rigid bodies provided in LSDYNA can solve any contact problems which very useful in crash testing (Livermore Software Technology Corporation, 2003). The code's origins lie in highly nonlinear, transient dynamic finite element analysis using explicit time integration.

"Nonlinear" means at least one (and sometimes all) of the following complications:

- Changing boundary conditions (such as contact between parts that changes over time).

- Large deformations (for example the crumpling of sheet metal parts).
- Nonlinear materials that do not exhibit ideally elastic behavior (for example thermoplastic polymers).

"Transient dynamic" means analyzing high speed, short duration events where inertial forces are important. Typical uses include:

- Automotive crash (deformation of chassis, airbag inflation, seatbelt tensioning)
- Explosions (underwater Naval mine, shaped charges).
- Manufacturing (sheet metal stamping).

3.3 Methods

In order to address the general and specific objectives of this thesis work a well-designed methodology will be followed. Various steps included in the methodologies are listed below and summarized in figure 3.5. Among the procedures the modeling and analysis stage have a more detail explanation and it is stated in detail on chapter four.

I. Literature review

Literature survey about vehicle structural response during impact load are the key methodology of this thesis work that will help to about what others done and identified, where the limitations does exist so that this work will be based on the research gap. Latest reviews and research work in area related to development, modification, design and analysis of BPV is collected and surveyed.

II. Data collection

In order to do the Numerical analysis, the necessary data about the existing Bishoftu pickup vehicle is collected. The necessary data will be collected by using primary data collection methods like questionnaires, interviews and secondary data collection through visiting various websites, journals, books and so on. Methodology of BPV which can also help in developing or modifying structural crashworthiness of BPV, the data are presented as follow:

- From Bishoftu Automotive Engineering Industry

The details of technical specification and necessary data of the existing Bishoftu Pickup vehicle has been collected from the company Bishoftu Automotive Engineering Industry. All the necessary information of Bishoftu Pickup vehicle is already showed in Table 3.1. In addition to this, when dealing with crashworthiness, the mass of the vehicle parts plays vital role. The load distribution of the Bishoftu pickup vehicle which are critical for the crash analysis were listed above on Table 3.1.

- From federal transport minister

The number of registered vehicles data in Ethiopia as a whole and as well as the number of specified available vehicle in every region in Ethiopia is collected from federal transport minister, and the data's are listed in Appendix –D.

- From federal police commission

The general road traffic accident data in Ethiopia and details of regional accident shares is collected in federal police commission. In addition to this number of human loss and also material losses are also collected on there for more, it is shown in Appendix –D.

III. Concept Generation

The concept generation process results a set of productive concepts from which we make the final specification and design. Different concepts towards the crashworthiness improvement of Bishoftu pickup vehicle structure is generated. This includes safety development concepts and structure modification methods. Figure 3.4 shows the concept for engineering approach.

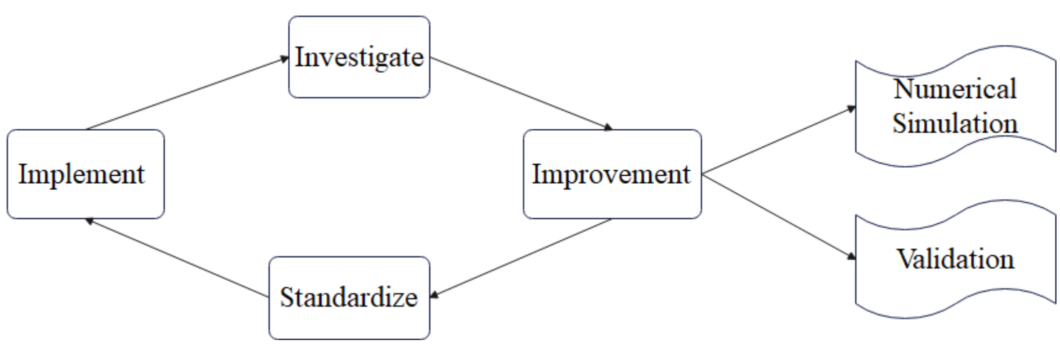

Figure 3.4: Approach to engineering research

IV. Modelling and Analysis of the existing model

The 3D modelling of parts and then assembling process of the Bishoftu pickup will be done by CATIA V5 and finally, mechanical simulation is done by CATIA V5. After finishing the 3D modeling of the Bishoftu pickup then analysis of crashworthiness will be carried out by LS DYNA software.

V. Modification Analysis

After carefully observing the crashworthiness behavior of the existing model, modifications and designs were made on critical parts of the vehicle. Then the modified parts were analyzed separately.

VI. Discussion

At this stage, the response of modifications is examined using engineering analysis and discussions. If the result were satisfactory the next stage of the research will take place but if not, the modification is to be re-designed and repeat the steps.

VII. Design and Analysis of the new model

The safety development or modifications which increase the crashworthiness of vehicles are fitted in to the existing model and further analysis is made using LS-DYNA. After that the numerical comparison between the existing model and modified model is done using different crashworthiness parameters such as energy absorbing ability, impact force, deformation and so on.

VIII. Verification

Without experimental data, the appropriateness of the values obtained on a computational model accurately represented by verification process. In case LS DYNA simulation, verification can be made by checking the quantity of energy balance, deformations, kinematics, kinetics and other quantities (Gulavani et al., 2014), the most common and logical ways are listed below:

- Energy balance
- Energy Ratio
- Ratio of Hourglass energy (HE) to Total energy (TE)

Energy Balance Curve

The energy balance of a system in an impact is governed by the law of conservation of energy. According to the law of conservation of energy, Energy can neither be created nor be destroyed, but it can be converted from one form of energy to another form. Applying the same principle to crash analysis, the amount of kinetic energy lost during impact must be converted to other forms of energy such as internal energy, sliding energy, hourglass energy and other forms of energy like heat energy.

Kinetic energy is the work input and internal energy is the work output. Internal energy is the energy absorbed by the system and is directly proportional to the product of force and deformation. It is also noted that, there may be negligible errors in calculating energy ratio because all the processes in this universe are irreversible and some losses are always included which deviates energy ratio slightly from one.

- The total applied energy should be constant throughout the simulation.
- The kinetic energy should be decreasing and internal energy should be increasing; and ideally the sum of kinetic energy and internal energy should be equal to total energy.
- The Hourglass energy should be less than 5% of total energy.

Energy ratio

The energy balance for an explicit time integration scheme is given by:

$$\underbrace{E_i + E_s + E_d + E_{ke} + E_h}_{\text{Total energy}} = \underbrace{W_{ext} + E_i^0 + E_{ke}^o}_{\text{initial total energy}} \quad \ldots\ldots(3.10)$$

Where: E_i : internal energy; E_h : hourglass energies

E_d : damping energy; W_{ext} : work done by the external forces

E_{ke} : kinetic energy, E_S : interface sliding (dissipated contact energy)

And the superscript 0 denotes the initial values.

The total sum of energies in the left-hand side of the equation represents the total energy of the system, and terms on the right-hand side of the equation represent the initial total energy plus the work done by the external forces (W_{ext}). The ratio of the ‘total energy’ to the sum of ‘initial total energy' and 'external work done 'is called the energy ratio. The energy ratio is also known as the 'energy balance'.

$$e = \frac{E_i+E_s+E_d+E_{ke}+E_h}{W_{ext}+E_i^0+E_{ke}^o} \quad (3.11)$$

An energy ratio with value of equal to 1 shows more stable and reliable FEA result, but most of it is difficult to achieve such value. This is due to the modelling error which may increases or decreases the total energy(Livermore Software Technology Corporation, 2003). There are two causes which can be considered when checking the energy ratio:

If e>1, which mean that artificially energy is added in the model and rises the total energy values, as a results instability occur, most of the time the rises of total energy is due to a numerical instability or through initial penetration.

If e<1, which indicates that the total energy reduces because of artificially absorbed energy, either by excessive hour-glassing or during stabilization of an ill-conditioned contact surface.

Generally, energy ratio simply is different from unity, and then there are high probability. Since it is difficult to obtain energy ratio equal to unity so, the acceptable value of the ratio is 1.00 +/- 0.07 the discrepancies in the ratio are due to spurious energy produced in the system and simulation error.

Ratio of TE/HE

Through analyzing the energy curves, the verification of the finite element model can also be determined using the ratio between the total energy to hourglass energy. Hourglass energy can cause a zero-energy model. If the hourglass Energy is less than 5% of the total energy, the finite element model is reliable (Gulavani et al., 2014).

The above-mentioned verification method is implemented at each simulation results report. The accuracy of the FEA model is checked by examining the different pattern exhibited by the simulation results. Following checkpoints are considered for simulation.

1. The results of Simulations of existing BPV frontal and side impact for respective simulations are imported and discussed.
2. The analysis results of the modifications are presented.
3. The results of Simulations of modified BPV frontal and side impact for respective simulations are imported and discussed.

At each section the main parameter which are going to be examined are the energy balance, absorbed energy, impact force, deformations and structural response.

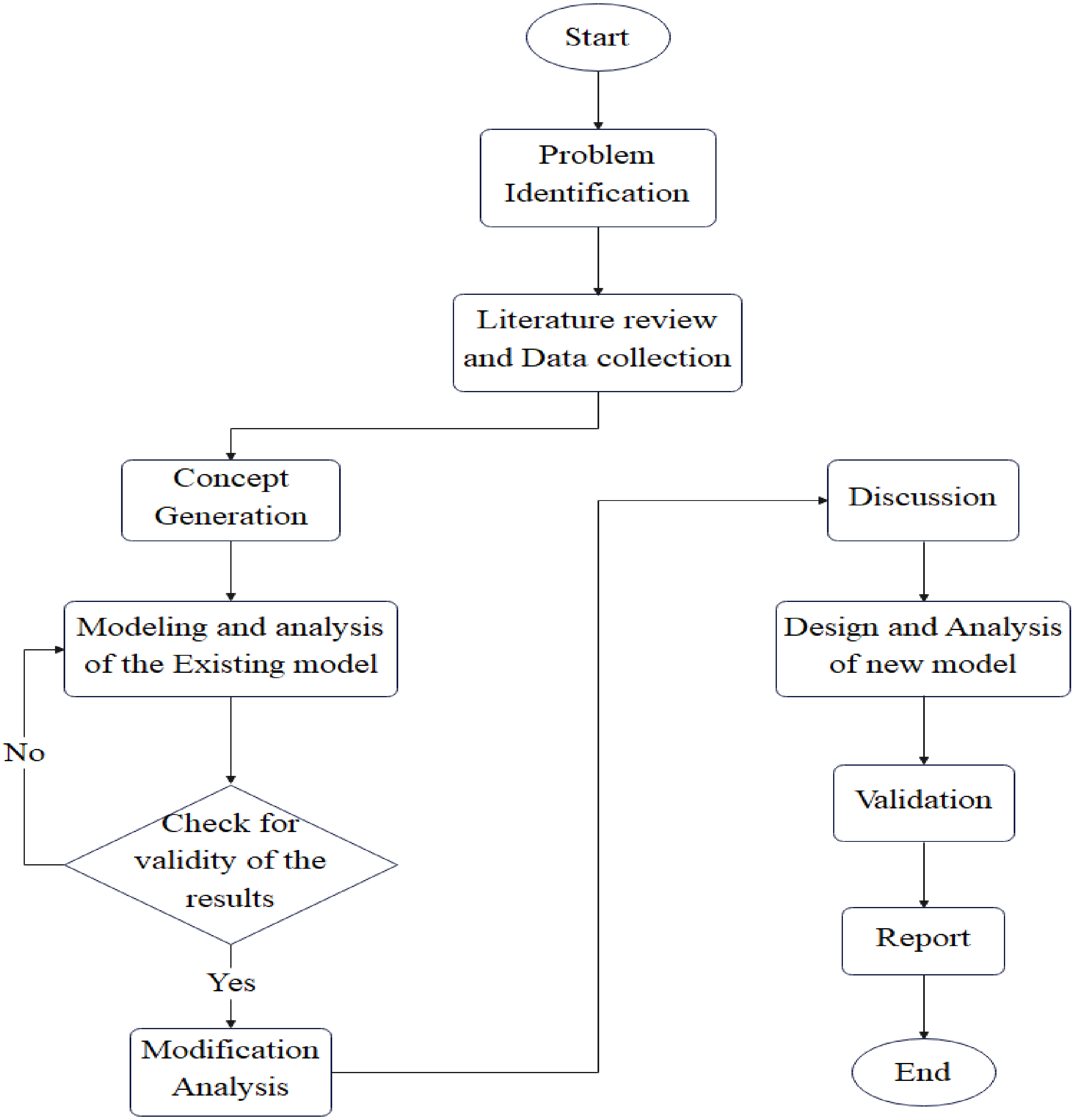

Figure 3.5: Research methodology

CHAPTER FOUR

MODELING AND ANALYSIS

Under this chapter the method used for analyzing and modifying the existing Bishoftu pickup vehicle are discussed. The work flow used were shown in Figure 4.1. These steps were used on the analyzing frontal and side impact of the existing and modified model.

4.1 Work flow of modeling and analysis

In performing the design and analysis of the Bishoftu pickup vehicle, CATIA V5 is used for modeling and then model was imported in to LS DYNA. Surface cleaning, meshing and other parameters of the model is done using LS DYNA workbench on LS-PREPOST. The crash analysis is being done in LS DYNA post process. The detail of each of the steps is mentioned on the figure 4.1 below.

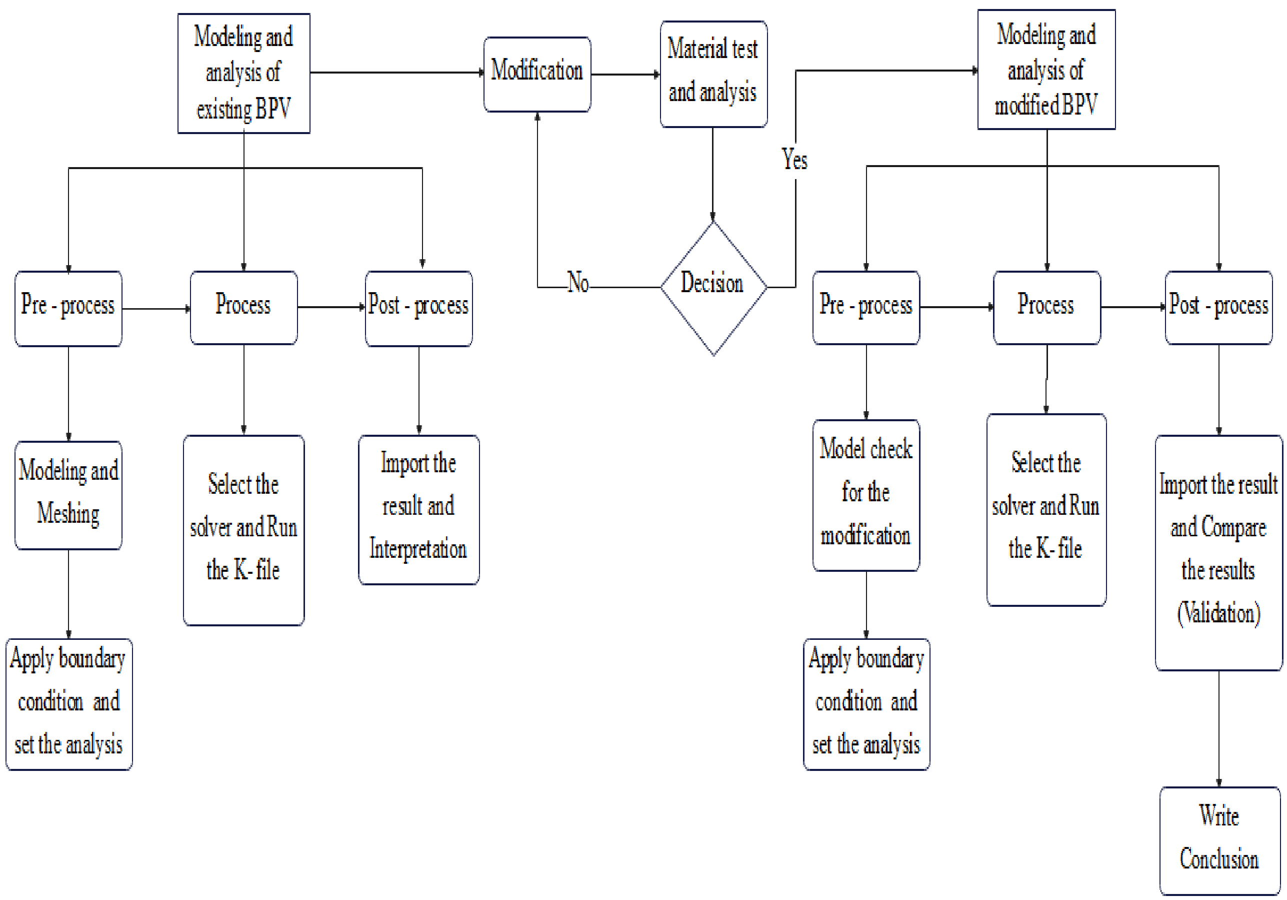

Figure 4.1: Work flow for modeling and analysis

4.2 Modeling and analyzing of the existing structure

4.2.1 Modeling of BPV

Geometry model of Bishoftu pickup Vehicle is modeled based on specification obtained from data collection on BAEI. Before attaching the geometry to LS DYNA, several steps are performed during modeling in CATIA V5. Sketcher is the initial stage of modeling in which the basic profile or part of the BPV. After that, the surface is generated, and the corresponding extruding (pad) thickness was given for each part. Finally, the parts are assembled for checking for dimension error. The parts were named separately in CATIA; these steps are shown on Figure 4.2, and the lists of parts modeled assembled are listed below:

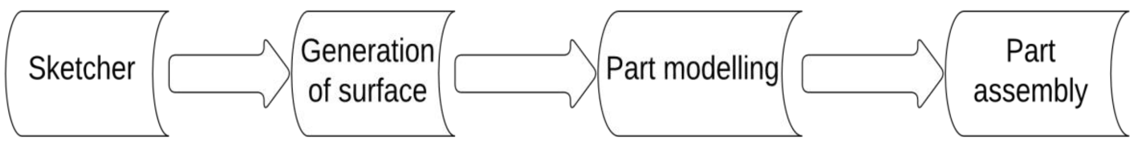

Figure 4.2: Modeling procedure

1. Front body structure: consists of bumper, hood, fenders, head light and others.
2. Cabin: it is driver compartment consists of dashboards, gauges, steering linkage and others.
3. Chassis and wheels: support the weight of whole vehicle and occupants and includes all front and rear suspension components and linkages.
4. Engine and other Components: this is modelled to consider the mass and space of the engine, gas cylinder and other missing rear parts including the mass of the occupants.
5. Rear body structure: covers the rear parts and used as carrying materials (luggage compartment). The modeled parts are shown on figure 4.3.

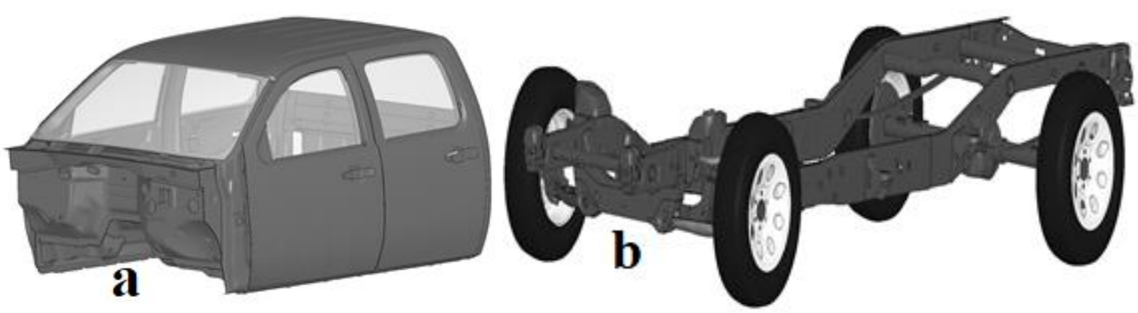

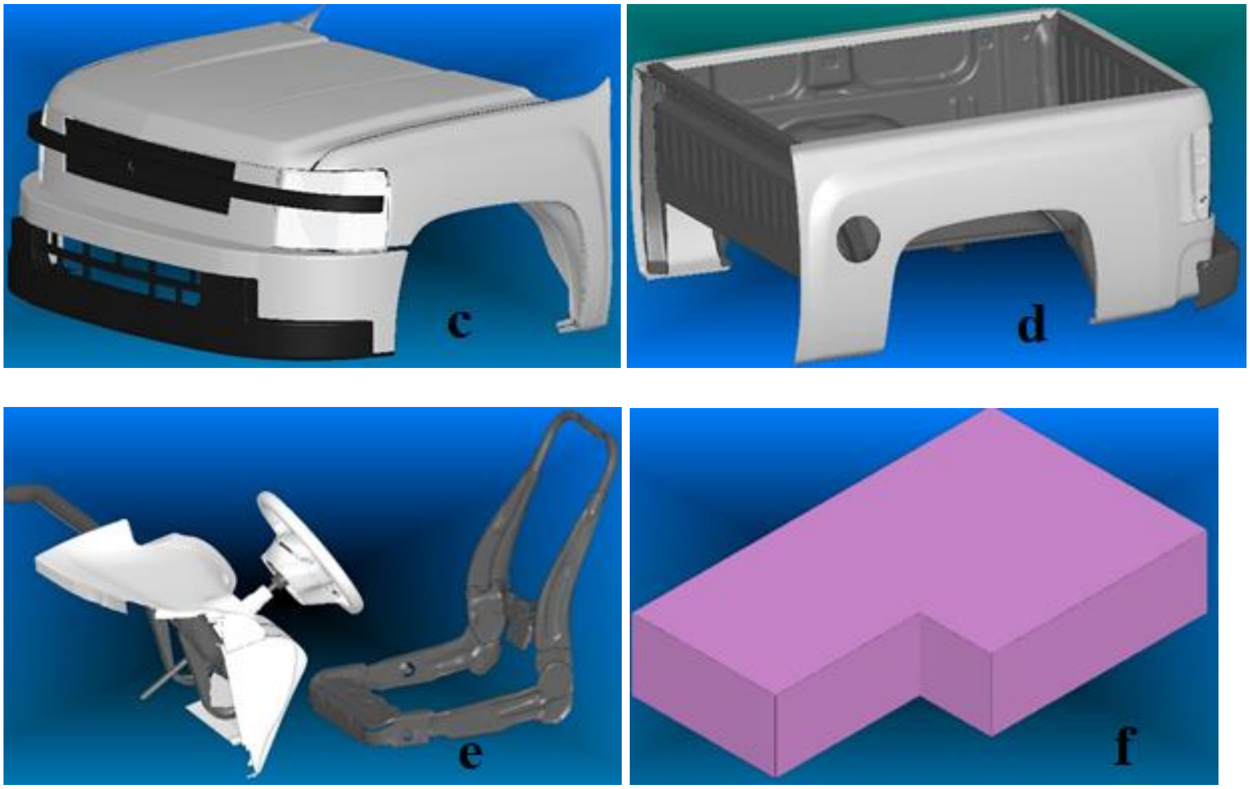

Figure 4.3: Model components of BPV (a) Cabin (b) Chassis and wheels (c) Front body structure (d) Rear body structure (e) Dashboard and seat (f) Engine and other missing parts

After modeling the above main components, the next procedure is to assemble the separated components in to one full model. The assembled 3D modeling and the real vehicle structure is shown on Figure 4.4.

Figure 4.4: (a) Isometric view of Bishoftu pickup vehicle model and (b) the real vehicle

4.2.2 Model check

After modeling the next step is model checking, Getting the Model 'Right' or model Checking consist of three basic stages and these are before, during and after analysis as shown in figure 4.5.

- Pre-analysis checking: Any checks to do before running your analysis in LS-DYNA.
- Checking during the analysis: Any checks you may want to do whilst the model is running.
- Post-analysis checking: Checks on your models after the analysis is complete. This includes feedback to access initial model data.

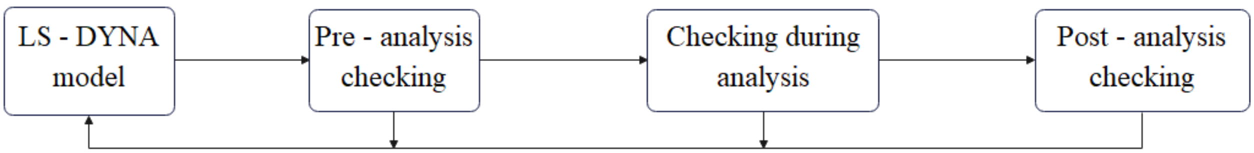

Figure 4.5: Model checking procedures

Pre-analysis checking

Before meshing: the Computer Aided Design (CAD) of the pickup model was converted by CATIA V5 software in to an Initial Graphics Exchange Specification (IGES) or STEP model. Then, the model was checked for whether modeling errors are available or not. Duplicated surfaces, unwanted lines, edges and part to part penetration etc., are checked and removed from the imported model on LS DYNA geometry tool. The next stage is to move the model to ls dyna pre-post meshing and for further deep checking's, LS dyna Pre-Analysis Checking includes:

- Checks on curves referenced by particular material types.
- Rigid body constraint clash checks.
- Tied (or not tied) contact checks/penetration checks.

Check for element quality, shell normal and crossed edge

Incorrect values in certain fields (for example a negative value when this is not valid). This errors usually leads to usually errors like the above will result in LS-DYNA not running, and a termination so when running in LS-DYNA it is important that the issue is picked up at the pre analysis checking stage, as it may go unnoticed. Normal check is for reviewing and reversing shell, segment, and thick shell normal. Consistent normal in a part may be required to meet mesh quality standards, for contact definitions in LS DYNA. After checking those, the next thing to do is to ensure that no crossed edges existed. The case where an edge of an element crosses another shell element mid surface, or face on a solid element, is not a penetration in a classical sense in LS-DYNA. But these mesh errors might lead to severe problems when running an analysis in LS-DYNA so, it is very important that such modeling is avoided (Redscan, 2017).

Check for Penetration

Initial penetration is a term used frequently to describe the amount of penetration that exists between a node and its closest master segment (in the case of classic node/ segment treatment) or between two interacting segments (in the case of `segment-based` treatment) during the initialization of the problem. The most obvious recommendation would be to have no initial penetrations at all. However, this is rather difficult due to the nature of the model building process and the number of design changes that usually occur during the course of the product lifecycle. Penetrations are checked for shell, beam and solid elements in LS DYNA, Penetration check by Parts and check by contact (LS-DYNA Support Site, 2022). Figure 4.6 shows penetration check by part. The arrow shown on the model shows the penetration and the magnitude is shown on the vector plot at right side of the model.

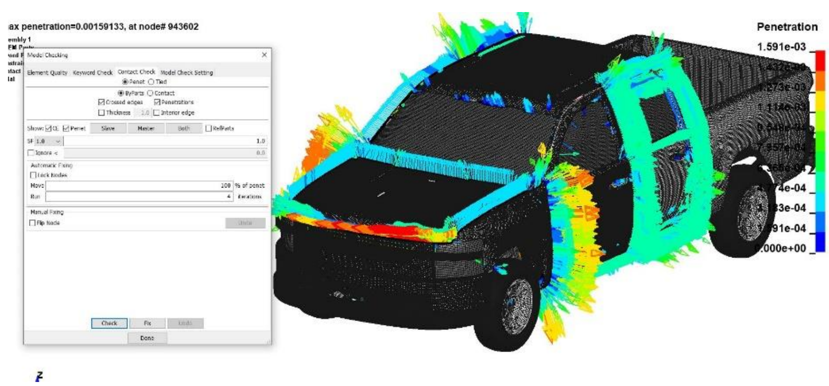

Figure 4.6: Initial Penetration

Penetration check by contact: By selecting a contact from the list of defined contact in the model, the elements included in the contact are displayed and the check is performed by taking care of all parameters that affects the contact thickness (SST, MST, SFST, SFMT, SHLTHK, SLDTHK, SSTHK, OPTT, SFT, TH, THSF) and which nodes/elements is to be checked against penetration to which elements.

Keyword check

Another way to tackle problems on the modeling process is to look for keyword check. The model is checked for keyword input error such as section, material, contacts and constraints. Figure 4.7. Shows the Model keyword report in which all the errors are removed and left with some warnings.

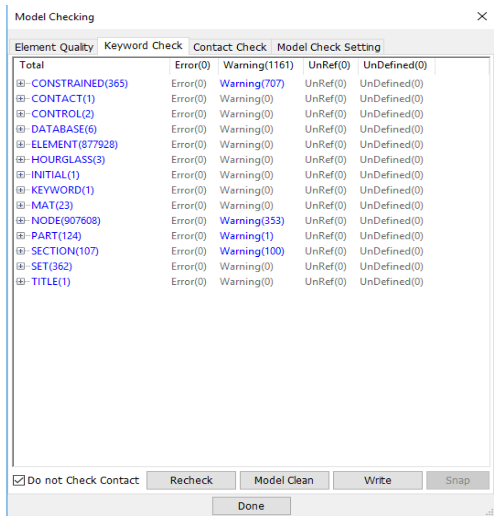

Figure 4.7: Keyword checks

During analysis

Under this section, penetrations and modeling error etc., were reported. So that a user can fix the problem by reading Warning in message file or on the running LS DYNA command window. Figure 4.8, shows the reported warning message. It reports the penetration detected between the ground and tire.

Figure 4.8: Warning during analysis

Post-analysis checking

Post-checking provides information about the model deformations, energy balance and other results. The deformations can also be reviewed from the test video. This information is useful for model checking especially for those parts with large permanent deformations. Although the relation of energy balance, hourglass energy and energy ratio is also checked. On this thesis work these checks are presented on result and discussion chapter.

4.2.3 Mesh generation

Mesh generation includes mesh type, size and geometrical attributes. There are three different mesh types, 1D, 2D and 3D, relevant to element dimension. Mostly, pickup components were a shell element, which means that the length and width of the structure is considerably larger than its thickness. Therefore, auto mesh type was used. The Bishoftu pickup vehicle geometry was meshed by LS DYNA software using mixing of linear quadrilateral 97.9% and triangular elements 2.1%. The element size for the whole model between 3mm and 7mm. The total number of elements for the whole meshed model were 1,154,037 and node 1,188,194. So, the whole meshed model is very complex and computationally “expensive”, see Figure 4.9.

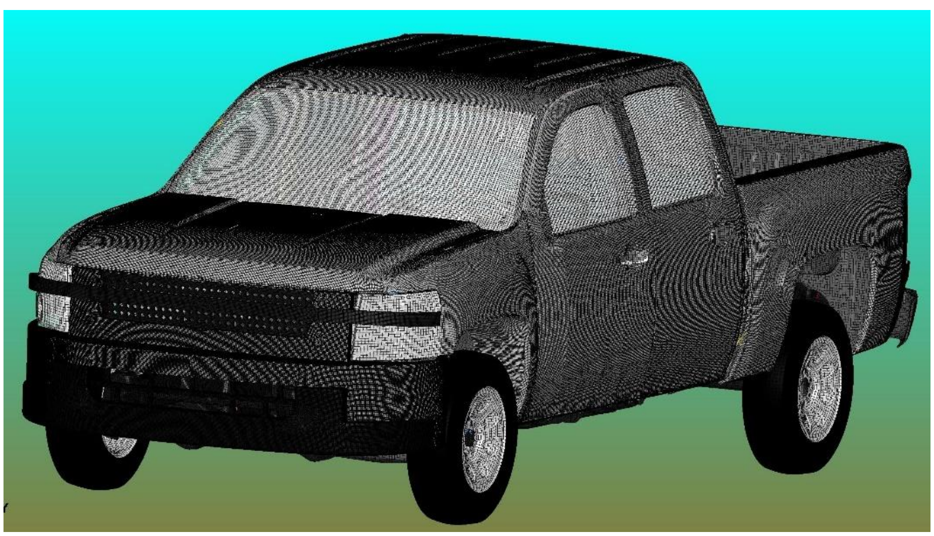

Figure 4.9: Meshed FE model of the pickup vehicle

4.2.4 Analysis setting

Material Definition

Vehicle material types and properties are the most important factors, which effect significantly the accuracy of the impact simulation. Moreover, material types and properties should fulfil the automotive criteria, such as safety, environment, lightweight, fuel consumption, cost and design. Mostly, the vehicle model consists of shells, which need to identify thicknesses for every single shell besides mechanical material properties.

Table 4.1: Material mechanical properties for vehicle part set

Vehicle parts	Mass density (kg/m^3)	Young's Modulus(Pa)	Poisson's ratio	Yield Stress (Pa)
Vehicle structure	7890	2.13e+11	0.28	2.45e+8
Bumper	2700	7.0e+10	0.33	2.76e+8
Chassis	7850	2e+11	0.26	2.50e+8
Windscreen	3150	7.39e+10	0.22	1.380e+08
Tire	1510	3.00e+09	0.45	

The vehicle components materials were selected by the ls-dyna material library. The keyword used for tire was modeled by MAT_ELASTIC. While MAT_PIECEWISE_LINEAR_PLASTICITY was used for windscreen, chassis and vehicle structures. Since some parts are not subjected to deformation so they were modeled by MAT_RIGID, these are axles, wishbones and engine components representation. Most vehicle components thicknesses were defined by section shell and the rest with solid element. For shell elements the value of the thickness is determined based on their density and mass value listed on above data collections. The material mechanical properties and shell thicknesses of the vehicle components are shown in Table 4.1 and Table 4.2.

Table 4.2: Thicknesses of the vehicle component

vehicle component	Thicknesses(mm)
Vehicle structure	1
chassis	4
Windscreen	4
Tire	7

Missing Components

To simplify the model, several of the components of the car were not modeled, but rather were represented as point masses and rigid bodies. The components acted mainly in series progressing from the front of the car through the middle to the rear, all interconnected to each other. This component representation was done to preserve the inertial properties of these components, which would be very important to create an accurate impact simulation of the BPV. These point masses were created in LS-DYNA by creating a single node on the part, and adding a mass using ELEMENT_MASS and the node is connected to any of the rigid part in the model using *RIGID TO RIGID. Masses were at both of the front wheels to represent the mass of the engine, transmission, brake, and steering assembly and also occupant masses. Mesh was only added for visualization purposes. This mass part is applied on the center of mass of the vehicle.

Element Formulation

This paper mostly uses 'fully integrated shell element modified for higher accuracy' element formulation, and some of them are default element formulation. Belytschko-tsay element formulation is used for default type shell element with 3-point integration point and 'fully integrated S/R solid' for solid elements.

Constraints

After meshing the individual parts, interactions have been defined between them. These interactions are defined between the surfaces of different parts and control the transmission of forces and moments between individual members. Kinematic joints have been defined for different parts of the vehicle. In LS-DYNA, the constraint between two deformable parts was given by the keyword CONSTRAINED_NODAL_RIGID_BODY in Entity creation. Also, to connect rigid to deformable body CONSTRAINED_GENERALIZED_WELD_SPOT is used, and constrained RIGID BODIES is another keyword used to connect rigid bodies with another rigid body. In addition, JOINT_REVOLUTE was used to constrain tire with the vehicle components.

Contact Definition

The contact between two parts is given to prevent penetration during the crash. There are a lot of contact types are available in the keyword manager. In this case, the contact is directly in within the components of the BPV like chassis, the front portion, cabin, etc., and between the road and the tires, between the impacting surfaces (BPV and external part) and various parts of the BPV. In order to define the interaction between different parts of the BPV, a set of parts (PART_SET) is defined then, the keyword CONTACT_AUTOMATIC_SINGLE_SURFACE used, and for defining two different objects like the vehicle and the ground and also the vehicle and the impacting surface, then the keyword CONTACT_AUTOMATIC_SURFACE_TO_SURFACE is used. The master and slave parts are listed in Table 4.3.

Table 4.3: Master and slave parts

Contact type	Slave	Master
Automatic surface to surface	Tire	ground
Automatic surface to surface	BPV	External part
Automatic single surface	Whole vehicle	non

4.2.5 Boundary Conditions and Simulation environment

The function of the boundary conditions is to create and define constraints and loads on finite element models. To simulate a full vehicle crash, all loads and boundary conditions that occur in the actual crash event need to be modeled. Just as a vehicle is subjected to gravitational loads in real life, the simulated model should have a representative gravity force applied. Friction forces between the tires and the road surface play an important role in how the vehicle behaves on impact, so these have to be accounted for in the simulation. A velocity has to be applied to the vehicle in a manner as to not impart any unrealistic acceleration or cause the simulation to run for an extended amount of time. Fortunately, Ls-Dyna provides methods to simulate all of these requirements(Liu, 2013a). In this section the setups for the simulation of front and side impact test will be presented. The Boundary condition and set up follows the standards indicted on literature. The detail of set ups and boundary condition in each of the crash scenarios are presented as follows.

Case 1. Frontal Impact

In front impact test, the BPV is crashing with a rigid wall which is stationary on opposite side with the pickup that has a speed of 60 km/h and the main purpose is to clarify the damages to BPV front body structure. Figure 4.10 shows front impacts SET UP is in three different views which we will analyze in the following section.

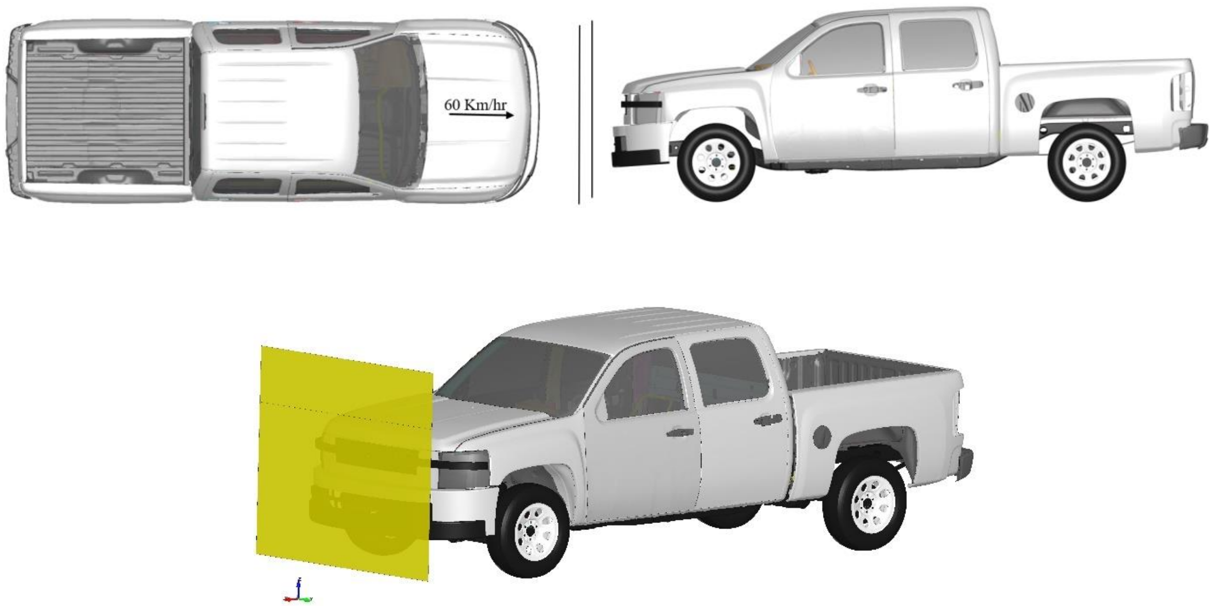

Figure 4.10: Simulation set ups and boundary condition of frontal crash

To simulate the Frontal impact, the BPV vehicle is subject to an initial velocity of 60 km/h and along the horizontal direction towards the rigid wall. The simulation is adjusted to 160ms.

Case 2. Side pole impact

In this test the Bishoftu pickup vehicle impacts the rigid pole laterally at a speed of 32 km/h as stated on NCAP test protocol, its line of forward motion forms an angle of 75 degrees with the vehicle’s longitudinal axis, simulating a real-world crash in which the vehicle hits a tree while sliding on the road. The rigid pole is a vertically oriented metal structure with:

- Diameter of 254 mm.
- Beginning no more than 102 mm above the lowest point of the tires on the struck side of the fully loaded test vehicle.
- Extending at least 150 mm above the highest point of the roof of the test vehicle.

The direction of vehicle motion is such that the pole is always aligned with the CG of the head of the driver (Singh, 2012). The LS-DYNA set-up for the side impact crash test of the BPV model with a pole is shown in Figure 4.11.

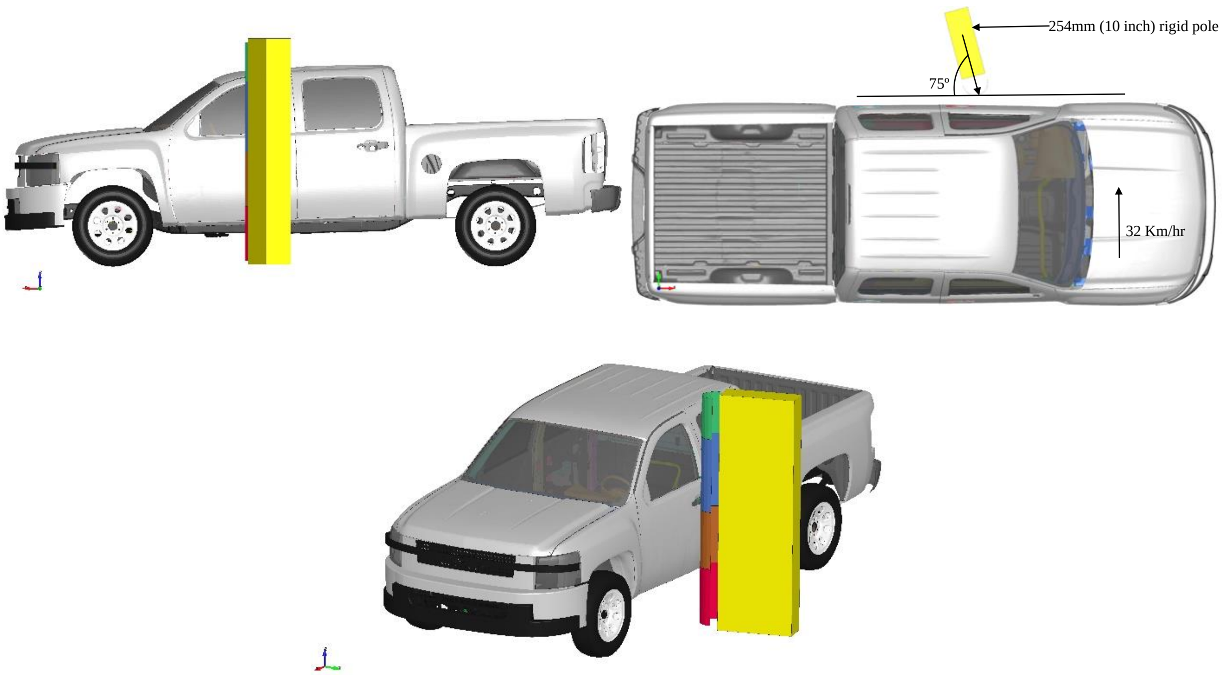

Figure 4.11: FEA set up for Lateral (side crash) Test

Control Simulation

Solution control has a significant influence on simulation stability and accuracy. CONTROL_TERMINATION was used to define the simulation termination time. It is used to control the time step and run time of the file. These cards are necessary to control the duration of simulation time. Run time of the key file is 160 ms (0.16 s). The results are plotted for the energies absorbed by the parts within 1 ms interval. DT min is the interval in which the codes are generated in processing the file in ls-dyna. It is the minimum time taken by the sound wave for travelling from one end to other of the shortest element. It is also used in plotting the graph i.e., for every 0.001s interval a point on the graph is plotted. Decreasing the value below 0.001s increases the smoothness of the curve but at the same time increases run time.

Other control cards are defined, these are control are:

- CONTROL_ACCURACY: control parameters that can improve the accuracy of the calculation.
- CONTROL_CONTACT: Change defaults for computation with contact surfaces.
- CONTROL_ENERGY: Provide controls for energy dissipation options.

- CONTROL_HOURGLASS: control zero energy formation.

Database options

Database options are given to obtain the output i.e., to generate results and to interpret plots. Database was used to define the expected results using American Standard Code for Information Interchange (ASCII) to define specific functions such as NODOUT, JNFORC, JSTIFR and DEFORC (Kunle et al., 2019). Generally, they are used to analyze the energy absorption characteristics that are discussed in next chapter on result and discussions. Some of the database plots used are:

- D3PLOT (database for complete output states and some default results)
- D3DUMP (complete database for restart when interruption occurs on running due to power or other)
- ASCII options (absorption energies (GLSTAT), material energies (MATSUM), wall force (RWFORC), Resultant contact forces (RCFORC) and so on.

4.3 Modification on the existing Bishoftu pickup vehicle

4.3.1 Introduction

For years now, the vehicles safety has become more and more important in the car development. The WHO has synthesized evidence-based measures called SAVE LIVES that can significantly reduce road traffic fatalities and injuries. Among the 6 strategies listed to reduce injuries and deaths from road crashes the first Standards states that, at event of frontal and side impact the vehicle should with stand a frontal or side impact crash and protect the occupants when tested at specific speeds (Desapriya, 2011). By keeping that in mind modification were made for the pickup vehicle. Generally, modifications are done by vehicles owners to give them a distinctive appearance, to improve their performance, to add desired features, change the engine (alternate or replacement engines), suspension, or to add a long-range fuel tank. Others modify their vehicles, so that they are better suited to a specialized purpose. In another hand, Excessive modifications can affect the road handling of the vehicles, such as, it may distract the original vehicle stability, fuel consumption due to addition of too much weight and other safety regulations which may result in wrong side of the law and perhaps insurance company. So, staying safe and legal is extremely important when modifying car. So that the improvement which were going to made on BPV should meet the following additional criteria:

- The vehicle must not have any rust or deficiencies in the areas to be modified or in the areas already modified.
- The vehicle must be structurally sound, without need of mechanical repairs and able to support/accommodate the needed adaptation (For & Vehicle, 2021).
- Do not affect the level of safety, strength or reliability of vital systems, like brakes steering and occupant protection systems.
- Have little or no impact on the vehicle's compliance with mandatory vehicle standards.

4.3.2 Safety Concept

The first thing to consider when making the modification is the occupants should be extensively protected from direct contact with obstructions and free from uncontrolled flight. To achieve this goal, the car body structure is also designed to be as safe as possible with some crashing zones to absorb energy but also a stiff protective cell for the occupants so called safety cage, the aim of this section is to modify and design BPV body structure as safe as possible with some crashing zones to absorb most of the impact energy but, also a stiff protective cell for the occupants. Here the intention is to achieve this aim by means of an energy absorbing component (deformation elements) of stable frame structure. The modifications were based on the study done on previous section of the existing model. The study indicates that small design changes could significantly enhance safety of BPV occupants. The location in which the modification was fitted are shown in Figure 4.13, and mountings is based on the study done on the existing model. The BPV is fitted with two main energy-absorbing zones, these were front and side parts of the BPV, see Figure 4.14.

The added energy absorbing parts are designed in order to have a controlled deformation. This deformation is used to absorb the maximum kinetic energy during a crash. This deformation zones not only absorbed the kinetic energy of impactor, but also the kinetic energy of the BPV itself, for example when the BPV fully crashed into full into a rigid wall. The beam element was act as a bumper and designed in such way that are capable of deformation and together with other linkages. The front bumper has functionality of reduce kinetic energy, minimizing the stress on the drivers and occupants' body. It should deform and absorbed the impact energy without affecting the occupants. By doing so they will significantly help during collisions of the BPV. In addition, the side door beams have been designed to meet the requirements of beams at event of side crash. They absorbed the side collision energy, reduce intrusion in to the BPV and reduce the force of impact transferred in to the occupants.

Figure 4.12: Existing structure before modification

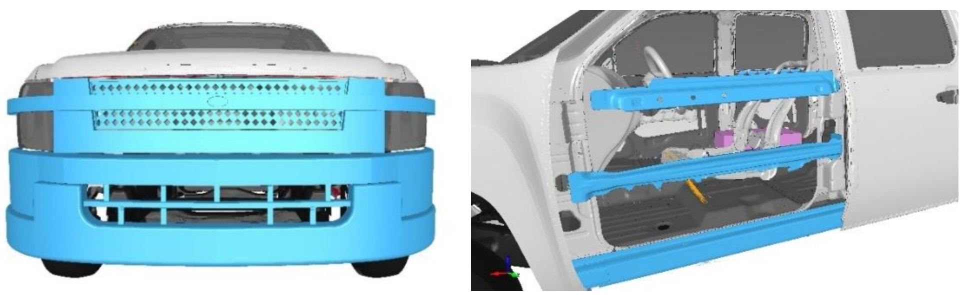

Figure 4.13: Modified BPV model parts

Stable frame structure

Maintaining the safety required to protect the driver and occupants makes high demands on the frame structure, particularly in the case of serious accidents. The final 3D model of the modified BPV is shown on Figure 4.14 below, in addition to the above safety concept, the new model has the same fuel consumption with the existing BPV because the total mass of the new model was made the same with the exiting by introducing the use of lightweight material. Since modifications were done symmetrically so the stability of the vehicle is not also affected by the modifications.

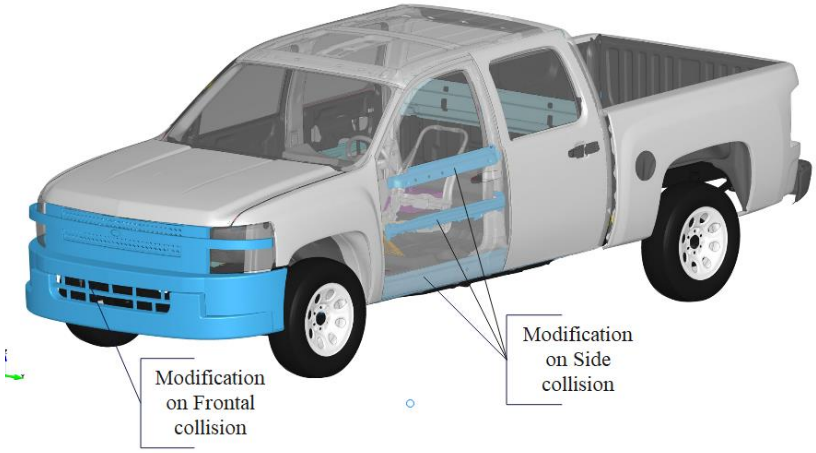

Figure 4.14: BPV isometric view of the modification

4.4 Bumper and Beam design

To improve the performance of vehicles at event of crash many technological developments is needed towards designing a successful lightweight and good energy absorbing unit. During crash, the energy absorbing members of the vehicle are expected to fold progressively, so as to absorb more energy and to ensure enough passenger space (Srikantha et al., 2017).

Automobile bumper and side door beam is a structural component or part of vehicle, which is mounted at the front and side (side doors) of the vehicle for improving crashworthiness or occupant protection during both crash cases. In low-speed collision, it used to prevent or reduce damage to the vehicle by absorbing the shock or impact forces. Most of the time, they are not designed as structural components that would significantly contribute to vehicle crashworthiness at high speed. Several design factors are considered on selecting a bumper and beam. The most important factors are:

- The ability of the system to absorb shocks or impacts.
- To stay intact at high-speed impacts.
- Weight, manufacturing process ability and cost are also the factors in design phase.
- Both initial cost and repair cost are also important.

Based on reading of a number of published papers, a summary is drawn that materials with different thicknesses can gain different crash performance. So, the purpose of this section is to check the performance between 0.886 mm and 2 mm thickness and select the best material thickness for the side beam. For the front bumper from 50 – 70 km/hr is checked and select the best speed for the front bumper of the vehicle, and to check the selected material strength, energy absorbing capabilities and deformation by varying the thickness and speed of the cross section.

4.4.1 Bumper and Beam material

On different surveys, it was observed that the performance of the bumper and beam at event collision is greatly depending on the material used. If it is properly selected, it produces a great impact on the vehicle performance by minimizing the weight (high fuel efficiency) without sacrificing the strength. Since, most of the fuel consumption (75%) due to the weight of the vehicle. It is also mentioned that, 6%–8% increase in fuel economy can be realized for every 10% reduction in weight (Tie Wang & Li, 2015). So, the use of Lightweight and good crash performance material will provide opportunities for reducing vehicle weight, thus increasing fuel efficiency and reducing emission of harmful pollutants. So, for the front bumper closed cell Aluminum foam and for the side door beams advanced high strength steel (AHSS) DP 980 steel material are taken into consideration to achieve the required performance. The advantages of Aluminum foam for automobiles are;

- High strength and stiffness to weight ratio
- Corrosion resistance
- Withstand great damage
- Light weight
- Can be made into complex geometrical forms easily
- Extremely strong and can absorb great deal of mechanical energy

Advantages of advanced high strength steel (AHSS) DP 980 steel material:

- Good crash performance
- Light weight as compared to conventional steels
- Cost effective solution

Aluminum foam is a material made from aluminum, which is also populated with a large volume of pores or cavities. It is a solid material filled with pores such that up to 95% of the volume consists of gas-filled voids, in two different kinds of structures. The pores can be sealed from each other (known as closed-cell foams) or can form an interconnected network (open-cell foams). It is both extremely durable and lightweight, with a large surface area to volume ratio. The non-flammable material inherits all of the excellent properties of its parent metal aluminum, such as recyclability, heat and corrosion resistance, strength, electrical and thermal conductivity, etc. but at a fraction of the weight, Aluminum foam has a high specific stiffness, especially compared to the original denser metal, and can withstand great damage with little deformation. Closed-cell aluminum foam is widely used as a lightweight construction material, both in its original format, and as sandwich panels, which are valued for their low density and very high stiffness. The main applications for this variety of foams are in the automotive industry as impact, acoustic and vibration absorbers, the aerospace industry. Metal foams, as a whole are not as cheap as sheet metals, or other polymeric counterparts. This is because of the number of processing steps and specific raw materials needed to facilitate their manufacture. However, the cost and energy benefits offered by using lightweight yet resilient foams such as aluminum foam in various applications of automotive industry can greatly offset these initial material costs (Aluminium Foam | Properties and Applications | Materials Hub, 2022). So, in this paper, the front bumper is mounted on the BPV for safety purposes. The mechanical properties will be directly used as the parameters in LS DYNA material options, and they are summarized in Table 4.4 below.

Table 4.4: Material properties of aluminum foam for LS-DYNA material

Properties	Units	Value
Foam density, ρ	kg/m^3	2670
Young's modulus, E	Pa	7.2e+10
Poisson's ratio, PR	-	0.25
Yield strength (stress), YS	Pa	1.8e+8
Ultimate tensile strength, UTS	Pa	3.2e+8
Shear modulus	Pa	9.2 e+8
Elongation at Break	%	0.15
Compressive modulus	Pa	5.0 e+8

Advanced high-strength steels (AHSS) are routinely used in numerous manufacturing applications due to their good combination of desirable properties such as high formability, high strength, good ductility, light-weight and low cost as well as high deformation hardening, which implies a high energy absorbing ability or “crashworthiness”. Weight reduction in automobiles is being accepted as one of the most efficient measures to lower energy consumption making AHSS the candidate of choice among steel alloys. Dual phase (DP) steel is part of the family of AHSS, and these steels are designated by their ultimate tensile strength (UTS) values. DP 980 is the current highest grade of steel, with a UTS of 980 MPa. Typically, DP steels have a microstructure consisting of a mixture of a soft ferrite matrix and hard martensite particles. DP steels are mainly used by the automotive industry primarily for safety parts in car bodies, e.g., bumpers, B-pillars, side impact beams, etc (Baltazar Hernandez et al., 2010). The mechanical properties of DP 980 steel materials are summarized in Table 4.5 below.

Table 4.5: Material properties of DP 980 steel material

Properties	Units	Value
Mass density, ρ	kg/m^3	7850
Young’s modulus, E	Pa	2.18e+11
Poisson’s ratio, PR	-	0.3
Yield strength (stress), YS	Pa	6e+8
Ultimate tensile strength, UTS	Pa	9.8e+8
Uniform elongation, ϵ	%	5.9
MARTENSITE	%	90

Material and Section definition

The geometric modelling of the front bumper and side door beam is done by using CATIA V5 modelling tools and mesh, boundary conditions, material properties and section properties are defined using on the Ls-pre post. Both the bumper and the beam are uniformly meshed with 4- and 3-mm element size respectively. They are meshed with shell elements. The ends of them are constrained in all the directions both in translational and rotational to the neighboring parts like body. The material model or keyword used to define the material is* MAT_PIECEWISE_LINEAR_PLASTICITY*.

Since the thickness of the bumper and the beam which is considered is very small comparing to its all length, a shell section is used to model them. The shell elements are formulated by ELFORM=2 (Belytschko-Tsay elements) for the bumper and ELFORM=16 (fully integrated shell element modified for higher accuracy) for the beam, because it gives better results with bending stress. Mixed (Rectangular and triangular) cross section is used as cross section of the beam and the bumper. It also provides good fitting space with the existing BPV frame structure when making modification. Different thicknesses of beam are taken into consideration to achieve the effect of thickness on impact performance of the side collision.

Boundary conditions

The different boundary settings for testing each of the bumper and the beam are represented by LS-DYNA's options as follows:

INITIAL_VELOCITY_GENERATION was used to define the velocity of the moving components like bumper and beam. CONTACT_AUTOMATIC_ SURFACE _SURFACE_ID between the bumper or beam and the rigid wall (in case of front) or rigid pole (in case of side impact). CONTROL_TERMINATION for the simulation time is set as 0.16 s, CONTROL_HOURGLASS is for zero energy mode of deformation for non-fully-integrated elements IHQ=4, IBQ=0 is used and for fully integrated shell elements IHQ=8, IBQ=0. For the output values in DATABASE_EXTENT_BINARY; D3PLOT, D3DUMP, ASCII options are selected.

Side bumper beam test

Side beam considered as one of important safety component which strengthen the side members of the BPV and helps on lowering the degree of injures to occupants during side collision. Under this section, door beam with advanced high-strength steels (AHSS) DP 980 material is designed for different thickness. Rectangular cross section used for the beam having different thickness of 0.886, 1, 1.25, 1.5, 1.7 and 2 mm. the reason for starting from 0.886 mm thickness is that when the material thickness was lowed from this value it showed some kind of failure mode. Among the listed ones, the best material thickness is selected based on parameters like, impact energy, Stress, energy absorption capacity and reduction in displacement.

The boundary conditions and the setups used are discussed below. The test consists of three components, these are the supports (red colors), the beam (blue) and rigid pole (yellow). The pole is represented by a rigid body, and discretized by solid elements. The beam and its supports utilize single-layered modelling approach, where only one layer of shell element is implemented for efficiency. The components are mainly meshed with quadrilateral elements (97%) with fewer triangular one (3%) and totally consists of 862,905 elements and 908,851 nodes. mat-rigid (MAT 20) is used for simulation of the rigid pole, and MAT_PIECEWISE_LINEAR_PLASTICITY (MAT 24) used for the supports and the beams.

The test procedure follows the same procedure used in the full crash test of the BPV. The supports were arranged in the same manner as point where the modification was made on BPV. The same distance that was set between the BPV and rigid pole was also set for the beam and the side pole. The beam is moving with 32km/h as stated on NCAP was collide with the rigid pole, see Figure 4.15.

- The rigid pole degree of freedom is all fixed (DOFs=0).
- The moving beam and its supports are fixed in all DOFs except for the moving direction.

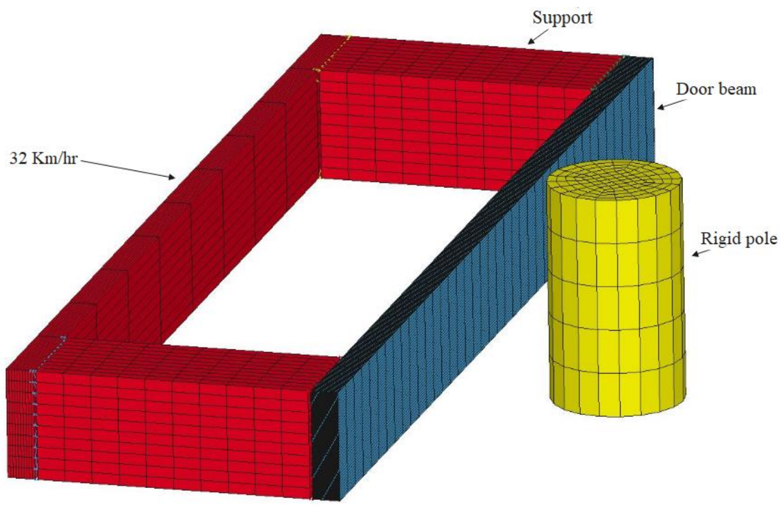

Figure 4.15: Side door beam test set up

Front bumper test

For any vehicle, front bumper is the most critical part which protect the occupants and the vehicle parts by deforming and absorbing much of the impact energy. A front bumper shown Figure 4.16 is mounted on the front part so that at the event of crash it absorbs the impact energy together with the front structural parts. Using the analysis method used in previous section different bumper speed are considered and based on the parameters such as deformation, impact force and internal energy, the best material speed is selected.

For the component reduction of BPV, it will be compensated by adding mass rigidly given to the reduced model using ELEMENT_MASS_PART. Therefore, the meshed reduced model totally consists of 157059 elements and 159626 nodes with much quadrilateral and fewer triangular elements. The total width of the front bumper is equal with the front track of the BPV. The speed of the bumper is varied from 50 Km/hr to 70 Km/hr. The test procedure follows the same procedure used in the full-frontal crash test of the BPV. The same distance that was set between the BPV and rigid wall was also set for the reduced models. The results of the above method used were discussed on the next chapter.

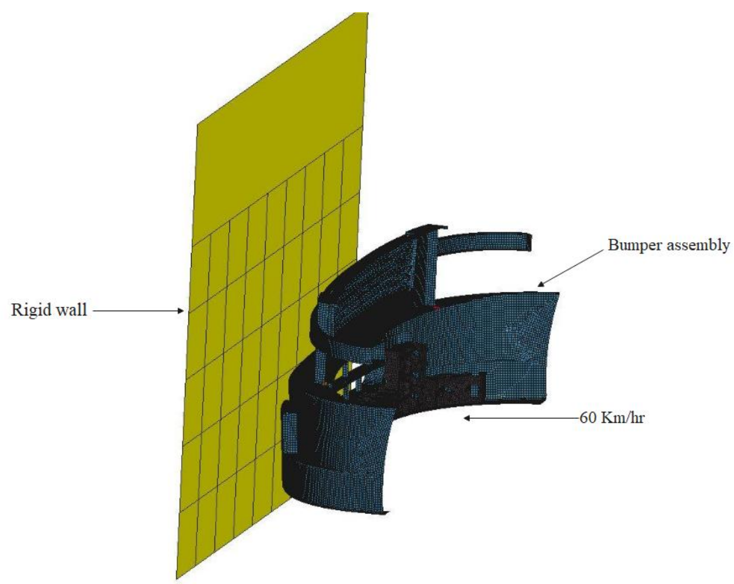

Figure 4.16: Front bumper test set up

CHAPTER FIVE

RESULT AND DISCUSSION

5.1 Introduction

In this chapter the results of the simulation of frontal and side crash of BPV is reported and comparative analysis carried out between the modified and existing vehicle model is also made. In addition, the detail discussion on the results is presented. But before entering into the report or result, the verification method for LS-DYNA simulation results is discussed below.

5.2 Result and discussion of existing model

5.2.1 Frontal collision

The analysis of the whole vehicle structure

The result of frontal crash simulation where the car moving with velocity of 60 km/h will collide with rigid wall which is stationary in opposite side of car and is discussed. Figure 5.1 shows the event and response of the whole vehicle structure during the time 160 ms. As it can be observed from the figure at t=0.027s, the first part of the BPV which is in contact with the opposite rigid wall and deformed the front bumper. After this point as the simulation time increase and reach 0.045s, the contact area increases, as a result the front structure of the vehicle parts like front fenders, bumper and hoods starts to deform progressively and have generated plastic deformation. When the time reaches 0.066s, the vehicle's lower support (chassis) of the BPV starts deformation, since the chassis of the BPV is relatively stiffer than the car front bumper so the car starts to deform together with BPV. At final stage, the front tires of the car deform and rotates at some angle and the rear tires starts to leave the ground. As result the frontal parts of the BPV deforms and high deformation at front structure occurs.

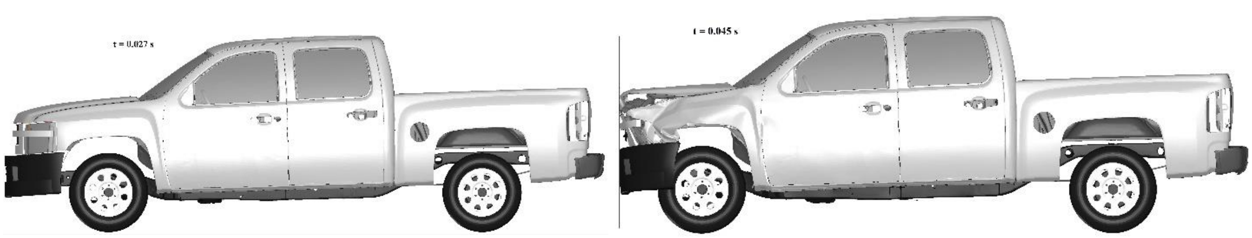

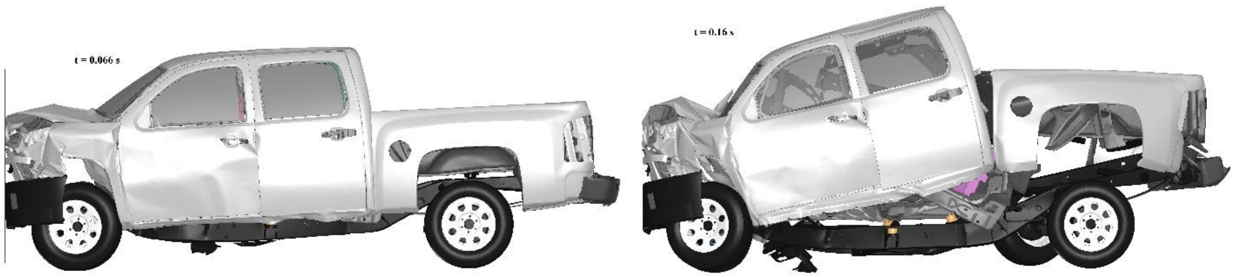

Figure 5.1: Sequence of front crash event

Total Energy-balance graph

According to Law of Conservation of energy, Energy can neither be created nor be destroyed, but it can be converted from one form of energy to other form. Applying the same principle to crash analysis, the amount of kinetic energy lost during impact must be converted to other forms of energy such as internal energy, sliding energy, heat energy and hour glass energy. From Figure 5.2 it can be seen that, initially the kinetic energy which is high at the start of the impact is equal with the total energy with value equal to 172 kJ and as the crash event starts to take place the kinetic energy of the system starts to slowly getting reduced and converted to other forms of energy and then finally reaches to 4.48 kJ of energy. From this difference, it can be observed that 167.52 kJ of energy is absorbed and converted to internal energy, sliding energy, heat energy and hour glass energy.

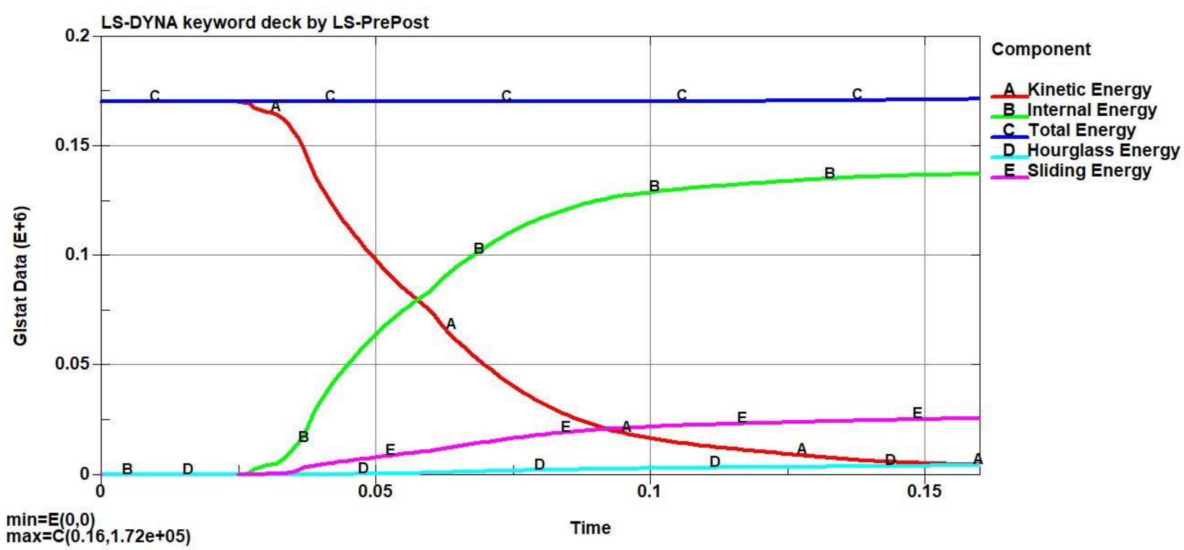

Figure 5.2: Energy balance curve

Energy absorbed by the vehicle

Among the loss of kinetic energy (167.52 kJ), 137 kJ or 81.78% of energy is converted in the form of internal energy as shown on Figure 5.3 and the remaining 18.2% energy is dissipated in the form of sliding, hourglass energy and heat energy.

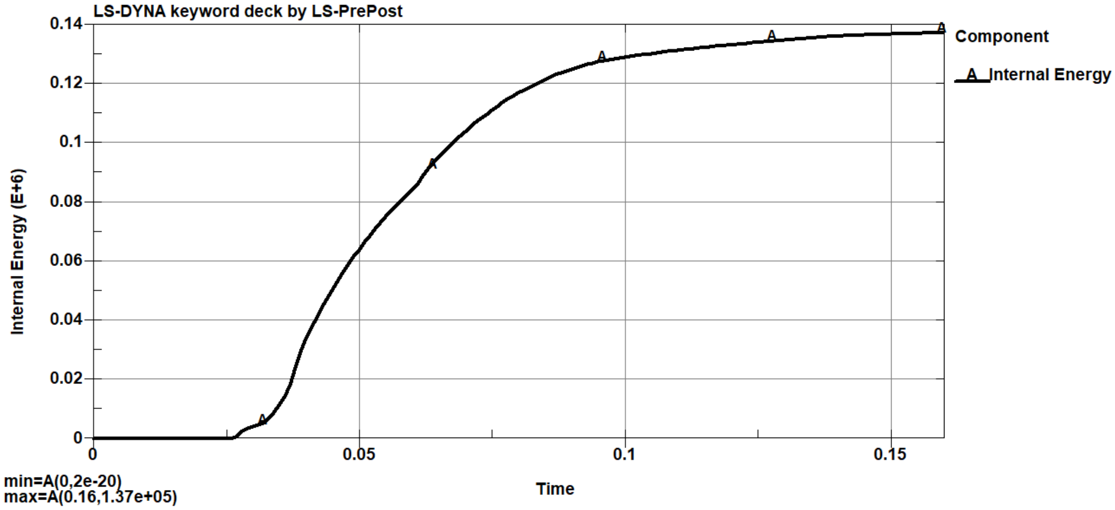

Figure 5.3: Total internal energy

On the other hand, Energy absorbed by BPV parts is shown on Figure 5.4 the energy graph shows the total internal energy absorbed by each of the vehicle frontal parts. The sum of total internal energy absorbed by the vehicle frontal parts are equal with 101.47 kJ, which is 74.07% of energy absorbed by the whole system (137 kJ). So, among the whole parts, most of the energy of the impact is absorbed by the front structure (hood and bumper which accounts 10.3 kJ and 13.3 kJ respectively) and the mainframe (chassis with value of 66.7 kJ). The maximum internal energy is obtained from the frontal structure (hood, bumper and chassis) with value of 90.245 kJ, this is due to that the collision first take place between the front structure and high impact force is transferred on it and this will lead to high deformation of the parts. Minimum value is from the axle, wishbones and engine, since they are modeled using the rigid material model so no deformation imposed on them.

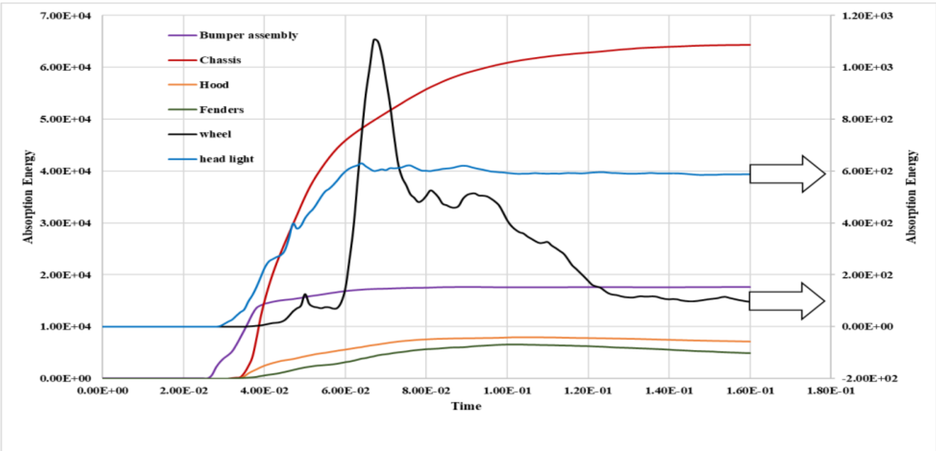

Figure 5.4: Energy absorbed by BPV parts

Generally, the front structure, which have shown large deformation takes effects in absorbing the energy. It causes the excessive stress surpassing the material bend stress greatly, so it can result in greater plastic deformation at the same, it can absorb the impact force mostly. At the same time, some amount of deformation is transferred to the rear vehicle structure and driver cabin.

Contact Force between the vehicle and rigid wall

The contact force pulse increases when the car is fully in contact with the rigid wall, so the simulation result of the maximum contact force for frontal crash of BPV at speed of 60 km/h was 499 kN at 38 ms. The values of contact force between the BPV and rigid wall is shown on Figure 5.5.

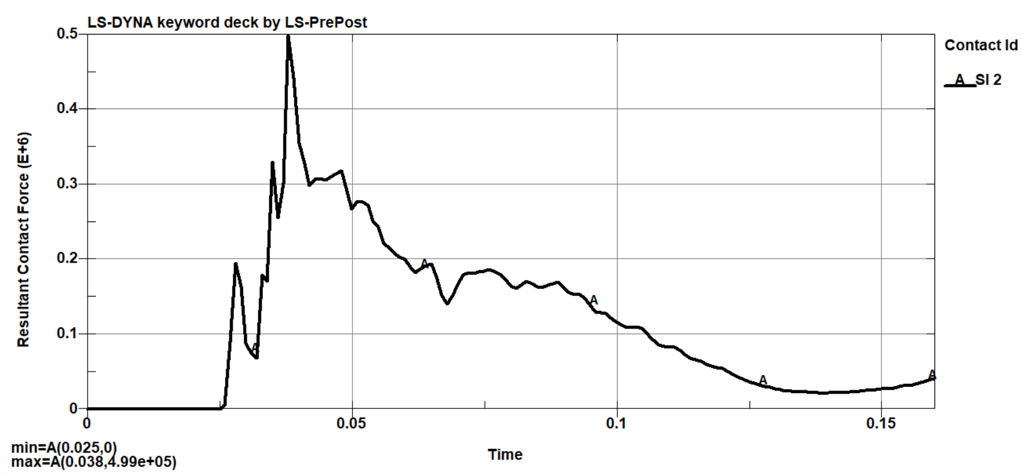

Figure 5.5: Contact force between BPV and rigid wall

Velocity of BPV components

To analyze the change of speed of varying vehicle section, I take the front most (lower bumper), front, middle and back section in all four points (node 115324, node 1247900, 508903 and node 879701 respectively). As the Figure 5.6 shows, initially the vehicles velocity for the BPV is given positive initial velocity of 16.6667 m/s in horizontal direction, the speed on node 115324 (lower bumper) falls down the most quickly because it is the point where the first impact contact occurs, and reach a velocity of 3.4 m/s at time 160 ms it has come down and then up which shows the rebounding of the part. The speed on node 1247900 (hood) initially starts to move with constant velocity of 16.6667 m/s until the body starts to deform and then decreases its speed with rebounding effect and finally reach a velocity of 0.1 m/s. Node 508903 (a point in the cabin of the vehicle) falls down linearly to 2 m/s at 160 ms without rebounding effect. Node 879701 (a point on the rear part of the vehicle) starts increasing the speed to 20.7 m/s then falls down with fluctuation, this reflects the phenomena that the vehicle would generate rebound after crash.

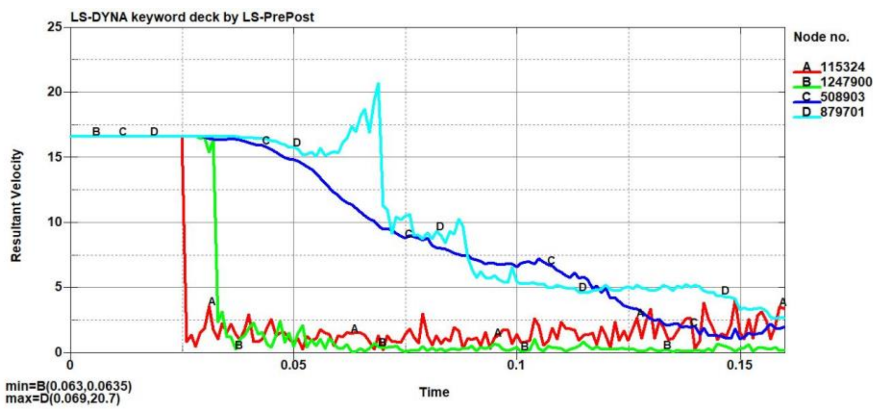

Figure 5.6: Velocity of nodes on BPV

Verification parameters

Energy ratio

From the energy balance curve, it has been seen that the system energy is not fully conserved and this is due to zero energy form of some elements. So, it may be noted that, all the processes in this universe are irreversible and some losses are always included which deviates energy ratio slightly from one. This can be observed in the energy ratio graph. As it is discussed before, to be accepted the energy ratio value should be 1.00 +/- 0.07. As shown in Figure 5.7, the simulation produce maximum value of 1.02 energy ratio and this value is approximately one with an error of 0.02% which is acceptable.

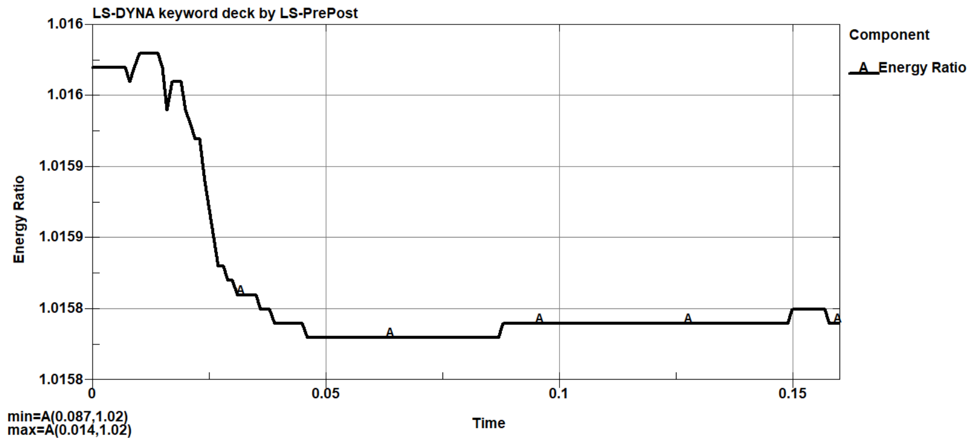

Figure 5.7: Verification: energy ratio

Ratio of TE/HE

Through analyzing the energy curves, the verification of the finite element model can also be determined using the ratio between the total energy to hourglass energy. Hourglass energy can cause a zero-energy model. If the hourglass Energy is less than 5% of the total energy, the finite element model is reliable. In the figure 5.8 below the hourglass energy graph is shown on the right-hand vertical axis vs time and the total energy graph is shown in the left-hand vertical axis vs time. As it can be seen the maximum value of hourglass is equal to 4.18 kJ and the total energy is equal with 172 kJ. Dividing these two gives 0.0243 (2.43 %) Because the hourglass energy is too small, i.e., HG < 5% it can be concluded that the result is reliable.

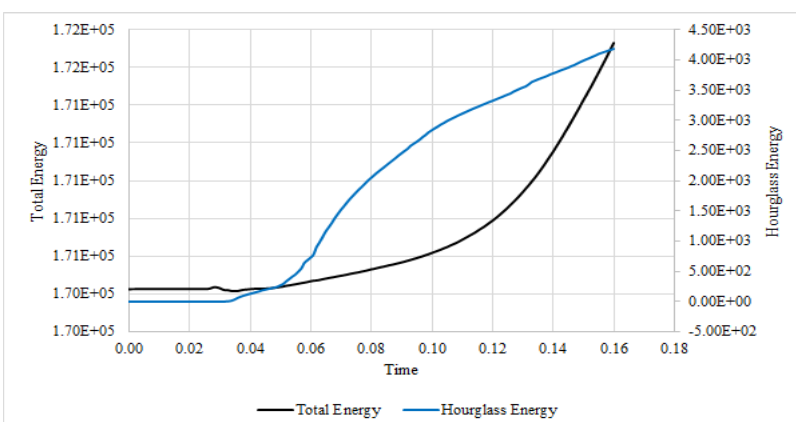

Figure 5.8: Verification: ratio TE/HE

5.2.2 Side pole collision

Vehicle structural response

The overall sequence of events during a side impact are shown on the Figure 5.9. It shows the response of the structure to the side pole collision. As it is seen in the Figure, when the collision process starts the vehicle starts to move in sideways. the whole process takes 0.16 s, at initial stages only small deformation of vehicle is observed until the time reaches 0.056 s. after this point, the force of impact increase as contact between the vehicle and pole increase as a result the vehicle body starts to respond with the same amount in which visible movements of damage of vehicle body is observed at t=0.08 s. Then when the time reaches 0.104 s, significant damage to the rear and fronts structure, roof structure and lower support like chassis, floor is observed and due to this BPV body is distorted too much. At the full stage of the simulation (t=0.16s), the vehicle structure is no more protecting the driver from external objects, this may result in high degree of injury to the driver body.

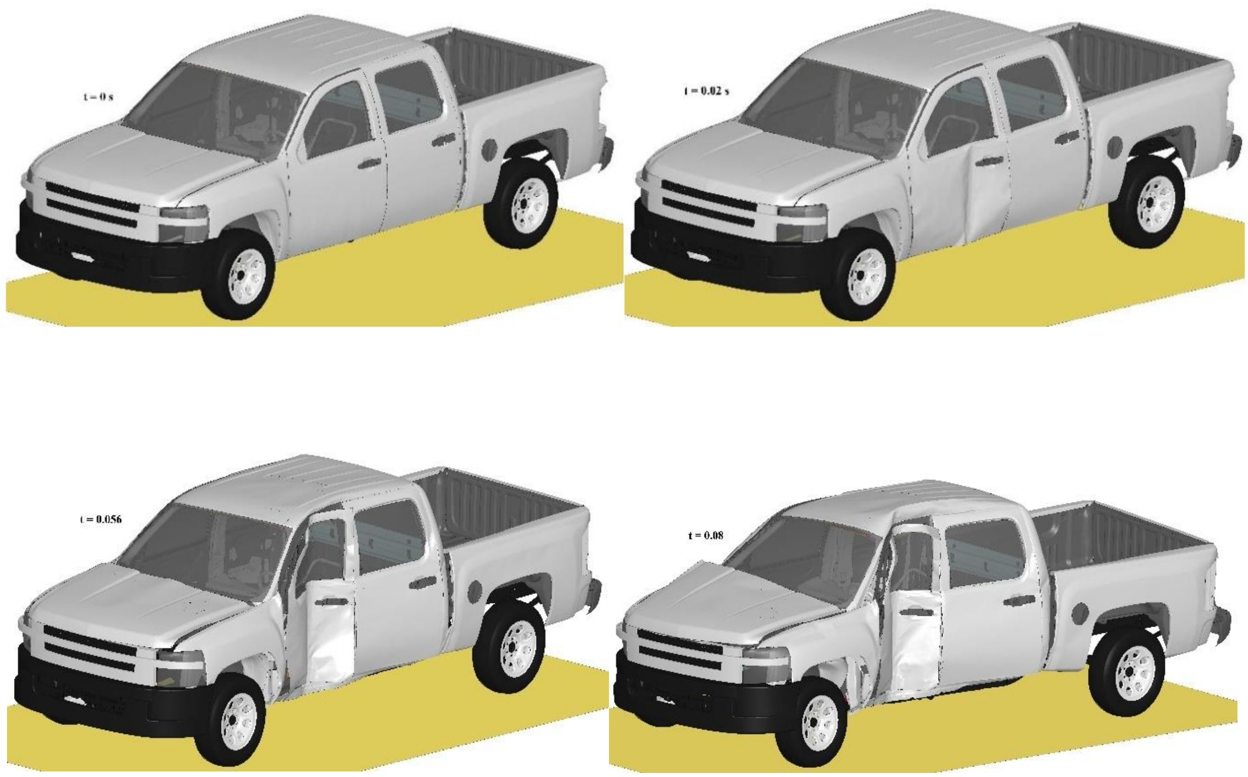

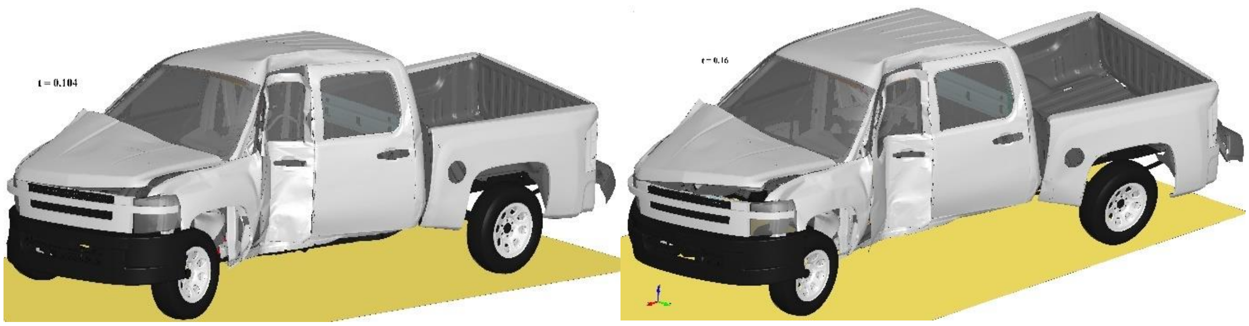

Figure 5.9: Sequence of side pole collision

Intrusion into the vehicle

Intrusion into the BPV is obtained by measuring the relative displacement of the node where there is no deformation with the node at another side where the deformation is more. Figure 5.10 shows the un-deformed and the final deformation of the BPV before and after impact with the rigid pole. As it can be seen, from the original width of the BPV, due to the side crash the side structure of the vehicle deformed 539 mm.

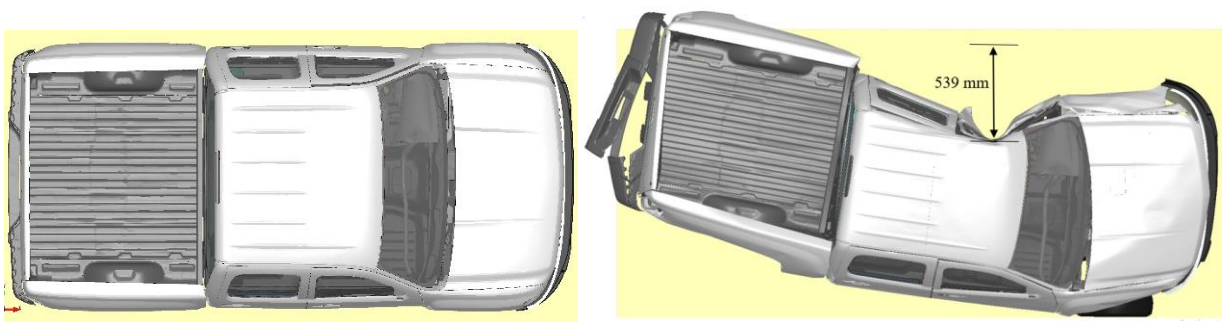

Figure 5.10: The original and deformed BPV vehicle structure

The maximum deformation is equal with 539mm. As shown on figure 5.11, Most of the deformation process takes place until 0.1 s and after this point only little deformation is observed. This is because initially the pole is in contact with the low stiff vehicle structure like the door or body. So, the deformation increases linearly until the vehicle structure collapsed and reaches the lower vehicle structure called chassis which is relatively stiffer. After this point the force of impact is decreased as a result only less deformation is observed.

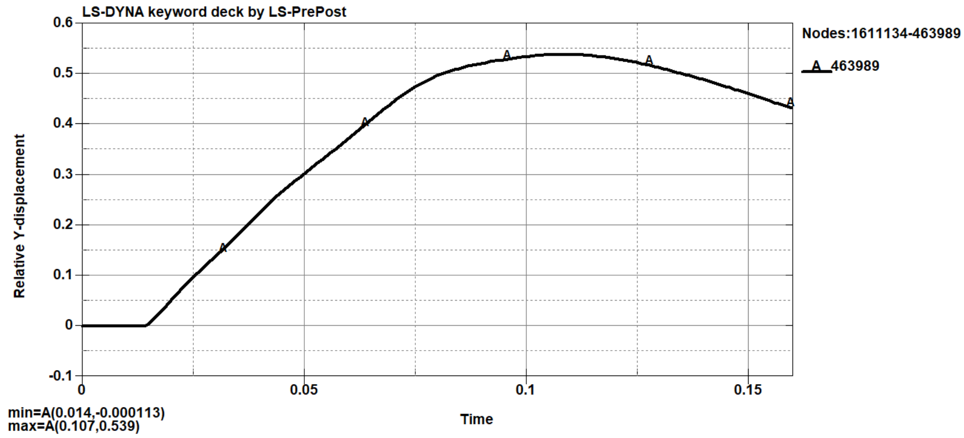

Figure 5.11: Deformation

Energy balance curve

The total energy of the system remains constant for the whole simulation with value equal to the initial kinetic energy which is 54 kJ. The kinetic energy of the whole system starts to decrease as the collision process starts and converted into internal energy which is increasing starting from zero energy. Most of the internal energy is gained due to the deformation of the structure. After 0.12s little deformation is observed, as a result the energy graph of the K.E and I.E become almost flat. The final kinetic energy is equal with 7.81 kJ and this can be interpreted as 14.46% of the initial kinetic energy or total energy. So, we can conclude that 46.19 kJ or 85.54 % of total energy (initial K.E) is converted to other forms of energy such us internal energy, hourglass energy, sliding energy or other forms. The energy versus time graph of the total system is shown in Figure 5.12.

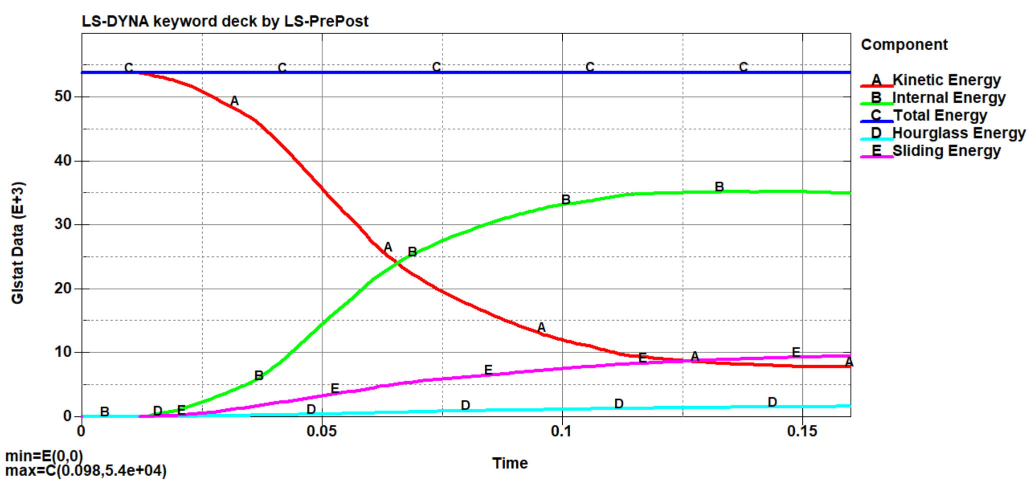

Figure 5.12: Side collision conservation of energy

Absorbed Energy by the Vehicle

From the total energy or initial kinetic energy, the internal energy is accounts for 35.3 kJ of energy which is 65.4% the total energy and the remaining energies are in the form of hourglass energy, sliding energy with value of 1.59 kJ, 9.53 kJ respectively and other form of energy. The total absorbed energy graph is shown on the Figure 5.13.

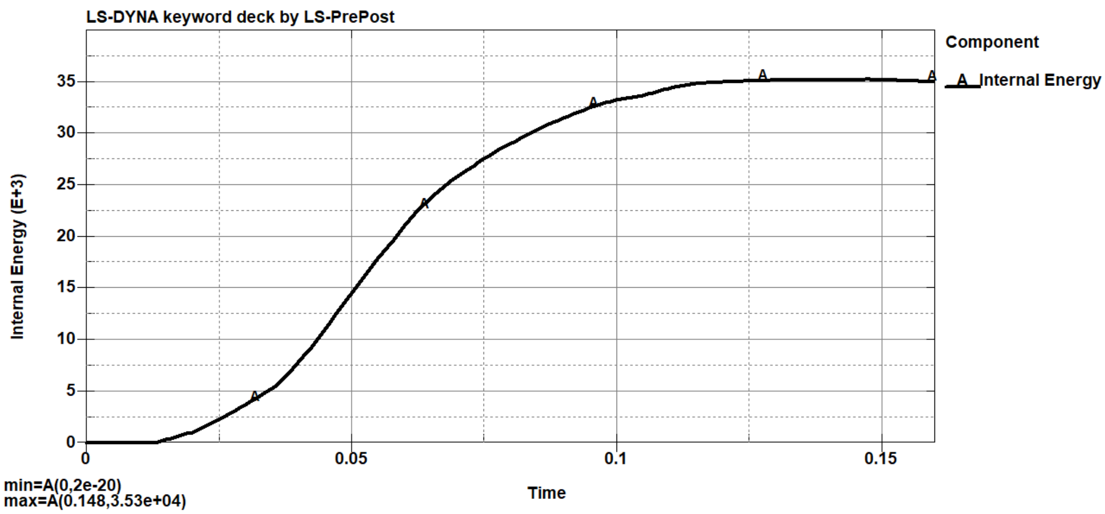

Figure 5.13: Side collision total Internal energy

From the total energy absorbed by the whole system, the energy absorbed by the BPV side parts is equal with 27.32 kJ as shown on the Figure 5.14. This shows that 77.4% of the total amount of energy is absorbed by the BPV side structure. Thus, the lower frame structure (chassis, floor) which support the front and rear structure, door and also roof structure have absorbed maximum of 21.59 kJ of energy which is 61.16 % of total absorbed energy. From the absorbed energy, the remaining 22.6 % of the energy (7.98 kJ) is obtained by the deformation of front and rear body structure. This is quite easy to predict because the pole has direct contact with the side structure. This is due to the force of impact transferred from the rigid pole to front and rear structure.

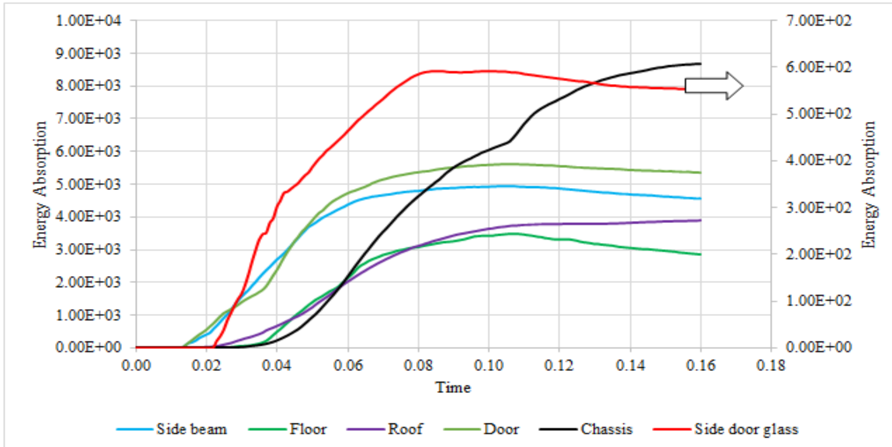

Figure 5.14: Energy absorbed by BPV side components during side collision

Contact force

The contact force between the BPV and the rigid pole is shown in the Figure 5.15. Initially the contact force is almost zero until the time reaches 0.012s. After this point the force starts to increase and shows some fluctuations. The fluctuations are due to the transient (time dependent) behavior of the simulation as a result the force on element is not always constant. The maximum force occurs when the pole is directly in contact with the stiffer structure of the BPV such as the lower frame structure (chassis). At this point the vehicle is highly damaged, the higher the force of impact the more damaged to the occupants. The force impact is reduced by introducing deformable elements on the structure. Otherwise, stiff elements will increase the force as the contact time is less.

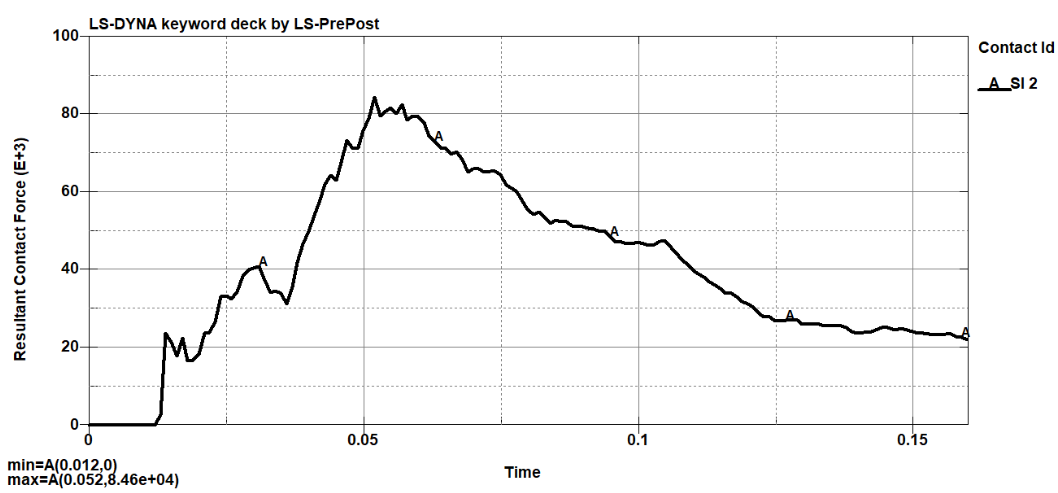

Figure 5.15: Contact force between the pole and BPV

Resultant velocity

Initially the velocity is 8.9 m/s and as the collision starts the resultant velocity reduces and reaches final value of 1.2 m/s. This shows that plastic deformation occurred on the BPV since the coefficient of restitution is low. The Figure 5.16 shows the resultant velocity of the vehicle.

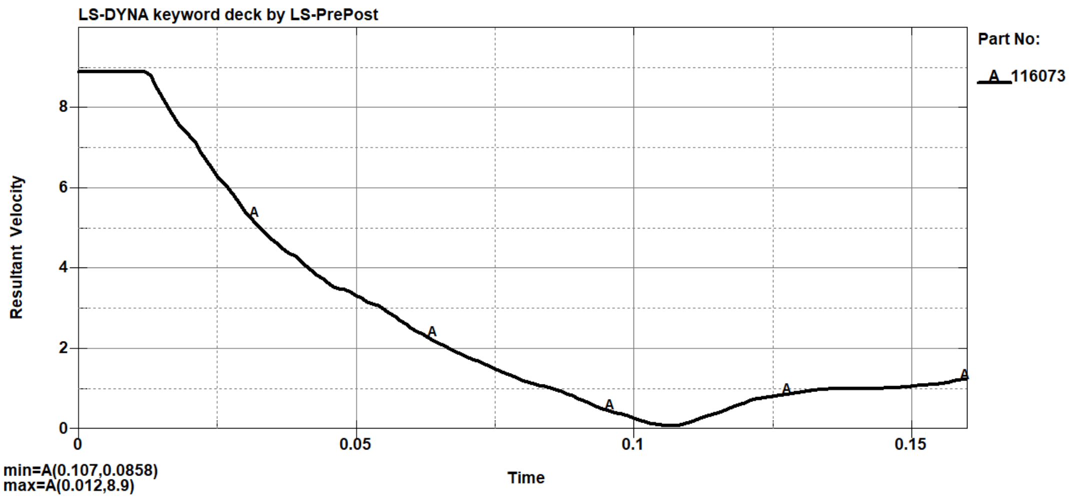

Figure 5.16: Velocity on the impact direction (resultant velocity)

Validation parameters

Energy ratio graph

As it can be seen on Figure 5.17, for the 0.16 s simulation the energy ratio value varies between 1 and 0.99978 which is within the range of acceptable value.

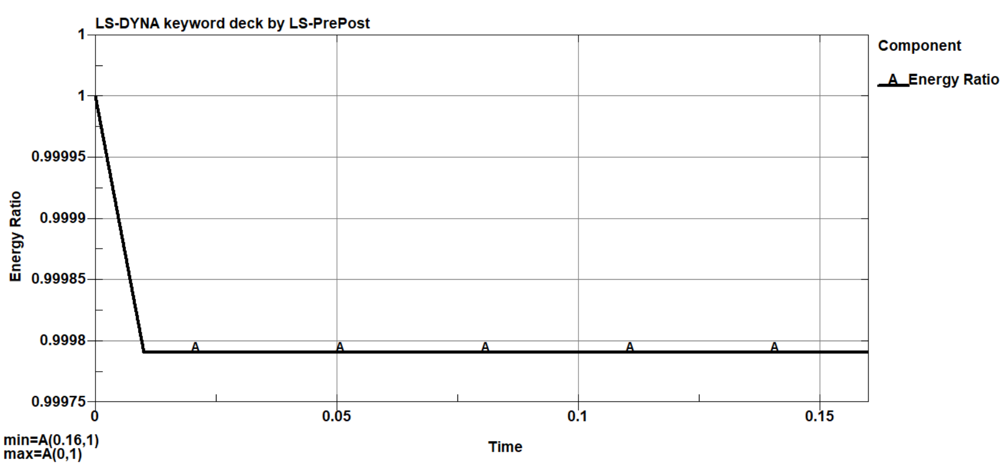

Figure 5.17: Verification: energy ratio

Ratio of TE/HE

Through analyzing the energy curves, the verification of the finite element model can also be determined using the ratio between the total energy to hourglass energy. Hourglass energy can cause a zero-energy model. If the hourglass Energy is less than 5% of the total energy, the finite element model is reliable. In the figure 5.18 below the hourglass energy graph is shown on the right-hand vertical axis vs time and the total energy graph is shown in the left-hand vertical axis vs time. As it can be seen the maximum value of hourglass is equal to 1.59 kJ and the total energy is equal with 54 kJ. Dividing these two gives 0.0294 (2.94 %) Because the hourglass energy is too small, i.e., HG < 5% it can be concluded that the result is reliable.

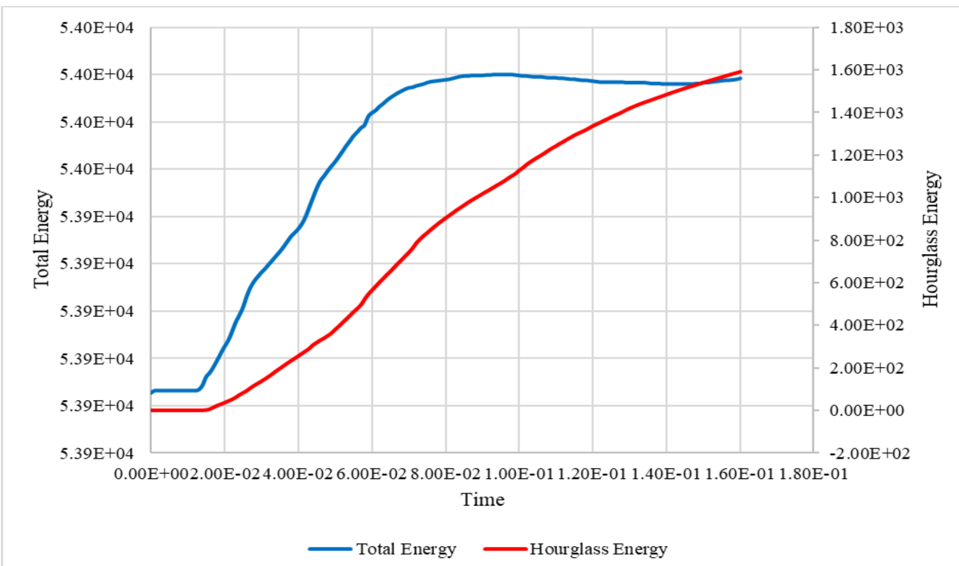

Figure 5.18: Verification: ratio TE/HE

5.3 Results of Front bumper simulation

Under this section the impact behavior of front bumper under different speed is analyzed based on parameters like force, displacement (deformation). When the material is changed due to the difference in density, the mass is changed and the mass percent decrease is 0.18% with in the same thickness. So, the modification gives an advantage on mass decrease. On the above studies, the deformation and energy absorbed have direct relation, so it is enough to study the energy absorbed in terms deformation. The speed considered were 50, 60, and 70 Km/hr. the result of the simulation is discussed below.

Deformation

As it is presented in graph, the behavior follows the same pattern in which the deformation increases as the speed increases. Initially until t=0.015 there is high deformation until the collision is in contact with high stiff material, then the collision starts to decrease the rate of deformation and finally, the structures were subjected to plastic deformation as shown on Figure 5.19.

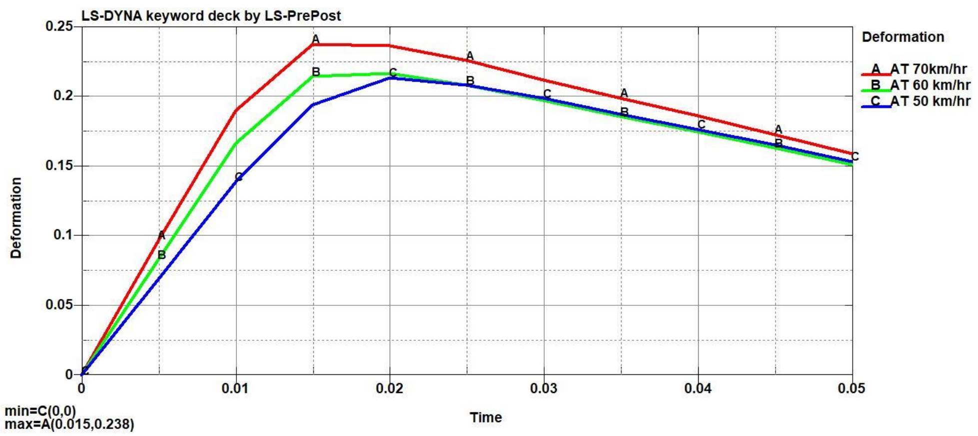

Figure 5.19: Deformation of front bumper for different speed

Energy absorption

As discussed on the above, the higher deformation of the bumper leads to more absorption of energy during the collision. The maximum amount of energy absorbed by the bumper is increases as the speed become increased as shown in the figure 5.20.

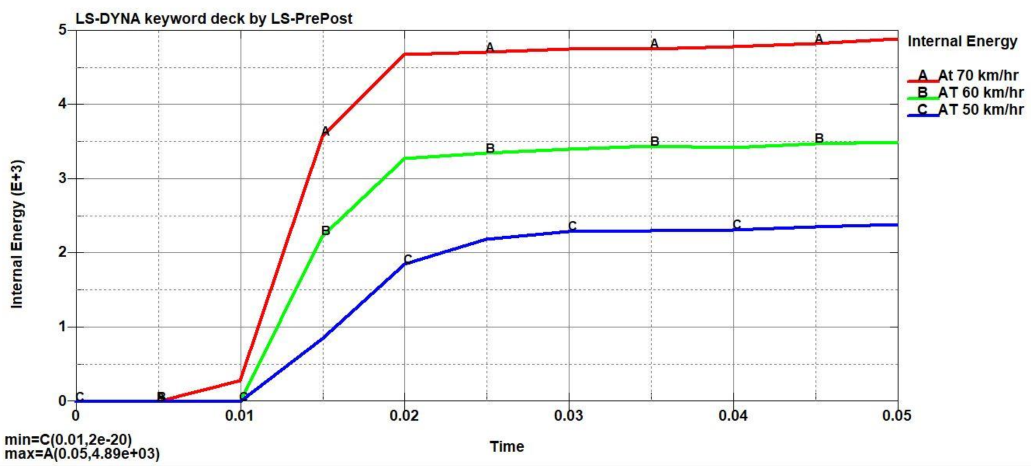

Figure 5.20: Internal Energy of bumper for different speed

Impact force

The fluctuation effect observed on the graph shown the compression and elongation effects occurs between the measuring nodal points of the bumper. From the deformation it can also concluded that the energy absorbed by bumper in increases with more deformation and decreases with les deformation. In another word the increase in vehicle speed results in more deformation and energy absorption. The contact force vs. time graph is shown in Figure 5.21. The graph reveals that as the speed increases the force of impact increases. The maximum impact force (81.4 kN) occurs when the bumper moves at 70 km/hr. This behavior is obvious as the momentum of the bumper increases with increase in speed of the front bumper. Generally looking at the above results it can concluded that the increases in speed results in high deformation, high energy absorption and high contact force. So, average speed (60 km/hr) is selected for the full car simulation in order to get low impact force, less deformation and good energy absorption.

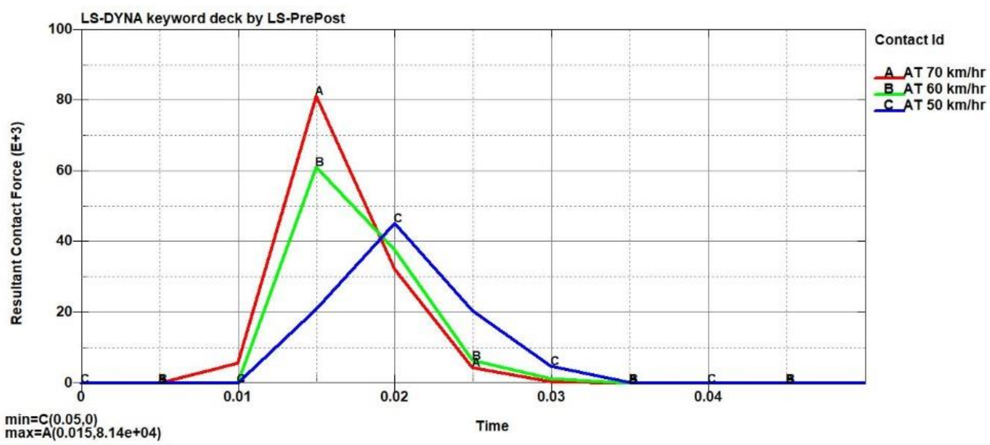

Figure 5.21: Resultant force of front bumper for 50, 60 and 70 km/hr speed

Effective von Moises stress

The effective van mosses stress of the front bumper as shown on Figure 5.22, the maximum stress value is equal to 0.54 Gpa at element 91719. The aluminum foam material strength and failure criteria are determined based on the material’s mechanical property. Since there is no dilatation of element was reported when running the simulation so based on that assumption the bumper is safe.

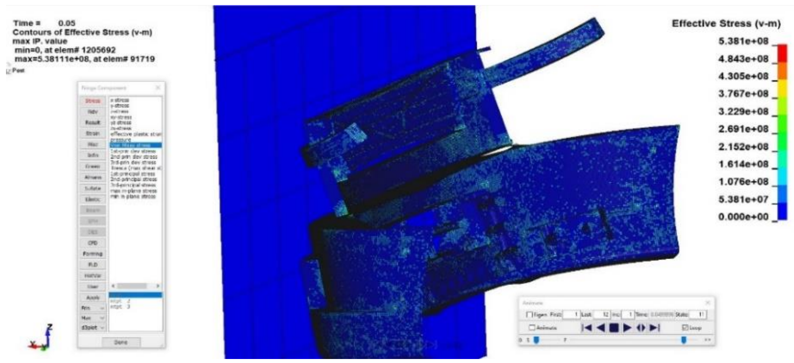

Figure 5.22: Effective von Moises stress of front bumper

Resultant displacement

The Resultant displacement of the front structure is shown on Figure 5.23. From the contour plot it can be seen that the maximum resultant displacement (deformation) of the structure is equal to 485.6 mm at node 74243.

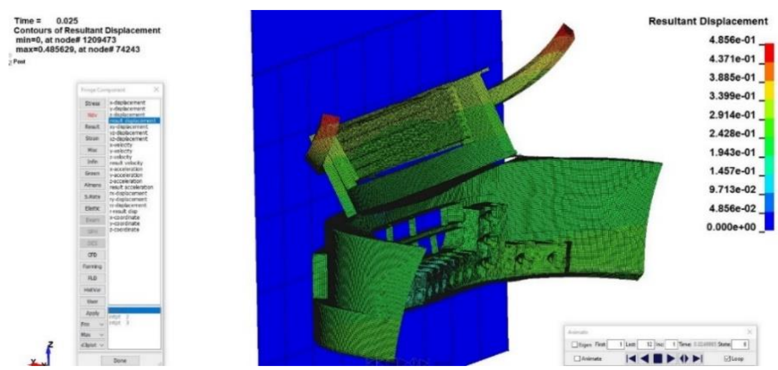

Figure 5.23: Resultant displacement

5.4 Results of Side door beam Simulation

The result for different thickness of beams is represented in graphs at regular interval of time as shown on the figure below. As the material is changed, due to the difference in density, the mass is also changed and the mass percent decrease is 0.2% with in the same thickness. So, the modification gives an advantage on mass decrease. Judgments were going to be made by observing the impact analysis results like force, stress, deformation and strain values.

Deformation

The deformation values are obtained by measuring the relative displacement from two nodes (one at the right or left end of the beam and the other at middle of the beam). With this measurement the value of deformation graph for different thickness of the beam was shown in the figure below. The thickness of the beam is 0.886, 1, 1.25, 1.5, 1.7, and 2 mm as shown in Figure 5.24. From the Figure shown, as the thickness of the beam increases from 0.886 mm to 2 mm, the maximum deformation of the beam decreases and the rate of decrease becomes also less with the increase of thickness. This does mean that abeam with less thickness is always better because more deformation means that there is probability of intrusion to the vehicle main compartments and also more energy is absorbed.

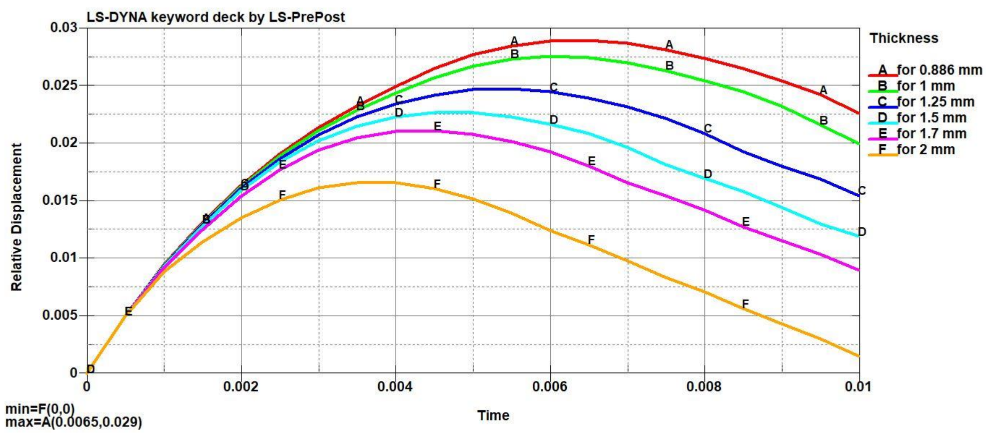

Figure 5.24: Deformation for Side beam with different thickness

Energy absorption

As discussed on the above, the higher deformation of the beam leads to more absorption of energy during the collision. The maximum amount of energy absorbed by the beam is reduced as the thickness become increased as shown in the figure 5.25.

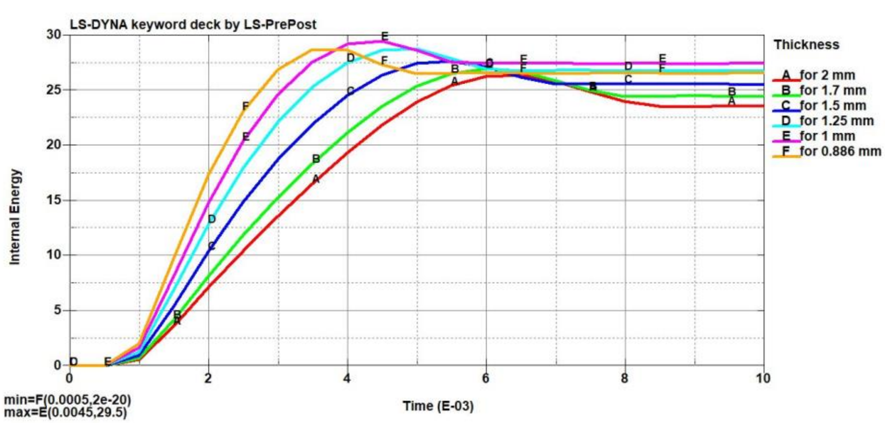

Figure 5.25: Energy absorption for side beam with different thickness

Impact force

Although maximum impact force between rigid pole and side door beam increase with the increase of thickness. This is obvious that with increase in thickness the mass of the beam increases as a result, high impact force is produced as shown in Figure 5.26. But that does not mean that beam with smaller thickness is better because the stress on the on the beam increases with the use of less thickness. Therefore, from the above results it can be concluded that neither abeam with less thickness nor with higher thickness is better, rather it depends on the application it is required for. The main purpose of this thesis work is to select a lightweight, good crash performance side door beam without sacrificing the impact behavior. From the viewpoint of impact performance, among the listed thickness taking the average value provides improved the level of performance relative of other for the body parts and passengers of BPV. Therefore, the door beam with 1.25mm thickness is better to be selected.

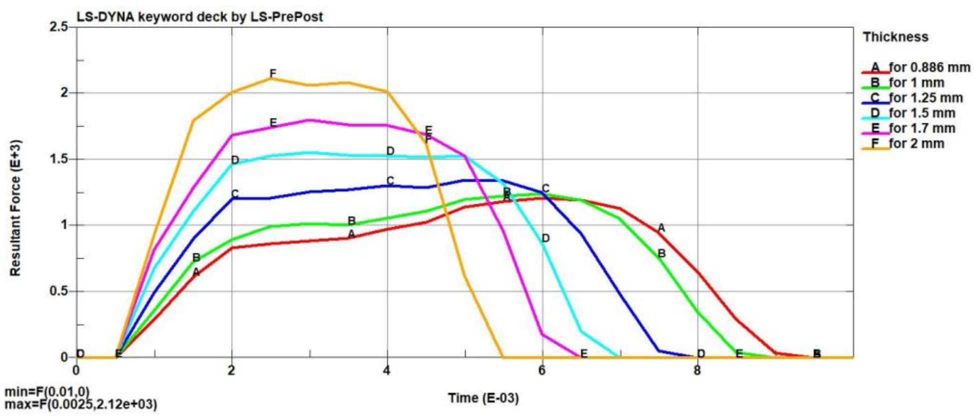

Figure 5.26: Impact force for Side door beam with different thickness

Effective von Moises stress

As it is indicated in Figure 5.27, the maximum stress value is equal to 0.8 Gpa at element 6255. The steel material strength and failure criteria are determined based on the material's mechanical property. Since there is no dilatation of element was reported when running the simulation so based on that assumption the beam is safe.

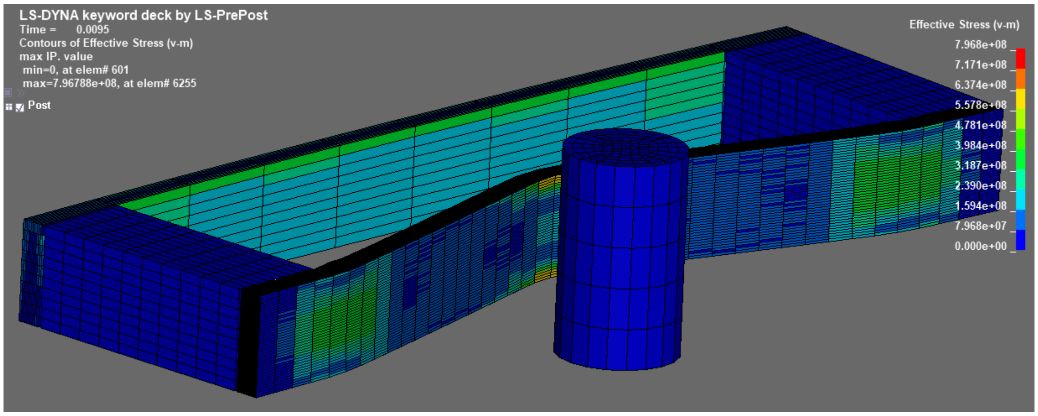

Figure 5.27: Effective von mises stress

Resultant displacement

As it is indicated on the counter plot, the maximum resultant deformation of the beam is 35 mm at node 3570. Deformation of the beam produce changes in the energy absorption of the beam. With this deformation, the intrusion is very less and the force of impact is gradually increase but the damage will be less as compared to the existing, see Figure 5.28.

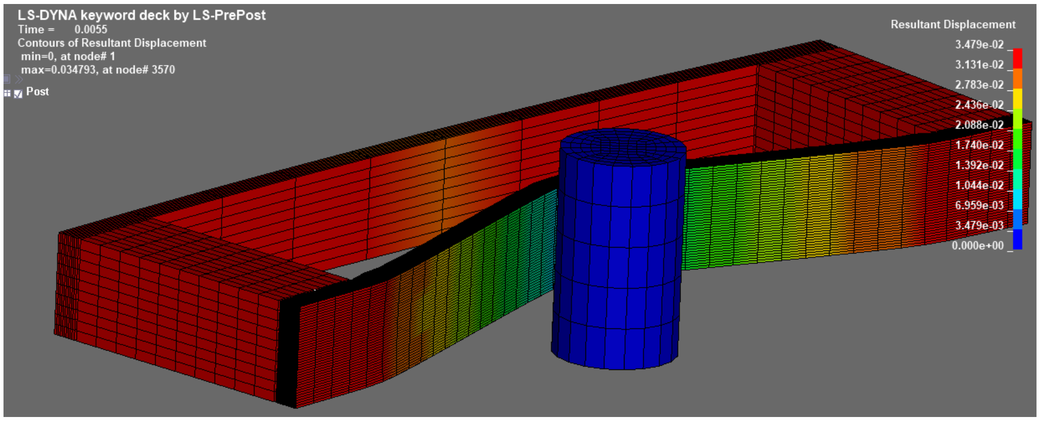

Figure 5.28: Resultant displacement

5.5 Result and discussion of Modified BPV

5.5.1 Frontal collision

Analysis of the whole vehicle's response

The simulation result of modified model BPV frontal crash is presented and discussed, the sequence and the appearance of the modified BPV at final state is shown on figure 5.29. The result of frontal crash simulation where the car moving with velocity of 60 km/h will collide with rigid wall which is stationary in opposite side of car and discussed. The Figure below shows the event and response of the whole vehicle structure during the time 160 ms. As it can be observed from the figure at t=0.029s, the first part of the BPV which is in contact with the opposite rigid wall and deformed the front bumper. After this point as the simulation time increase and reach 0.048s, the contact area increases, as a result the front structure of the vehicle parts like front fenders, bumper and hoods starts to deform progressively and have generated plastic deformation. When the time reaches 0.07s, the vehicle's lower support (chassis) of the BPV starts deformation, since the chassis of the BPV is relatively stiffer than the car front bumper so the car starts to deform together. At final stage, the front tires of the car slightly deform and rotates at some angle. As result the frontal parts of the BPV deforms and high deformation at front structure occurs. Due to the material modification on the front bumper high energy is absorbed during the collision so, there will be less impact force transferred to the occupant which will probably save human life or reduce injury on the occupant. Therefore, the modification made on the vehicle is highly acceptable.

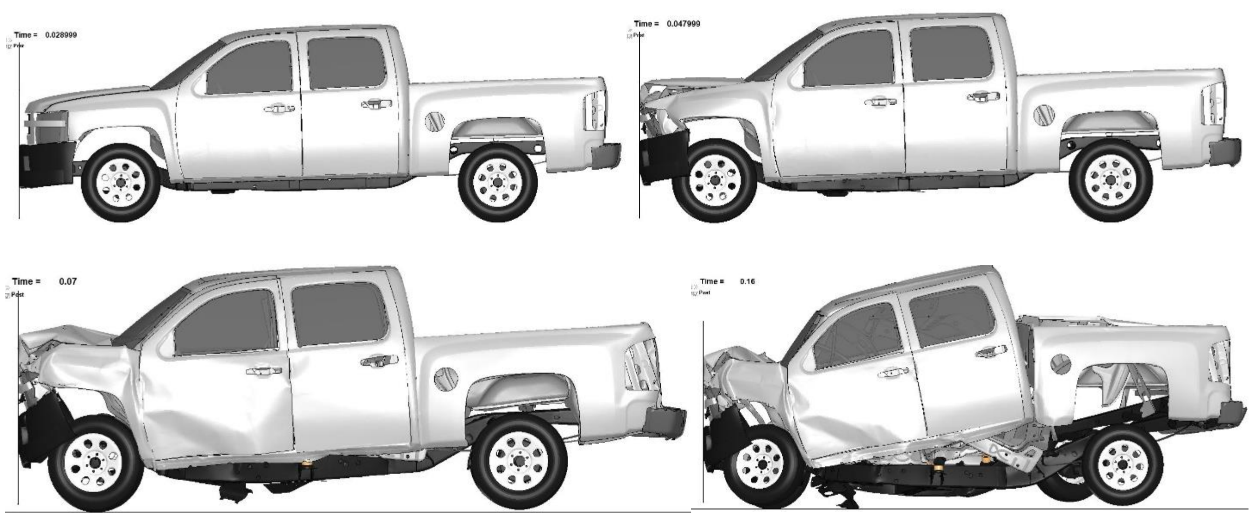

Figure 5.29: The Sequence and appearance of the modified BPV during front crash event

Energy balance

The energy versus time graph of the total system is shown in Figure 5.30. As it is shown through the simulation the Conservation of energy principle is obeyed in which the amount of kinetic energy lost during impact is converted to other forms of energy such as internal energy, sliding energy and hour glass energy. The total energy graph remains approximately constant. Initially the kinetic energy is equal with total energy with value equal to 175 kJ but as the vehicles starts motion the KE value decrease and get converted into internal energy and other forms. As a result of final state, it reaches energy value equal to 4.27 kJ this indicate that 97.56 % of kinetic energy is lost and converted in to other forms of energy.

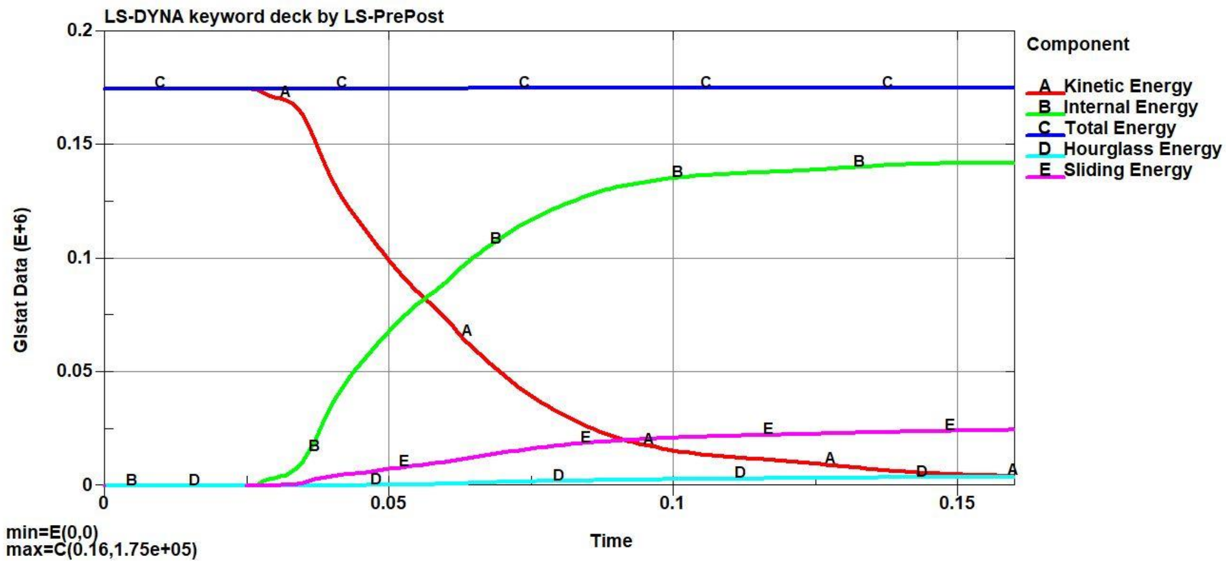

Figure 5.30: Modified model energy balance curve

Energy absorbed by modified BPV

Among the lost kinetic energies, 142 kJ (81.15%) of energy is in the form of internal energy as shown Figure 5.31 and the remaining 18.85% is converted in to other forms of energy like sliding energy, hourglass energy or other forms of energy.

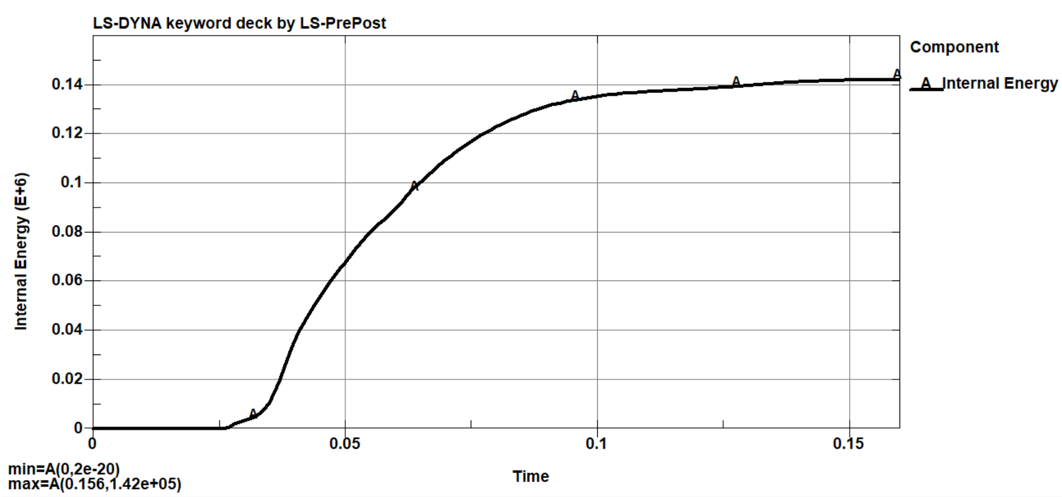

Figure 5.31: Modified model internal energy

From the energy absorbed by the whole system, front parts of the modified BPV contributes107.09 kJ of absorbed energy. This covers 75.4% of the total energy absorbed by the whole system. Figure 5.32 Show the energy absorbed by BPV frontal parts with primary and secondary axis versus time. As indicated the parts listed under primary axis absorbed much of energy by covering 99.35% of the energy absorbed by BPV parts. The front structure (bumper and front body structure) is responsible for most of the energy absorbed as it is very near to the collision contact area.

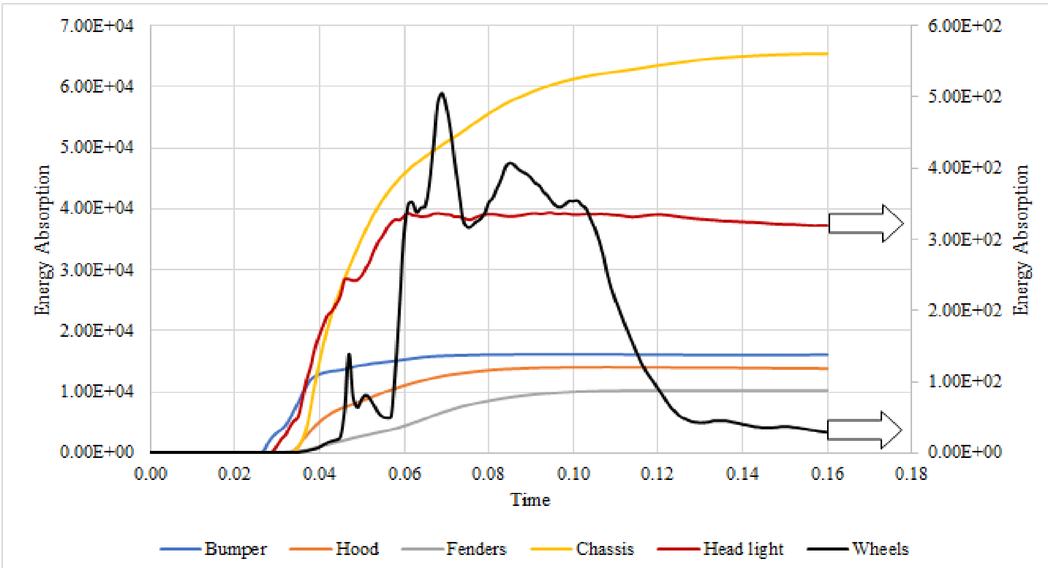

Figure 5.32: Energy absorbed by modified BPV parts

Contact force

The contact force between the modified BPV and the rigid wall is shown on Figure 5.33. As shown the Contact force pulse data shows maximum force at 0.039 s. This maximum force is equal to 460 kN. This force is due to the high contact force occurred as the rigid wall is in contact with the front portion of the chassis of BPV.

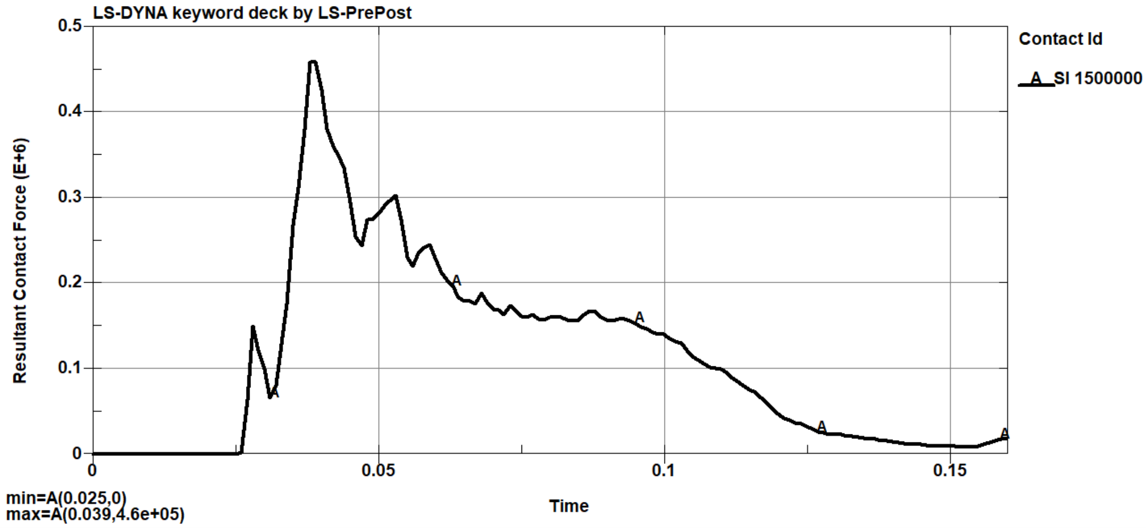

Figure 5.33: Contact force for Modified BPV

Resultant velocity

The resultant velocity of the whole system is shown on Figure 5.34. As it is shown below the velocity before the start of the collision is equal to 7.7 m/s but as it indicates as the collision process starts to take place the initial velocity value gets decreased and reaches final value of 0.814 m/s this shows the car collides to a rigid wall so the velocity value gets minimized.

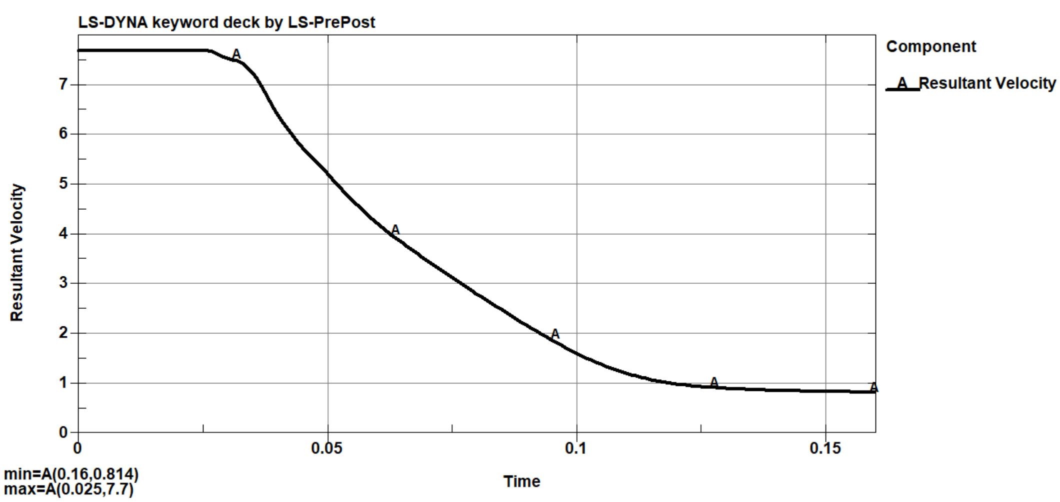

Figure 5.34: Resultant velocity

Verification

The above obtained values are verified by the energy ratio and ratio of HE/TE, the graphs are presented as follow:

Energy ratio

The energy ratio of the whole system is presented on Figure 5.35, the energy ratio value varies between 1.0159 and 1.0157. This value in the range stated above is acceptable.

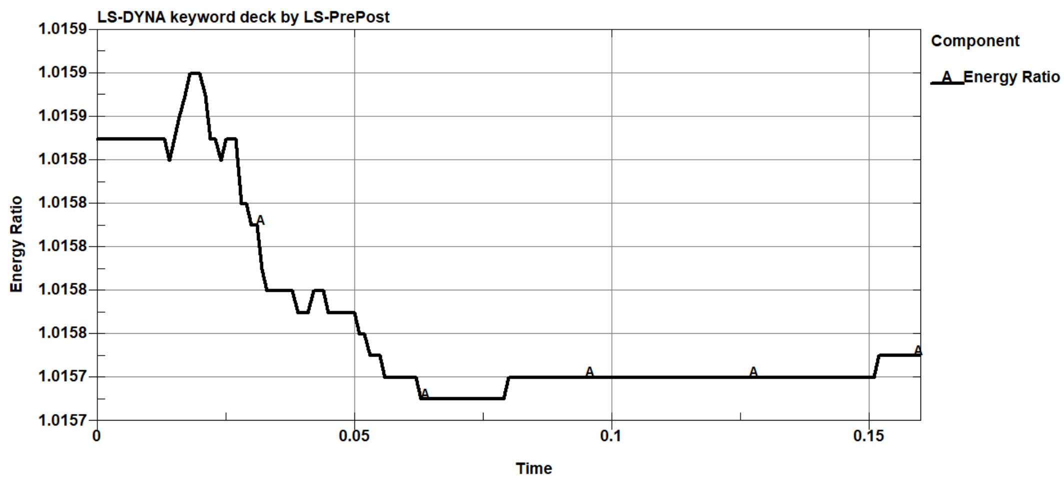

Figure 5.35: Energy ratio

Ratio of HE/TE

As it can be easily seen from Figure 5.36, the value of hourglass energy is very less as compared to the total energy. The ratio resulted in 0.0226 or 2.26%. Since the energy ratio is less than 5% so the results are acceptable.

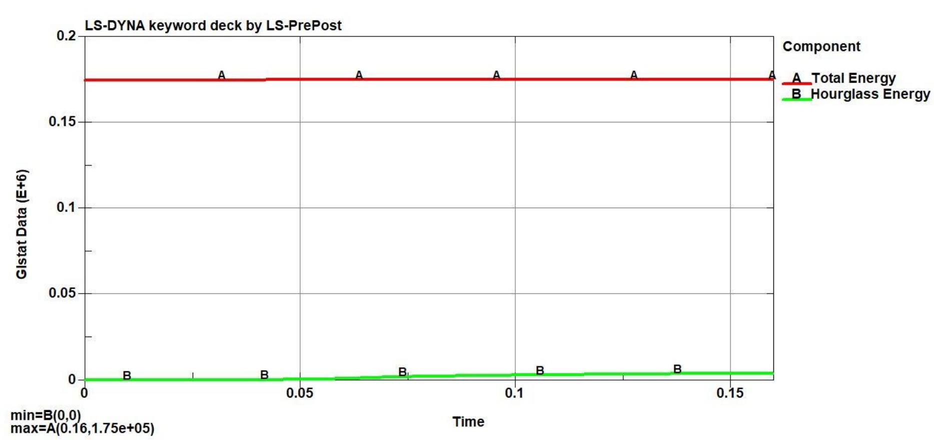

Figure 5.36: Ratio of HE/TE

5.5.2 Side pole collision

Intrusion into the vehicle cabin

The intrusion into the modified BPV model due to the side pole collision is shown on Figure 5.37. The Intrusion is obtained by measuring the relative displacement between two nodes of the model. The Figure shows the final deformation of the BPV after impact with the rigid pole. As it can be seen, a pole intrudes 337 mm in to the modified model. The original width of the BPV in lateral direction is 1725 mm. This shows that the modified model remains with 1388 mm space on lateral direction.

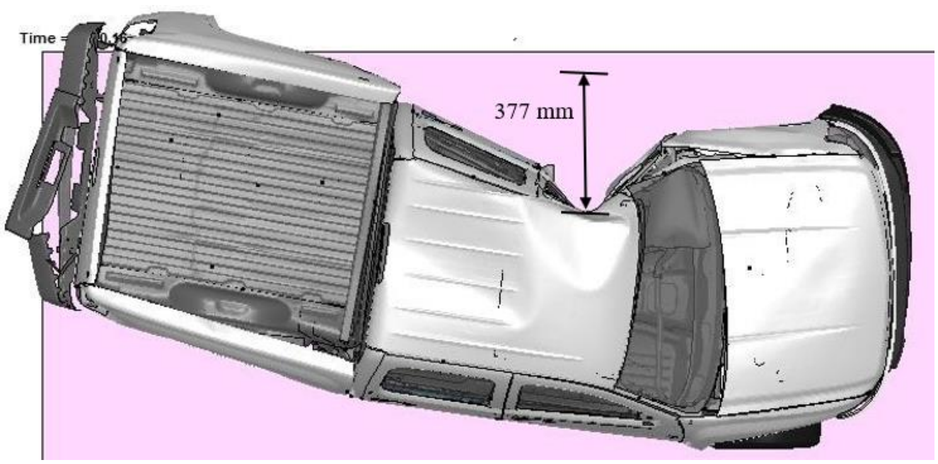

Figure 5.37: Side Intrusion into the vehicle

Deformation

The resultant displacement of the modified model in lateral direction is shown on Figure 5.38. From the graph, the maximum displacement is equal with 377 mm. The maximum deformation occurs at 0.105 s and after this point the deformation decrease. This is due to the reduction on speed of the BPV rebounding and the contact between stiff elements. Although after this point the force of impact is decreased as a result only less deformation is observed.

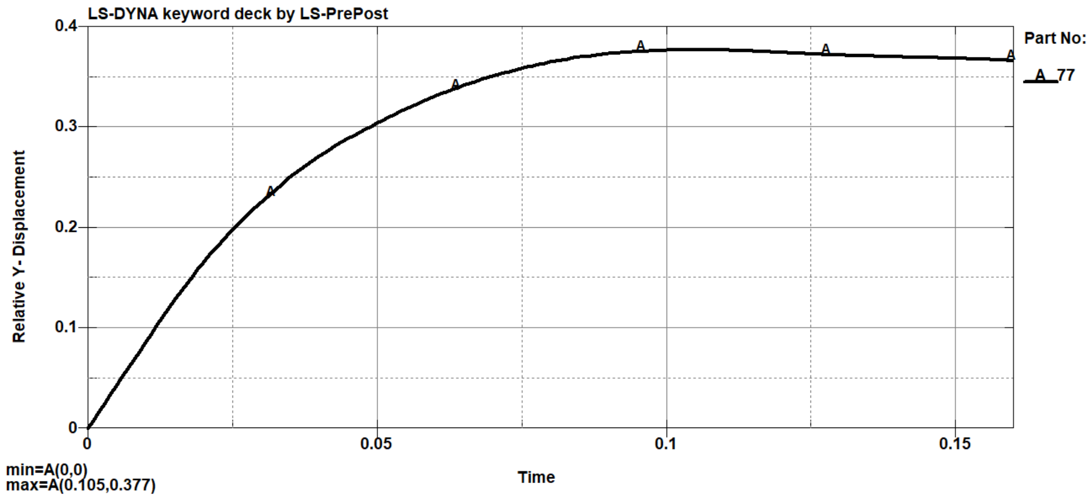

Figure 5.38: Relative Displacement of Modified BPV model

Energy balance curve

The energy versus time plot of the total system is shown in Figure 5.39. As it is shown the total energy of the system remain almost constant for the whole 0.16s simulation with value equal to the initial kinetic energy which is 54.7 kJ. On the other hand, the kinetic energy of the whole system starts to decrease as the collision process starts and converted into internal energy, hourglass energy, sliding energy or other forms of energy. Which is increasing starting from zero energy. Most of the absorbed energy is due to the deformation of the structure.

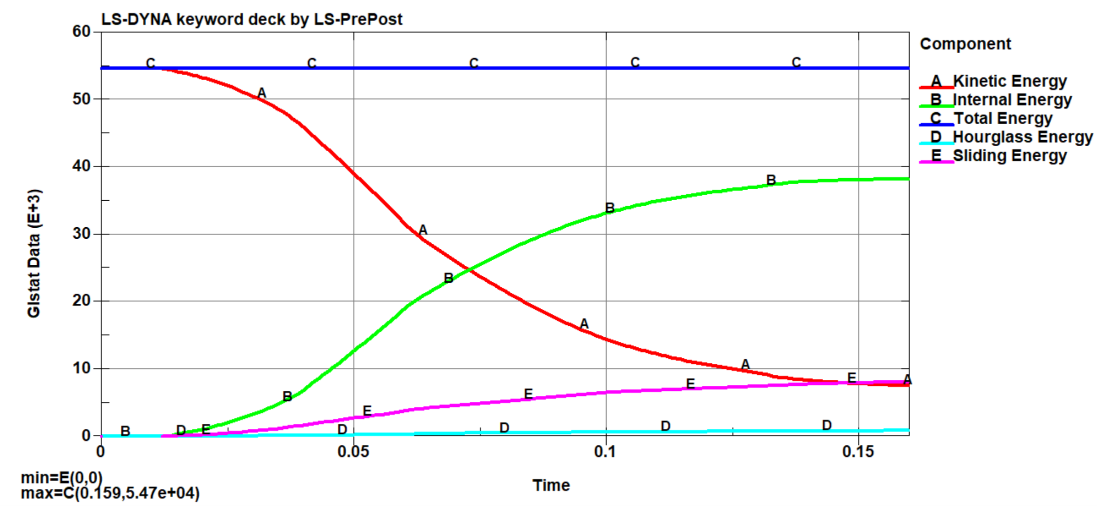

Figure 5.39: Energy balance of modified BPV model at event of side collision

At 0.16s the kinetic energy value is equal with 7.54 kJ and this indicate that 47.16 kJ kinetic energy is lost and converted in to other forms of energy such as Internal energy (I.E), Hourglass energy (H.E) and other form of energy.

Absorbed Energy by BPV Vehicle

From the total energy or initial kinetic energy 38.2 kJ of energy is in the form of internal energy as shown on figure 5.40. This mean that internal energy takes 81 % of the dissipated or lost KE. The remaining 8.96 kJ of energy is in the form of hourglass and sliding energy.

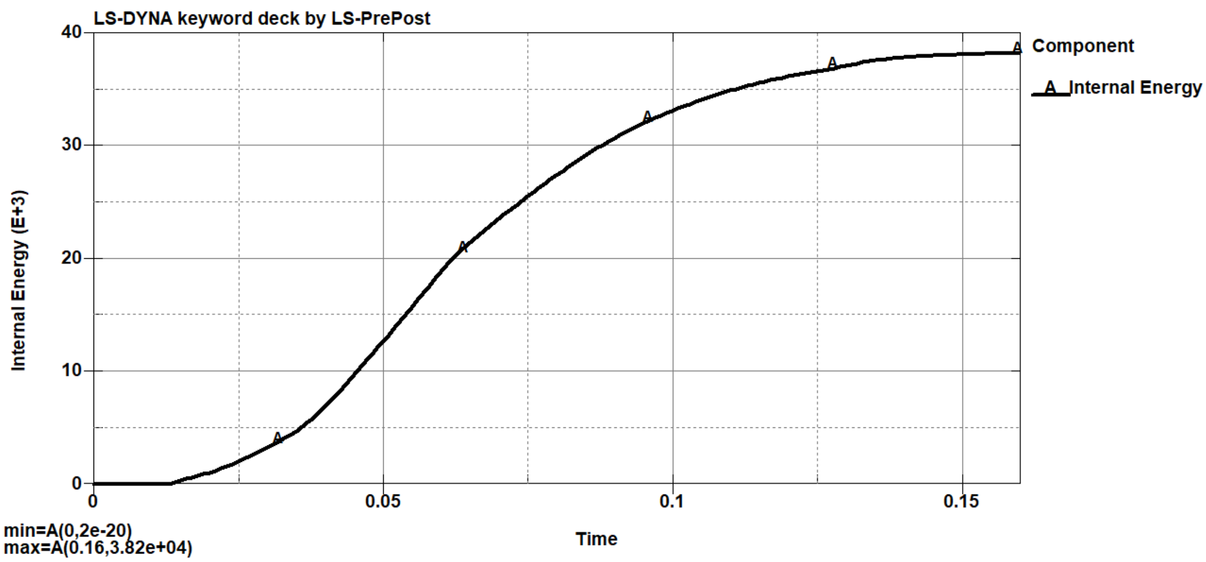

Figure 5.40: Internal energy of modified BPV model at event of side collision

From the total energy absorbed by the whole system, the energy absorbed by the BPV side parts is presented on the Figure 5.41. from the figure below, the primary axis (left vertical axis) shows the BPV parts with the highest energy absorption such as side door body structure, roof support frame, main lower frame (chassis), floor and the secondary axis (right vertical axis) shows the parts with lower absorption of energy. The total amount of energy absorbed by the side structure of BPV is equal with 26.692 kJ which accounts 69.87 % of the absorbed energy. This shows that most of the energy is absorbed by the BPV side structure. Among the parts which are listed under primary (left) axis are absorbed 97.55% and the remaining 2.45% is absorbed under the right axis.

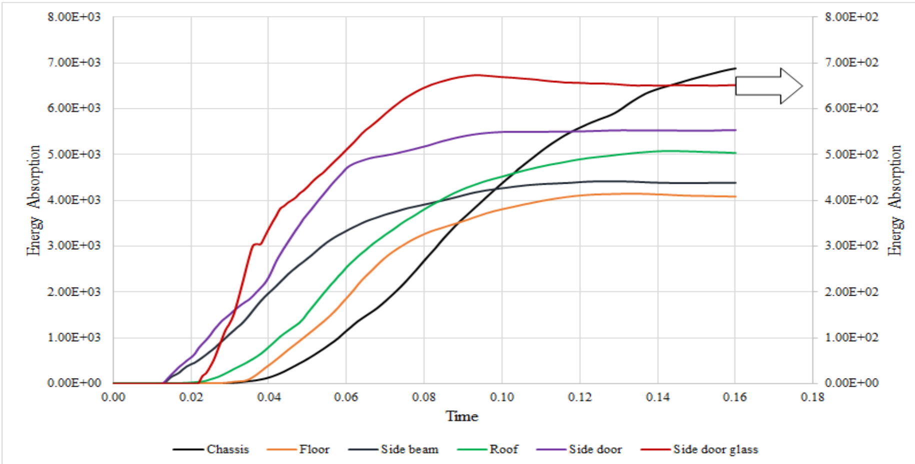

Figure 5.41: Energy absorbed by BPV parts at event of side collision

Contact force

The contact force between the BPV and the rigid pole is shown in the Figure 5.42. Until the time reaches 0.012 s it is minimum. After this point the force starts to increase and shows some fluctuations. As mentioned before the fluctuations are due to the transient (time dependent) behavior of the simulation. The maximum resultant force occurs at t=0.058 s with value equal to 72.4 kN. This value is maintained only for 0.01 s and then drops down, higher force of impact may cause more damage to the occupants.

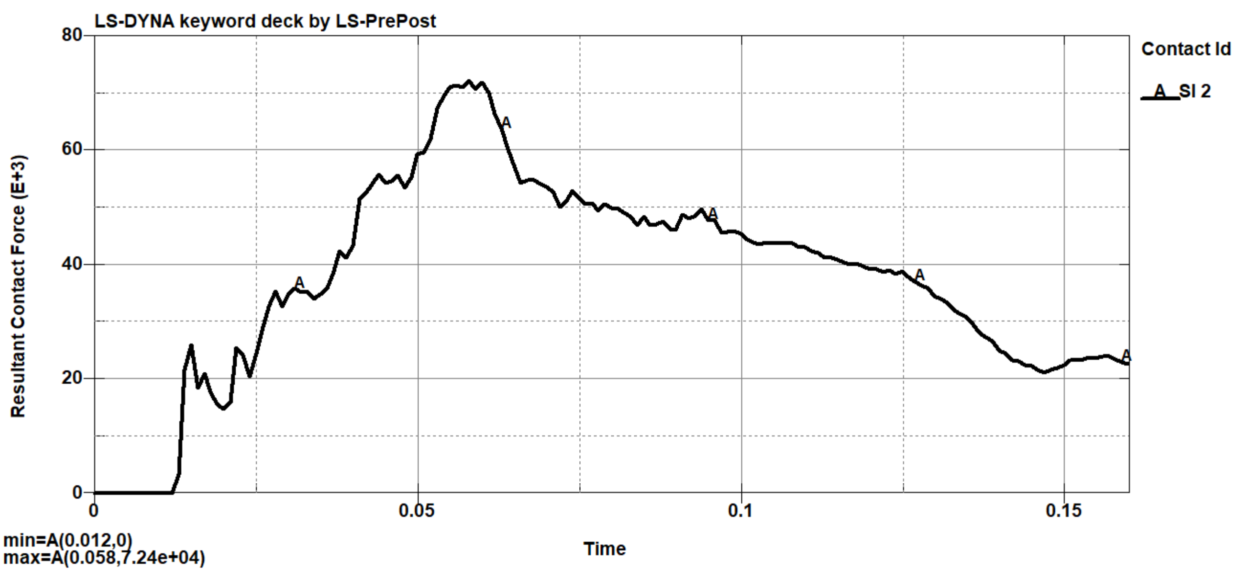

Figure 5.42: Contact force between the side pole and BPV

Resultant velocity

The resultant velocity shows in Figure 5.43. Initially the velocity is 2.19 m/s and as the collision starts the resultant velocity reduces and reaches final value of 0.158 m/s. This shows that plastic deformation occurred on the BPV since the coefficient of restitution is low.

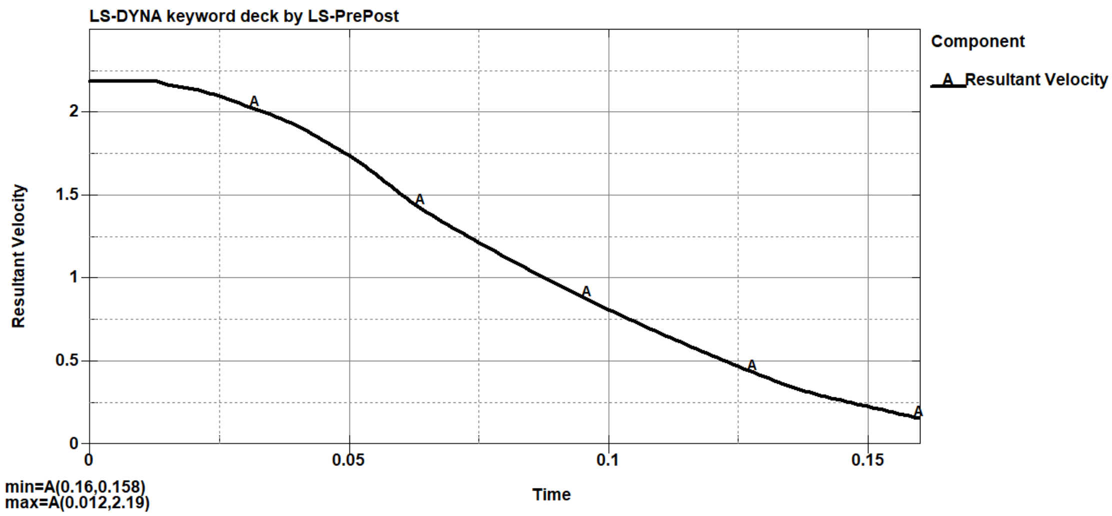

Figure 5.43: Resultant velocity

Validation parameters

Energy ratio

As it can be seen on Figure 5.44, for the 0.16 s simulation the energy ratio value varies between 1 and 0.99978 which is within the range of acceptable value.

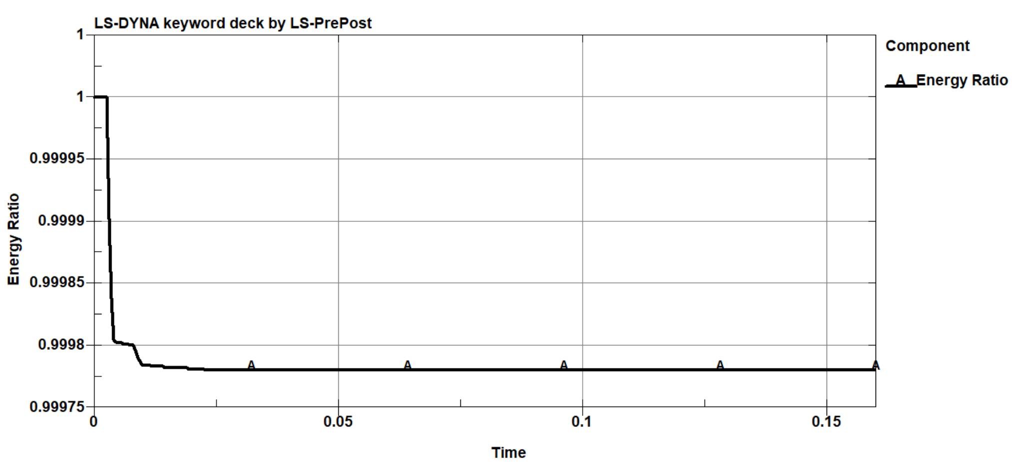

Figure 5.44: Verification: Energy ratio

Ratio of HE/TE

Another means for validating the FEA result is the ratio between the total energy to hourglass energy. As indicated on the graph the energy graph of the hourglass energy is shown on the right vertical axis vs time and the total energy is the left vertical axis vs time. The maximum hourglass energy is equal with 0.833 kJ and the total energy is 54.7 kJ. The ratio between this values (HE/TE) is less than 5%. If the hourglass Energy is less than 5% of the total energy, the finite element model is reliable. Figure 5.45 shows the TE/HE graph.

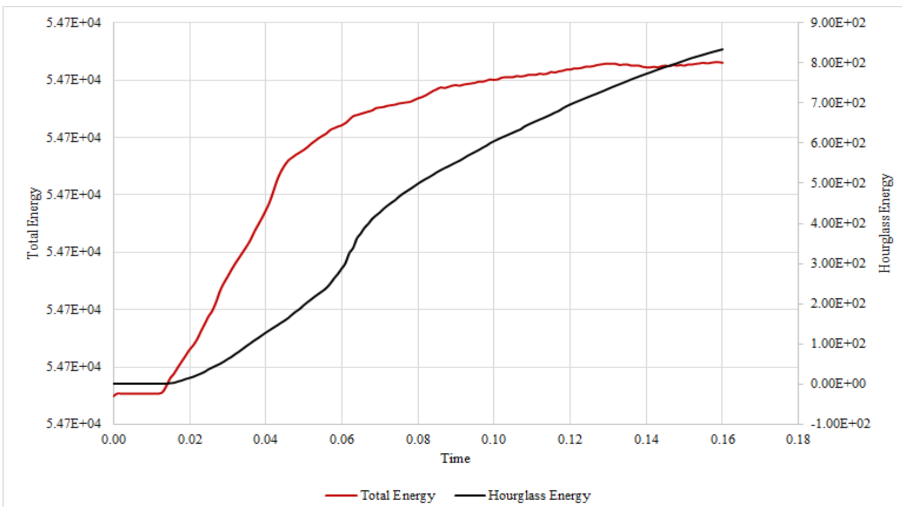

Figure 5.45: Verification: ratio HE/TE

5.6 Comparison between the existing and modified model of BPV

Under this section the crashworthiness ability of the existing and modified model will be compared based on the comparison parameters these are:

- The structural response
- Relative Displacement (Deformation)
- Energy absorption
- Force of impact (contact force)

For each of the crash scenarios the comparisons are discussed as follow.

Frontal crash

Structural response

Figure 5.46 shows the structural response of the existing and modified BPV for 0.16S simulation. From the figure, the structural deformation of the existing BPV vehicles looks more as compared to the modified for example the front fenders of the existing model damage to much whereas the very less for modified one and also the rear wheels of the existing model leaves the ground and rotate whereas slight (little) on the modified. Generally, the structural response of the BPV were determined by comparing the internal energy absorbed and impact energy after collision.

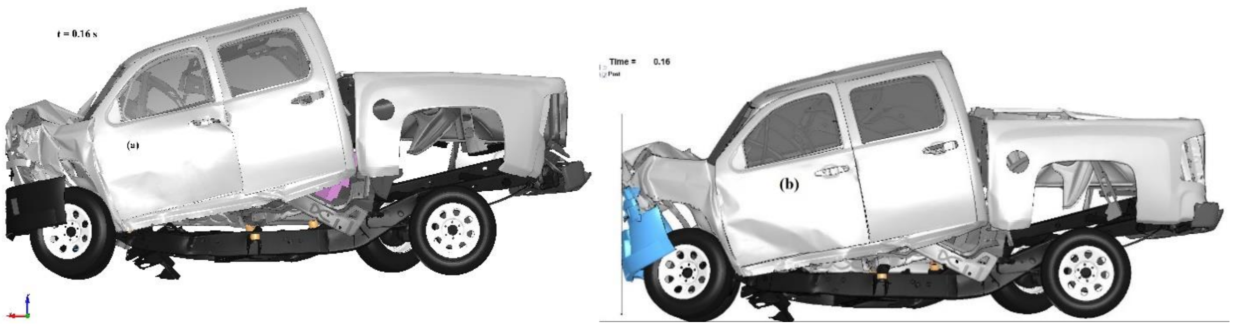

Figure 5.46: Structural response of the existing (a) and modified model (b)

Internal energy

The total energy absorbed by the existing and modified model is shown on figure 5.47. As it can be seen the maximum amount of energy is absorbed during the modified model. This is due to the material properties of bumper used for the modification, as a result these may deformed more and produces more absorption. Their difference in absorption is 5 kJ (3.52 % improvement in energy absorption).

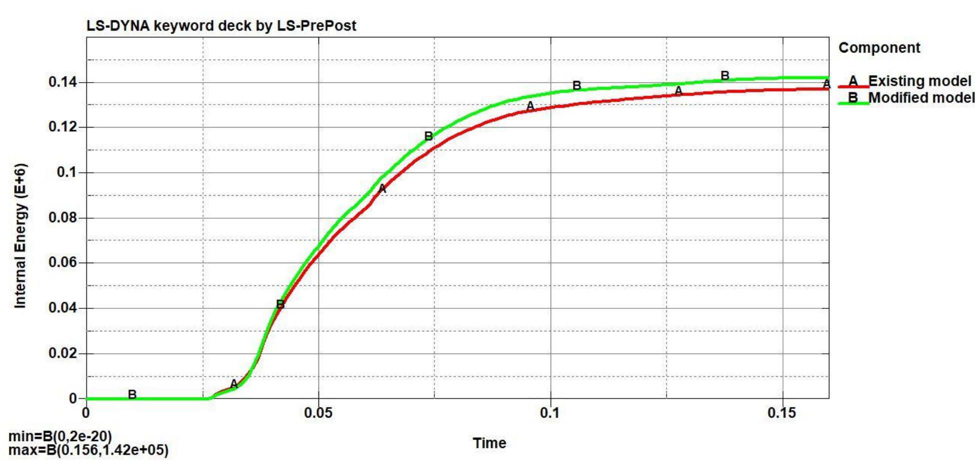

Figure 5.47: Internal energy of modified and existing model

Impact force

In addition to internal energy, the force of impact for the modified model is better as shown on figure 5.48. The maximum impact force occur on the existing model is equal to 499 kN, whereas the modified produced 460 kN, the difference is 39 KN (7.82 % improvement in impact force). This will minimize the driver injury level.

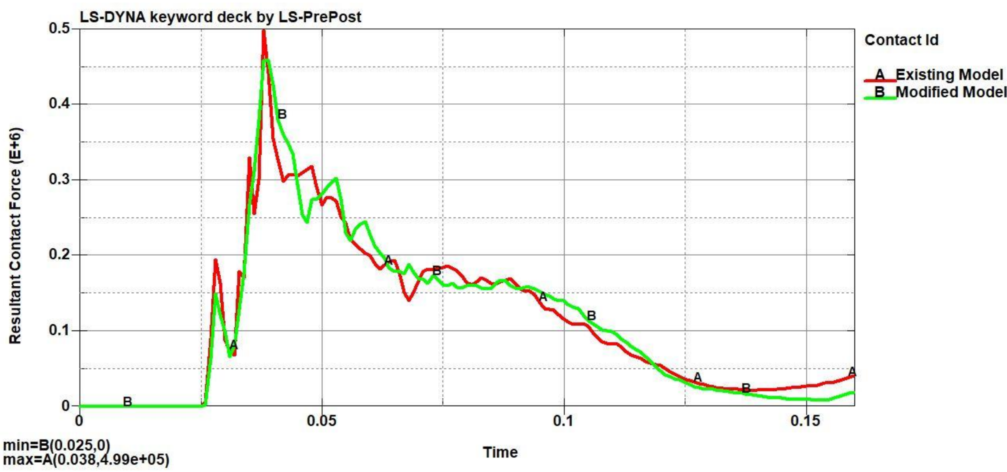

Figure 5.48: Force of impact for modified and existing model

Side crash

Structural response

Figure 5.49 shows the structural response of the existing and modified BPV for 0.16S. The parameter used to compare the structural response is the occupant's living space (intrusion) remains after collision. The pole intrudes 539 mm in case of existing model and 377 mm in case of modified one. The original lateral spacing of the modeled before collision is 1725 mm. Subtracting the intruding distance from the original width will give as the remaining space the existing and modified BPV model remain with 1186 mm and 1348 mm respectively. This shows that the modified model has remain with 162 mm more living space after side pole collision.

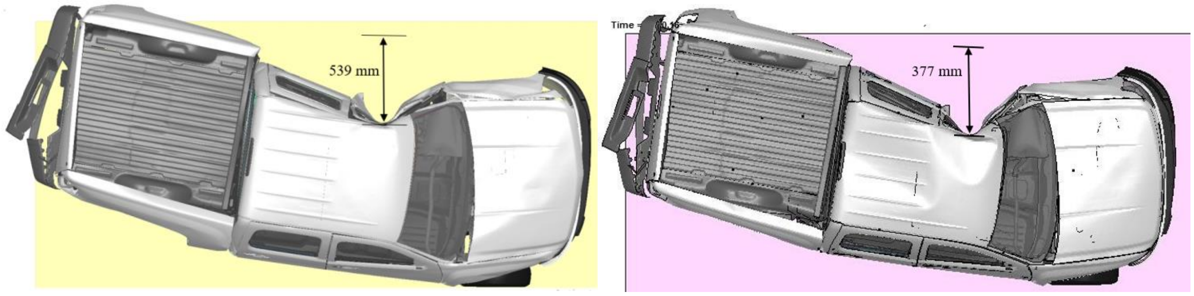

Figure 5.49: The intrusion for the existing model (Left) and for the modified (right)

Relative Displacement

The deformation results on the existing and modified models are shown on Figure 5.50. The red line shows the displacement of the existing BPV and the green line indicate the modified model. The maximum deformation for existing model and modified model is equal to 539 mm and 377 mm respectively. It is clear that the maximum deformation occurs on the existing model.

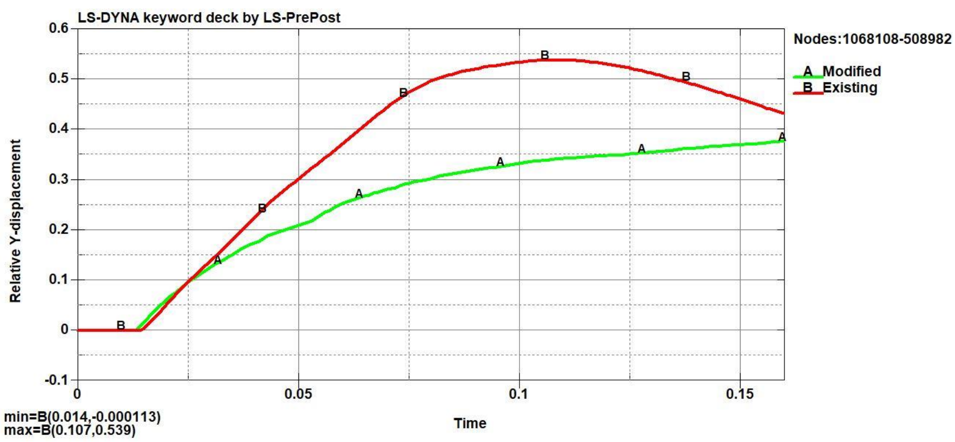

Figure 5.50: Comparison of displacement

Force of impact

The contact force between the BPV and the rigid pole for existing and modified model is shown in the Figure 5.51. The red line indicates existing model and the green one shows the modified model force of impact. From the figure below, the maximum impact force occurs at the existing model with value 84.6 KN whereas the force on the modified model is equal to 72.4 KN. so, their difference equals 12.2 KN. this much difference in force can create more momentum to the vehicle as a result the vehicle is highly damaged. Higher force of impact may cause more damaged to the occupants. So, it can be summarized that the modified model will decrease the impact force on the occupants.

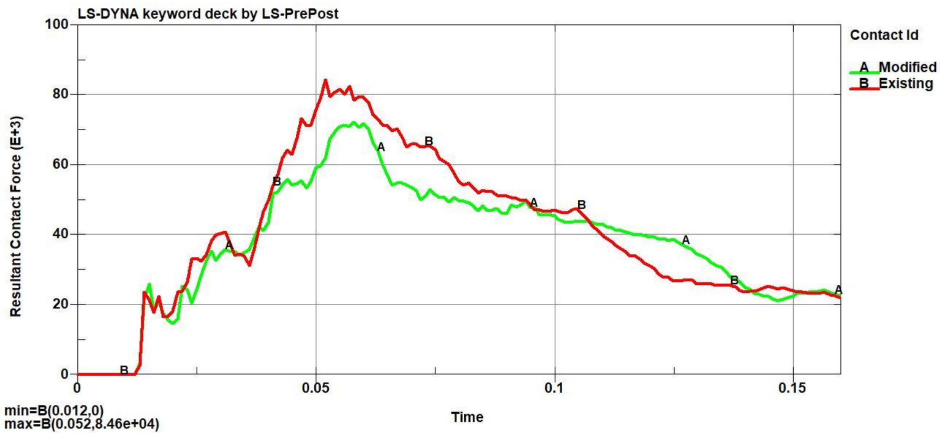

Figure 5.51: Comparison of impact force of the existing and modified BPV

Energy absorption

The absorption energy of the modified and existing model is shown in Figure 5.52. Since the same conditions are applied in the simulation of both models so, the energy absorption capacity of the models is determined by using the total internal energy graph. The models' internal energies are shown with green (modified) and red lines (existing). As it is indicated on the graph among them maximum amount of kinetic energy is absorbed in case of modified model with value equal to 38.2 kJ of internal energy. The existing model remain with 35.3 kJ. This show that for the same condition, the modified model have the ability to absorb more kinetic energy with less deformation. This helps in reducing the energy transferred to the occupants of BPV.

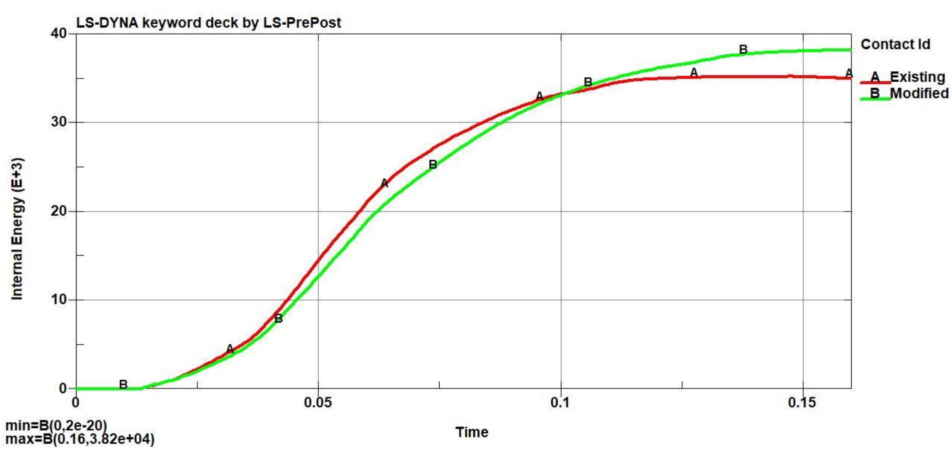

Figure 5.52: Comparison of internal energy

Table 5.1: Summary of comparison between existing and modified material tests

		Existing model	Modified model
For front bumper	Maximum deformation(mm)	212	217
	Maximum Impact force (kN)	65.9	61.3
	Maximum Internal energy(kJ)	3.23	3.51
For side beam	Maximum deformation(mm)	36.1	27.6
	Maximum Impact force (KN)	1.36	1.24
	Maximum Internal energy(J)	25.8	27

Table 5.2: Summary of comparison between existing and modified the whole BPV model

		Existing model	Modified model
For frontal crash	Maximum deformation(mm)	479	493
	Maximum Impact force (kN)	499	460
	Maximum Internal energy(kJ)	137	142
For side crash	Maximum deformation(mm)	539	377
	Maximum Impact force(kN)	84.6	72.4
	Maximum Internal energy(kJ)	35.3	38.2

Validation

In addition to verification and comparison, the finite element model analysis is validated with a real-time crash of the NCAP crash test. As it can be seen from the figure the simulation result is much similar to the real crash. The fact that/ there is a slight difference on the hood of the FEA model Vs the real model due to that, the material model of the FEA Bishoftu pickup is not the same as other pickups. Figure 5.53 show the simulation sequence of FEM of BPV vs the real crash of pickup.

Figure 5.53: Sequence of Frontal crash FEA Vs real NCAP crash test

Figure 5.54 shows that the sequence of BPV side pole test to validate with NCAP real time test. As shown in the figure, the FEM simulation is much similar to the real time test. There is little difference on the side door glass, that is the property given in the FEM model is piecewise linear plastisty. The other difference between the two are in NCAP real time test the vehicle is rotated to 75° to the rigid pole whereas in FEM the pole is rotated 75° to the vehicle.

Figure 5.54: Sequence of side pole crash FEA Vs real NCAP crash test

CHAPTER SIX

CONCLUSION AND RECOMMENDATION

6.1 Summary of the Study

As it has been indicated in the introduction part, the main objective of this thesis work was to improve the crashworthiness of Bishoftu pickup vehicle for frontal and side collision. Before inter in to the modification the required data about the vehicle is collected. Then the analysis of the existing frame structure is done with different speed ranges and select the average speed of 60 km/hr for frontal and 32 km/hr for side collision for comparison. For both cases NCAP regulation is used throughout the simulation.

In doing so CATIA and LS DYNA software is used for 3D modeling and analysis of crashworthiness respectively. The results of the existing vehicle is checked for verification by using energy ratio and the ratio between hourglass and total energy. After analyzing the existing vehicle for both collision cases, weak and strong parts are identified and modification is done based on this.

Modification is done on both frontal and side parts of the vehicle. The material properties used for both is selected based on their cases. For the frontal case, more deformable, high-energy absorbent and low impact energy is needed because it has a space up to the driver cabin. For this reason, closed cell aluminum foam is used for its performance on the criteria. Before assembling in to the vehicle the material is tested individually and get improvement of 6.98% in impact force and 7.98% in internal energy.

For the side case, good crash performance and low intrusion to the occupant because there is small space between the occupant seat and side door. For this reason, DP 980 AHSS is used, and analysis is done with the same as the existing. When the material is tested, 8.82% in impact force, 4.45% in internal energy and 23.55% in intrusion to the cabin is improved during side collision. By doing the modification all the objectives are achieved. And finally, the validity of the crash process is checked by the structural response between the FEM and real time NCAP test. The mass of the modified vehicle is minimized and the percentage decrement also stated.

6.2 Conclusion

The study clearly states the problems exist on BPV at event of each of the crash scenarios. Thus, NCAP standards and regulations are used to numerically analyze the crashworthiness of the current BPV. The frontal and side collision of the existing BPV is analyzed. In addition, based on the results obtained from the existing model an attempt was made to modify the structural crashworthiness of the vehicle. As a result, the modified BPV has improved crashworthiness features and gives better safety for occupants.

The modified model shows better protection by deforming more as compared to the existing model during frontal collision, it gives protection to the occupant compartment after collision: -

- Among the initial kinetic energy, 167.52 kJ of kinetic energy which is 97.3% is lost in the existing model where as for the modified model, the loss of kinetic energy is 170.73 kJ which is 97.56% of the total energy or the initial kinetic energy during frontal collision.
- The total energy absorbed by the modified model is more as compared to the existing model, in addition the force of impact is also less. This is due to the mechanical properties of the material used for the modification, as a result they deformed more and produces more absorption and low impact force as compared to the existing one. The modified model provides 7.82% less contact force and 3.52% more energy absorption. So, the absorption capacity of the modified model is better. When considering the mass, the modified model decreases the mass by 0.18%.

When considering side collision, the modified model gives better protection by deforming less as compared to the existing model.

- Among the initial kinetic energy, 46.19 kJ of kinetic energy which is 85.54% is lost in the existing model where as for the modified model, the loss of kinetic energy is 47.16 kJ which is 87.33% of the total energy or the initial kinetic energy during side collision.
- The structure of the modified model has produced more living space than that of the existing model by only deforming 377 mm whereas the existing model deformed 539 mm this shows that at event of side collision the modified model provides more protection to the occupants and the vehicle sensitive parts.

- The impact force produced due to the collision of the vehicle in to the pole is less for the modified model. A reduction of contact force implies that the transferred impact energy to the occupants is reduced (minimized). So, a reduction of 12.2 kN (14.42%) force was obtained by the implementation of the modifications. And also decreases the mass by 0.2% as compared to the existing model.
- The modified model also absorbs more energy than the exiting model. It absorbed additional 2.9 kJ (7.59%) energy.

6.3 Recommendation

Based on the studies done on this thesis work the following points are recommended:

- It can be observed that with little modification the safety of the current BPV can be improved, so that the owners and manufacturers shall implement some of the safety developments concepts discussed on this thesis work to improve the crash worthiness of the BPV.
- As the study shows even with average and less speed the BPV has causing more sever damages, so it is better if the government and concerning bodies implement the crash and safety regulation for pickups which are play avital role on the economy of our country.

6.4 Future scope of the work

Considering the review of the existing research limitations and results the motivations for future research are suggested as follows:

- The present work evaluated the crash behavior of existing Bishoftu pickup vehicles by considering the response of the structure and this work can be extended to evaluating the response and injury level to occupants at different crash scenarios.
- This work does not include rear impact and rollover test. So, it does not include the effect on rear components of the BPV as well as the roof, so the effect of both rear and rollover collisions on the components of the vehicle can be studied in the future.
- BPV is hard for making body maintenance specially by arc welding this is because of the material used so, for the future research should be done on this area to increase the quality of the pickup.

Research Fund Acknowledgment

I would like to sincerely thank ASTU for the opportunity it has given me to complete my masters study. This research project is funded by Adama Science and Technology University under the grant Number ASTU/SM-R/644/22, Adama, Ethiopia.

REFERENCES

A. E. Ikpe1*, I. B. O. and P. S. (2017). Design optimization of a B-pillar for crashworthiness of vehicle side impact. Journal of Mechanical Engineering and Sciences, 1(69), 2693–2710.

Abdulqadir, S. F., & Tarlochan, F. (2022). Composite Hat Structure Design for Vehicle Safety: Potential Application to B-Pillar and Door Intrusion Beam. Materials, 15(3). https://doi.org/10.3390/ma15031084

Aluminium Foam | Properties and applications | Materials Hub. (2022). https://www.materialshub.com/material/aluminium-foam/

AMBATI, T., SRIKANTH, K. V. N. S., & VEERARAJU, P. (2012). Simulation of Vehicular Frontal Crash-Test. International Journal of Applied Research in Mechanical Engineering, 1, 262–267. https://doi.org/10.47893/ijarme.2012.1047

Asefa, F., Assefa, D., & Tesfaye, G. (2014). Magnitude of, trends in, and associated factors of road traffic collision in central Ethiopia. BMC Public Health, 14(1), 1–11. https://doi.org/10.1186/1471-2458-14-1072

Aysha, M. (2020). CATIA, all you need to know about this CAD software. In 3Dnatives. https://www.3dnatives.com/en/catia-cad-310720204/#!

Baltazar Hernandez, V. H., Panda, S. K., Okita, Y., & Zhou, N. Y. (2010). A study on heat affected zone softening in resistance spot welded dual phase steel by nanoindentation. Journal of Materials Science, 45(6), 1638–1647. https://doi.org/10.1007/s10853-009-4141-0

Chen, D. Y., Wang, L. M., Wang, C. Z., Yuan, L. K., Zhang, T. Y., & Zhang, Z. Z. (2015). Finite element based improvement of a light truck design to optimize crashworthiness. International Journal of Automotive Technology, 16(1), 39–49. https://doi.org/10.1007/s12239-015-0004-7

Dagdeviren, S., Yavuz, M., Kocabas, M. O., Unsal, E., & Esat, V. (2016). Structural crashworthiness analysis of a ladder frame chassis subjected to full frontal and pole side impacts. International Journal of Crashworthiness, 21(5), 477–493. https://doi.org/10.1080/13588265.2015.1135522

Dange, M. V, Buktar, R. B., & Raykar, N. R. (2015). Design and Analysis of an Automotive Front Bumper Beam for Low-Speed Impact. IOSR Journal of Mechanical and Civil Engineering Ver, 12(2), 2320–2334. https://doi.org/10.9790/1684-12241727

Desapriya, E. (2011). Vehicle safety standards. Traffic Safety, 201–222.

driverseducationusa.com. (2021). What forces are involved in a crash ? (pp. 1–2).

Duan, L., Sun, G., Cui, J., Chen, T., Cheng, A., & Li, G. (2016). Crashworthiness design of vehicle structure with tailor rolled blank. Structural and Multidisciplinary Optimization, 53(2), 321–338. https://doi.org/10.1007/s00158-015-1315-z

For, G., & Vehicle, A. (2021). Guidelines for Authorizing Vehicle (pp. 1–4).

Friedman, K., Mihora, D., & Hutchinson, J. (2018). Heavy truck front-end deployable system opportunities for crash compatibility with passenger vehicles. International Journal of Crashworthiness, 23(2), 161–172. https://doi.org/10.1080/13588265.2017.1290735

Frontal crash test with limo. (2022).

Gao, G., & Wang, S. (2019). Crashworthiness of passenger rail vehicles: a review. International Journal of Crashworthiness, 24(6), 664–676. https://doi.org/10.1080/13588265.2018.1511233

Georgiou, G., & Zeguer, T. (2018). On the assessment of the macro-element methodology for full vehicle crashworthiness analysis. International Journal of Crashworthiness, 23(3), 336–353. https://doi.org/10.1080/13588265.2017.1328723

Ghadianlou, A., & Abdullah, S. Bin. (2013). Crashworthiness design of vehicle side door beams under low-speed pole side impacts. Thin-Walled Structures, 67, 25–33. https://doi.org/10.1016/j.tws.2013.02.004

Gu, X., Sun, G., Li, G., Mao, L., & Li, Q. (2013). A Comparative study on multiobjective reliable and robust optimization for crashworthiness design of vehicle structure. Structural and Multidisciplinary Optimization, 48(3), 669–684. https://doi.org/10.1007/s00158-013-0921-x

Gulavani, O., Hughes, K., & Vignjevic, R. (2014). Explicit dynamic formulation to demonstrate compliance against quasi-static aircraft seat certification loads (CS25.561) -Part I: Influence of time and mass scaling. Proceedings of the Institution of Mechanical Engineers, Part G: Journal of Aerospace Engineering, 228(11), 1982–1995. https://doi.org/10.1177/0954410013506333

Horstemeyer, M. F., Ren, X. C., Fang, H., Acar, E., & Wang, P. T. (2009). A comparative study of design optimisation methodologies for side-impact crashworthiness, using injury-based versus energy-based criterion. International Journal of Crashworthiness, 14(2), 125–138. https://doi.org/10.1080/13588260802539489

Huh, H., Kim, K. P., Kim, S. H., Song, J. H., Kim, H. S., & Hong, S. K. (2003). Crashworthiness assessment of front side members in an auto-body considering the fabrication histories. International Journal of Mechanical Sciences, 45(10), 1645–1660. https://doi.org/10.1016/j.ijmecsci.2003.09.022

Ibrahim, T. M. H. T., Hafeez, T. M. (2014). a Study of Crashworthiness Characteristic of Woven. January.

Ikpe, A. E., Orhorhoro, E. K., & Gobir, A. (2017). Design and reinforcement of a B-pillar for occupants safety in conventional vehicle applications. International Journal of Mathematical, Engineering and Management Sciences, 2(1), 37–52. https://doi.org/10.33889/ijmems.2017.2.1-004

Kiani, M., & Yildiz, A. R. (2016). A Comparative Study of Non-traditional Methods for Vehicle Crashworthiness and NVH Optimization. Archives of Computational Methods in Engineering, 23(4), 723–734. https://doi.org/10.1007/s11831-015-9155-y

KiranKumar, K. N., Rajasekhar, D. A., chander, D. P. R., Reddy, Y. M. M., & K, V. (2019). Design Evaluation & Improvement Analysis of Vehicle Structural Crashworthiness using CAE in IIHS Frontal Crash Test. International Journal of Engineering and Advanced Technology, 9(1), 1575–1582. https://doi.org/10.35940/ijeat.f8597.109119

Kocabas, O., & Modelling, P. (2019). Structural crashworthiness analysis of a pickup truck subjected. April.

Krusper, A., & Thomson, R. (2010). Energy-absorbing FUPDs and their interactions with fronts of passenger cars. International Journal of Crashworthiness, 15(6), 635–647.

https://doi.org/10.1080/13588265.2010.491714

Kumar Nijagal Honnagangaiah. (2016). Design and evaluation of composite car-front subframe rails in a sedan and its corresponding occupant crash injury response. May.

Kunle, M. A., Farah, M. J., Ahmed, A. /hakim, & Mohamed. (2019). Auto Rickshaw Impacts with Pedestrians - A Computational Analysis of Post- Collision Kinematics and Injury Mechanics A Thesis Submitted to Cardiff University for the Degree of Doctor of Philosophy By. September.

Lebaal, N., Jeyanthi, S., Davidson, J., Leninbabu, M. C., Prabhaharan, S. A., Balaji, G., & Annamalai, K. (2022). Numerical simulation of crashworthiness parameters for design optimization of an automotive crash-box. International Journal for Simulation and Multidisciplinary Design Optimization, 13, 1–11. https://doi.org/10.1051/smdo/2021036

Lefer, B., & Rebolloso, I. (2012). Car-to-Truck Frontal Crash Compatibility. http://publications.lib.chalmers.se/records/fulltext/160351.pdf

Li, Q. Q., Li, E., Chen, T., Wu, L., Wang, G. Q., & He, Z. C. (2021). Improve the frontal crashworthiness of vehicle through the design of front rail. Thin-Walled Structures, 162(February). https://doi.org/10.1016/j.tws.2021.107588

Liu et al. (2021). Collaborative Optimization Of Vehicle crashworthiness under frontal impacts based on displacement oriented structure. International journal of Automotive Technology.

Liu, Y. P. (2013a). Simulation of vehicle's frontal crash with dummy inside. Advanced Materials Research, 760–762(Iccsee), 1244–1249. https://doi.org/10.4028/www.scientific.net/AMR.760-762.1244

Liu, Y. P. (2013b). Simulation of vehicle's frontal crash with dummy inside. Advanced Materials Research, 760–762, 1244–1249. https://doi.org/10.4028/www.scientific.net/AMR.760-762.1244

Livermore Software Technology Corporation. (2003). L{S}-{DYNA} - {K}eyword {U}ser's {M}anual, Version 970: Vol. I (Issue May).

LS-DYNA support site. (2022).

M. Ozan KOCABAŞ, Eren ÜNSAL, V. E. (2014). STRUCTURAL ANALYSIS OF PICKUP TRUCK SUBJECTED TO POLE SIDE IMPACTS.

Mahajan, G. B., & Kamble, D. N. (2016). Crash and impact strength analysis of structural component of the vehicle for occupant safety. International Journal of Science, Engineering and Technology Research, 4(12), 4288–4293.

Marzougui, D., Kan, C. D., & Opiela, K. S. (2014). Crash Test & Simulation Comparisons of a Pickup Truck & a Small Car Oblique Impacts Into a Concrete Barrier. 13th International LS-DYNA Users Conference, 1–18.

Mihradi, S., Golfianto, H., Mahyuddin, A. I., & Dirgantara, T. (2017). Head injury analysis of vehicle occupant in frontal crash simulation: Case study of ITB's formula SAE race car. Journal of Engineering and Technological Sciences, 49(4), 534–545. https://doi.org/10.5614/j.eng.technol.sci.2017.49.4.8

Muhammad, N. S., Hambali, A., Rosidah, J., Widodo, W. S., & Ahmad, M. N. (2017). A review of energy absorption of automotive bumper beam. International Journal of Applied Engineering Research, 12(2), 238–245.

NHTSA Crash Test - Consumer Reports. (2014). In Consumerreports.Org. https://www.consumerreports.org/cro/2011/08/crash-test-101/index.htm

Pahlavani, M., & Marzbanrad, J. (2015). Crashworthiness study of a full vehicle-lumped model using parameters optimisation. International Journal of Crashworthiness, 20(6), 573–591. https://doi.org/10.1080/13588265.2015.1068910

Park, C. K., Kan, C. D., & Hollowell, W. T. (2013). Investigation of crashworthiness of structural composite components in frontal and side NCAP tests. SAE Technical Papers, 2(6). https://doi.org/10.4271/2013-01-0650

Patel, S., Vusa, V. R., & Guedes Soares, C. (2019). Crashworthiness analysis of polymer composites under axial and oblique impact loading. International Journal of Mechanical Sciences, 156(December 2018), 221–234. https://doi.org/10.1016/j.ijmecsci.2019.03.038

Peng, Y., Wang, S., Yao, S., & Xu, P. (2017). Crashworthiness analysis and optimization of a cutting-style energy absorbing structure for subway vehicles. Thin-Walled Structures, 120(September), 225–235. https://doi.org/10.1016/j.tws.2017.09.006

Rajappan, R., & Vivekanandhan, M. (2013). Static and modal analysis of chassis by using FEA. International Journal of Computational Engineering Research, 3(4), 63–73.

Redscan. (2017). What is a Penetration Test? In Redscan Blog (Issue Mar, pp. 1–10). https://www.redscan.com/news/what-is-a-penetration-test/

Reichert, R., Kan, S., Arnold-Keifer, S., & Mueller, B. (2018). IIHS Side Impact Parametric Study using LS-DYNA. 15th International LS-DYNA USers Conference, 1–12. https://www.dynalook.com/conferences/15th-international-ls-dyna-conference/occupant-protection/iihs-side-impact-parametric-study-using-ls-dyna-r

Seyedi, M. R., Jung, S., Wekezer, J., Kerrigan, J. R., & Gepner, B. (2020). Rollover crashworthiness analyses–an overview and state of the art. International Journal of Crashworthiness, 25(3), 328–350. https://doi.org/10.1080/13588265.2019.1593290

side crash in NE Harris County - Free Texas Accident Report. (2022).

Singh, H. (Edag I. . (2012). Mass Reduction for Light-Duty Vehicles for Model Years 2017-2025 Final Report. Report No. DOT HS 811 666, August, 582.

Soltani, M., Topa, A., Karim, M. R., & Sulong, N. H. R. (2017). Crashworthiness of G4(2W) guardrail system: a finite element parametric study. International Journal of Crashworthiness, 22(2), 169–189. https://doi.org/10.1080/13588265.2016.1243636

Song, L., Fender, J., & Duddeck, F. (2015). A Semi-Analytical Approach to Identify Solution Spaces for Crashworthiness in Vehicle Architectures. 24th International Technical Conference on the Enhanced Safety of Vehicles, 1–12. https://www-esv.nhtsa.dot.gov/proceedings/24/files/24ESV-000183.PDF

Srikanth, K. M., & Prakash, R. V. (2009). Assessing the structural crashworthiness of a three-wheeler passenger vehicle. The 2nd International Conference on Research into Design., 152–159.

Srikantha, K., S, M. B. N., & K, M. K. (2017). Impact Analysis of Toyota Land Cruiser Car Bumper Using Ansys Autodyn 3D. 4(12), 29–37.

https://doi.org/10.26562/IJIRAE.2017.DCAE10087

Teng, T. L., Chang, K. C., & Nguyen, T. H. (2008). Crashworthiness Evaluation of Side-Door Beam of Vehicle. Technische Mechanik - European Journal of Engineering Mechanics, 28(3–4), 268–278. https://journals.ub.ovgu.de/index.php/techmech/article/view/848

Toy, E. L., & Hammitt, J. K. (2003). Safety impacts of SUVs, vans, and pickup trucks in two-vehicle crashes. Risk Analysis, 23(4), 641–650. https://doi.org/10.1111/1539-6924.00343

Tuljapure, S. B. (2015). Study of Energy Absorption of Rectangular Tube of Bumper of Light Commercial Vehicle. 3175–3181. https://doi.org/10.15680/IJIRSET.2015.0405100

Tulu, G. S., Washington, S., & King, M. J. (2013). Characteristics of Police-reported Road Traffic Crashes in Ethiopia over a Six Year Period. 1–13.

Vangi, D., Begani, F., Gulino, M. S., & Spitzhüttl, F. (2018). A vehicle model for crash stage simulation. 51(2), 837–842. https://doi.org/10.1016/j.ifacol.2018.04.018

Vedantam, R. (2018). Automotive Rear-End Crash Simulations According To Fmvss 310R for Evaluation of Structural Damage and Prediction of Occupant Potential Injuries Through Linear Regression. December.

Wang, D., Zhang, J., Ma, Y., & Jin, Y. (2021). Analytical modeling and collaborative optimization of the dynamic responses for barrier-vehicle-occupant system considering crashworthiness and compatibility. Structural and Multidisciplinary Optimization, 64(1), 349–367. https://doi.org/10.1007/s00158-021-02877-4

Wang, Tao, Wang, L., Wang, C., & Zou, X. (2018). Crashworthiness analysis and multi-objective optimization of a commercial vehicle frame: A mixed meta-modeling-based method. Advances in Mechanical Engineering, 10(5), 1–12. https://doi.org/10.1177/1687814018778480

Wang, Tie, & Li, Y. (2015). Design and analysis of automotive carbon fiber composite bumper beam based on finite element analysis. Advances in Mechanical Engineering, 7(6), 1–12. https://doi.org/10.1177/1687814015589561

WHO. (2020). Motorcycle ABS to Save Lives 1.

https://extranet.who.int/iris/restricted/bitstream/handle/10665/330720/9789290227441-eng.pdf?sequence=1&isAllowed=y

Xu, T., Sheng, X., Zhang, T., Liu, H., Liang, X., & Ding, A. (2018). Development and validation of dummies and human models used in crash test. Applied Bionics and Biomechanics, 2018. https://doi.org/10.1155/2018/3832850

Yadav, S., & Pradhan, S. K. (2014). Investigations into dynamic response of automobile components during crash simulation. Procedia Engineering, 97, 1254–1264. https://doi.org/10.1016/j.proeng.2014.12.404

Yang, Y., Chen, H., Zhang, R., Chen, H., & Qiang, X. (2014). Vehicle seat structure optimization in front and rear impact. Open Mechanical Engineering Journal, 8(May), 599–606. https://doi.org/10.2174/1874155x01408010599

Yu, L., Gu, X., Qian, L., Jiang, P., Wang, W., & Yu, M. (2021). Application of tailor rolled blanks in optimum design of pure electric vehicle crashworthiness and lightweight. Thin-Walled Structures, 161(January), 107410. https://doi.org/10.1016/j.tws.2020.107410

Zahedan, N., Ahmadi, H., & Liaghat, G. H. (2022). Experimental and numerical investigation on the multi-optimization of reinforcing the side members of the vehicle structure. Archives of Civil and Mechanical Engineering, 22(1), 1–18. https://doi.org/10.1007/s43452-021-00351-y

Zegeye, K. (2020). Modification and Crash Analysis of Frontal Frame Structure of a Small Car with Different Composite Materials for Improving Self Protection in a Frontal Crash. International Journal of Mechanical Engineering Research (IJMER), 1(4), 48–55.

Zhu, P., Pan, F., Chen, W., & Viana, F. A. C. (2013). Lightweight design of vehicle parameters under crashworthiness using conservative surrogates. Computers in Industry, 64(3), 280–289. https://doi.org/10.1016/j.compind.2012.11.004

Zhu, T., Xiao, S., Lei, C., Wang, X., Zhang, J., Yang, B., Yang, G., & Li, Y. (2021). Rail vehicle crashworthiness based on collision energy management: an overview. International Journal of Rail Transportation, 9(2), 101–131. https://doi.org/10.1080/23248378.2020.1777908

Appendix – A

Vehicle dimension

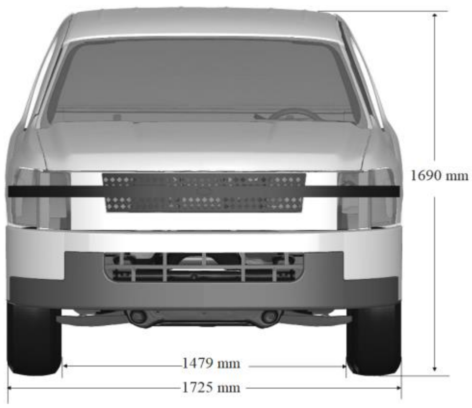

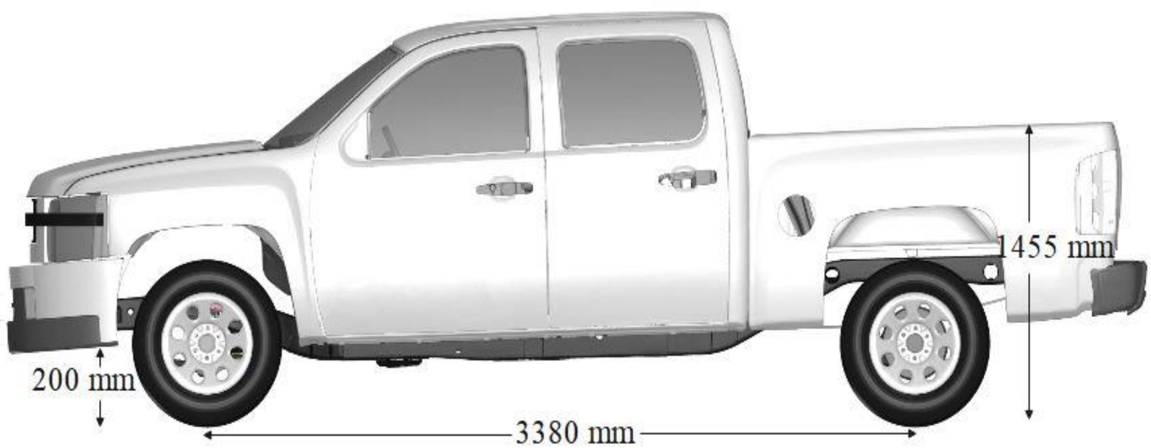

Appendix – B

Results for frontal existing

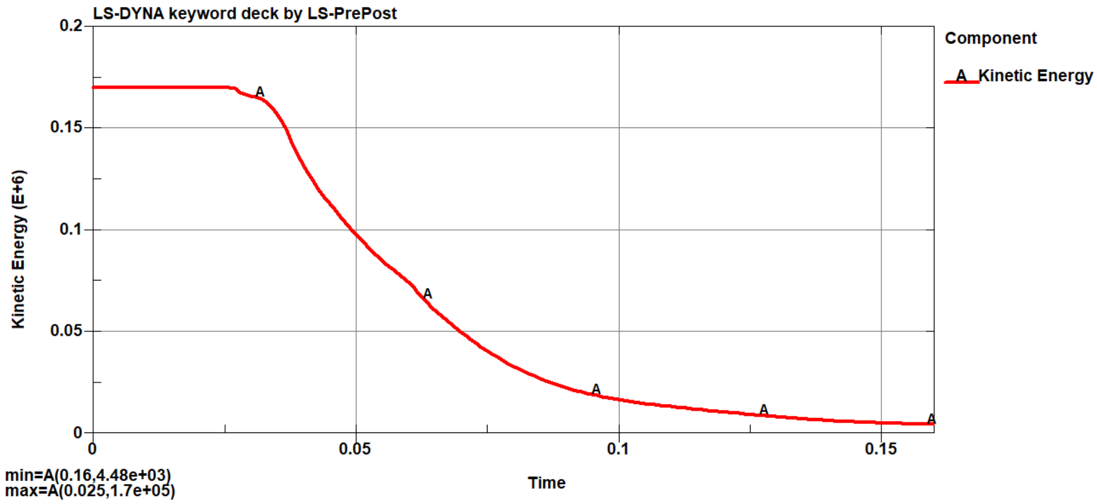

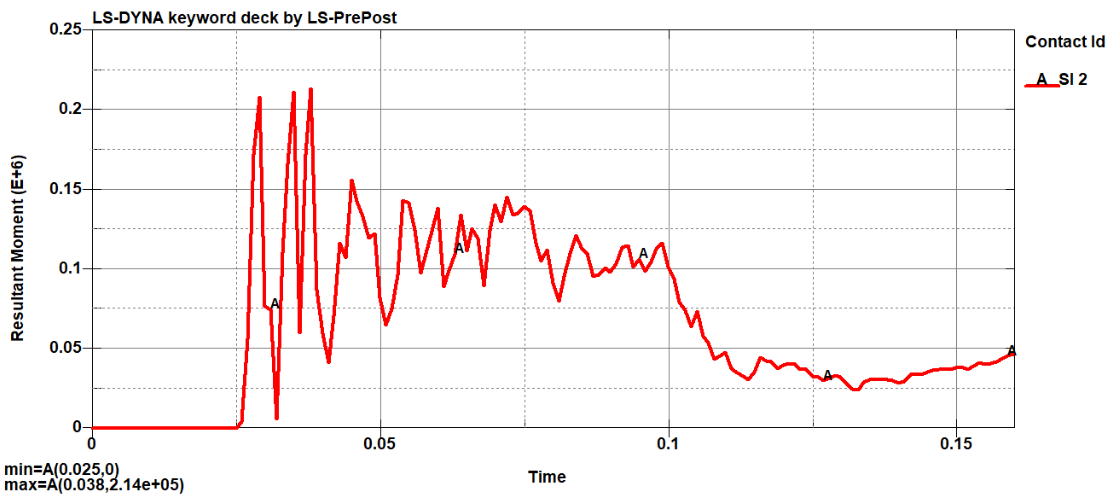

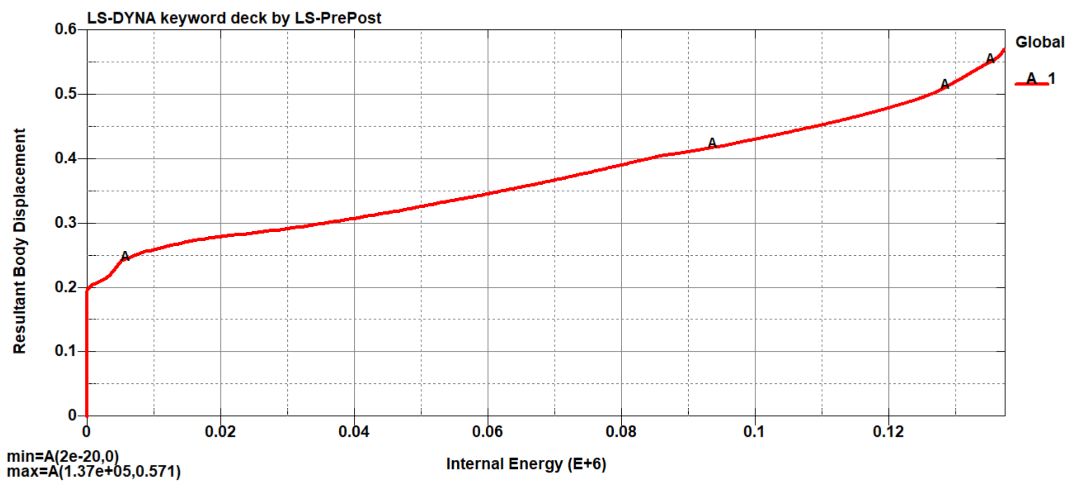

Results for side existing

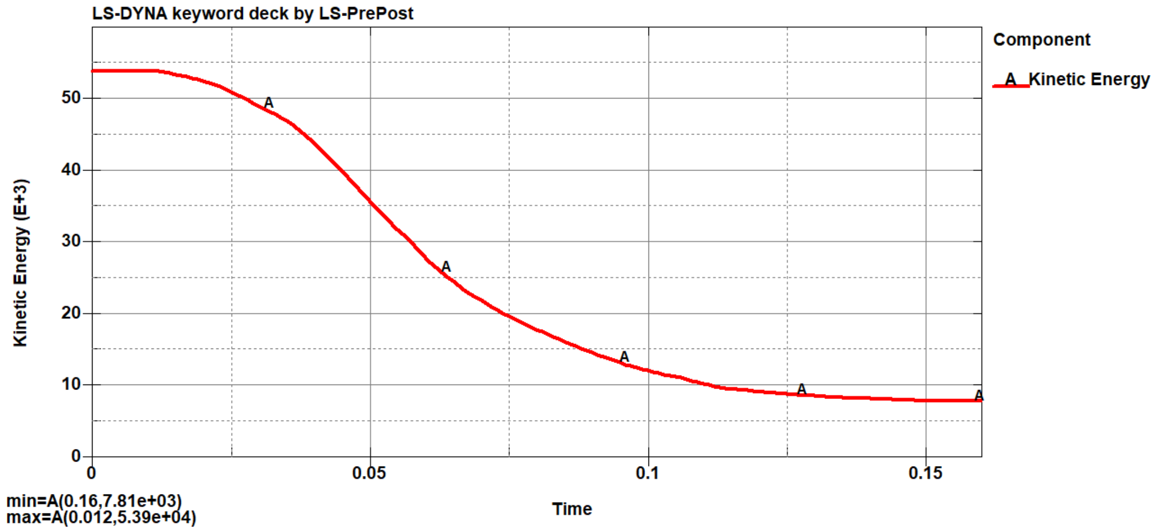

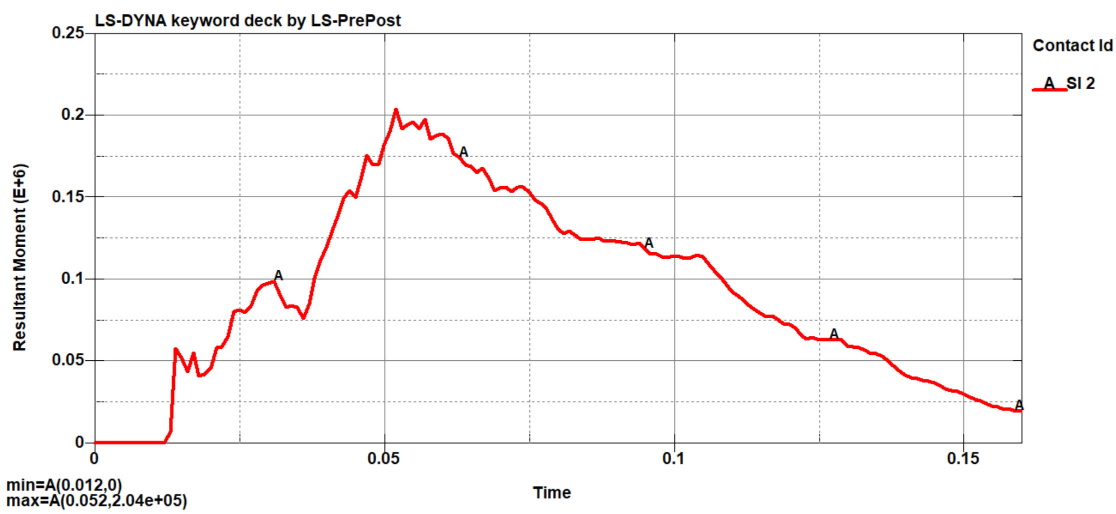

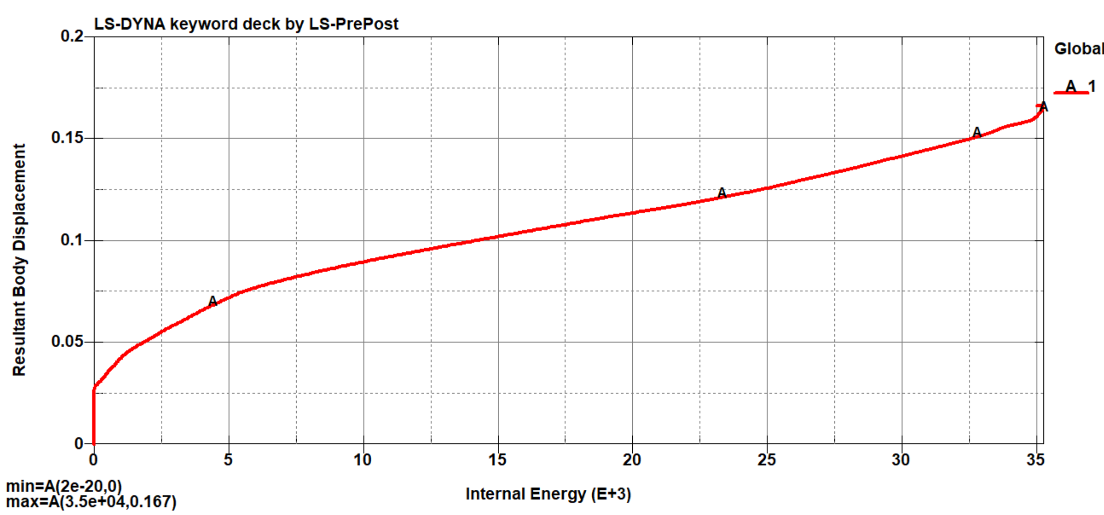

Results for frontal modified

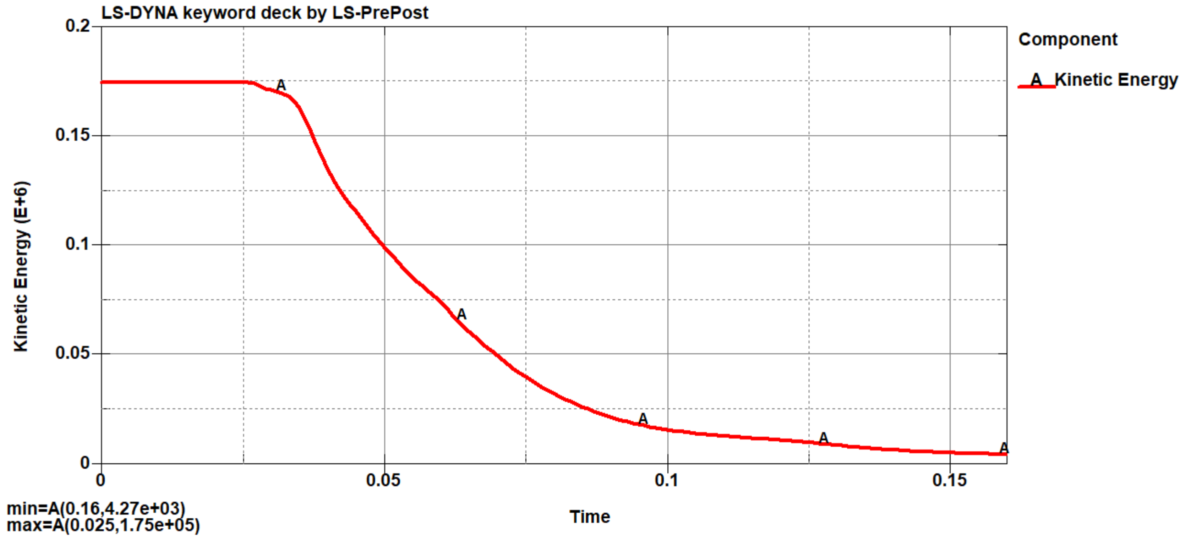

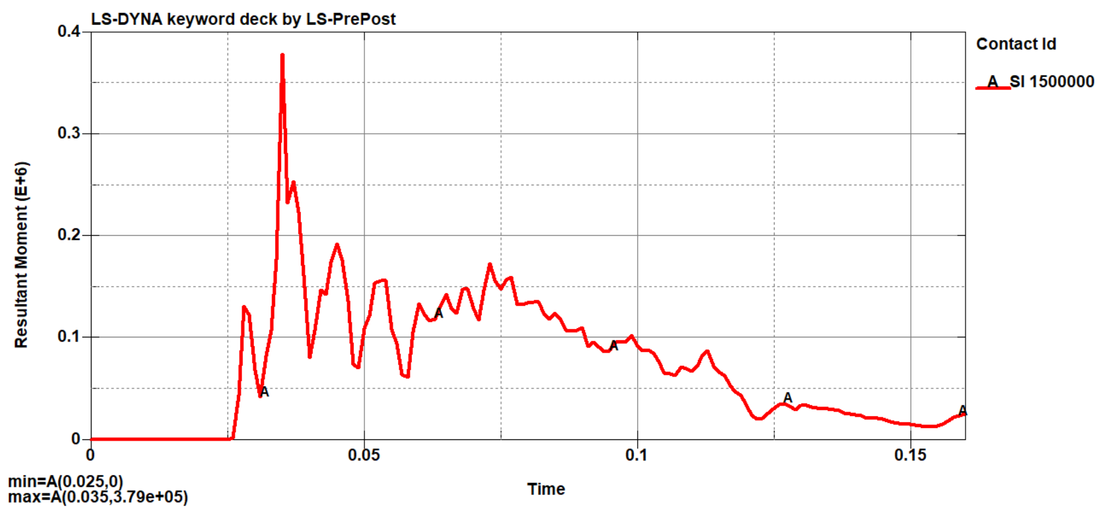

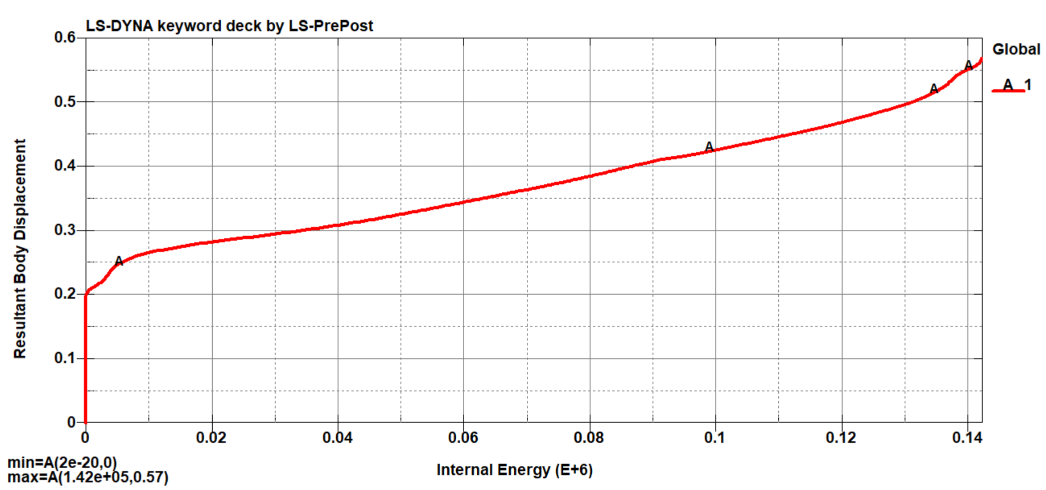

Results for side modified

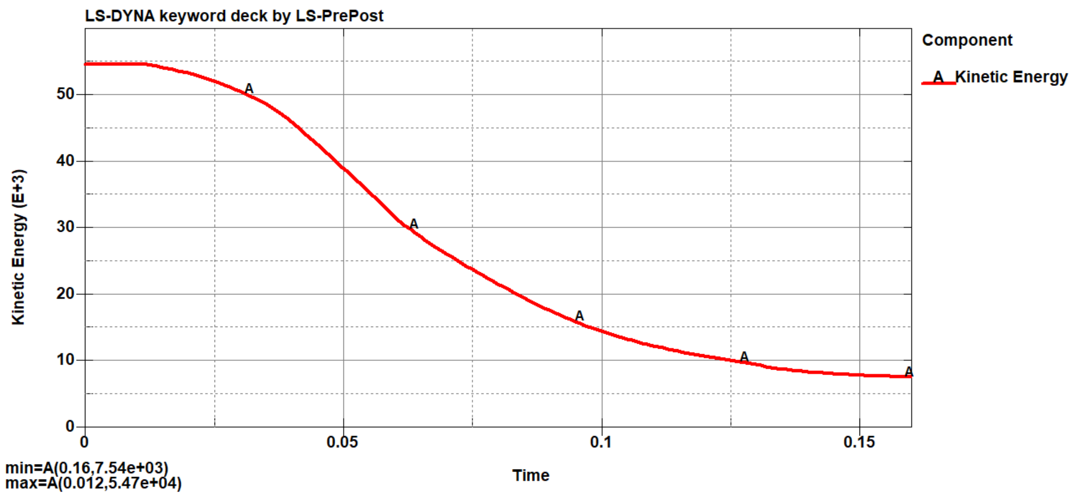

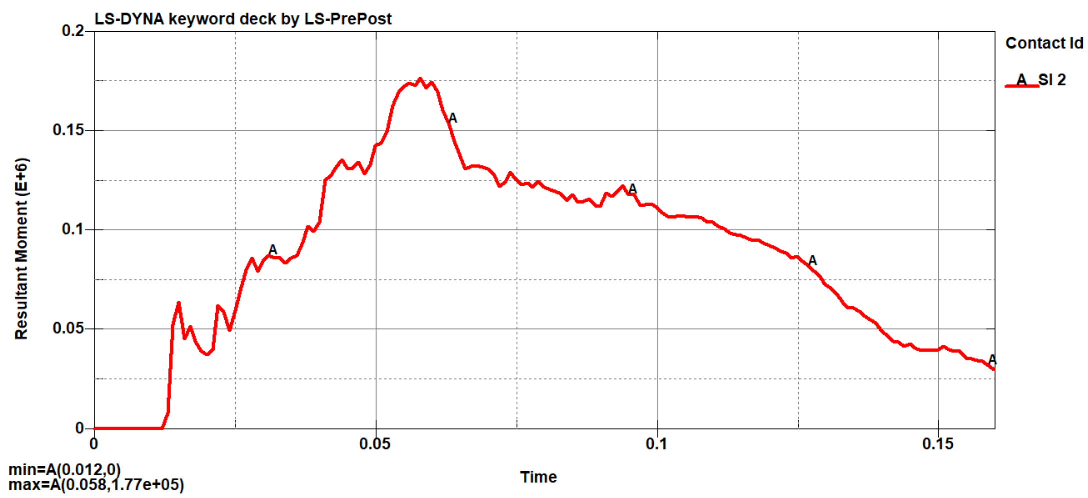

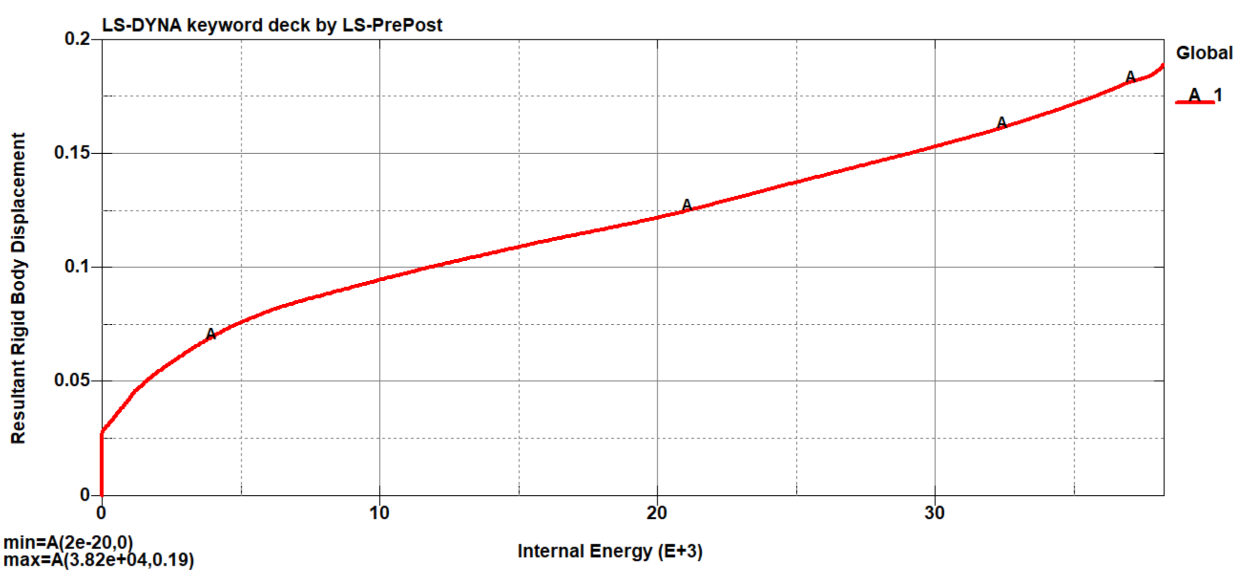

Appendix – C

Data collected from traffic polices (from Pilot study)

Questions for pilot study

Location: Adama, Wonji mazoria.

1. Is Bishoftu pickups are available in this area?

   ☑ yes ☐ no

2. At what age range bishoftu pickup drivers (users) are?

   25 – 40

3. What type of job do expect that mostly the pickup drivers (users) do?

   Contractors

4. Have you seen bishoftu pickup caused accident before?

   ☑ yes ☐ no

5. If your answer is yes, how frequently accidents occur on the pickups?

   at list in two weeks

6. What are the opposing materials that collides with this pickup?

   mostly heavy duty Vehicles -

7. What type of severity appear to the occupant?

   mild – fatality.

8. What do you think about the causes of the accident?

   fast turning

9. What type of collision did frequently occur on the pickup?

   side of the pick ups.

10. During what type of collision, occupant severity increases?

    during side impact mostly sever injuries occure.

11. What do you think about minimization of occupant injury?

    – minimizing ~~[illegible]~~ speed during turning.
    – follow traffic polices [illegible] sign

Questions for pilot study

Location: ADAMA , Mebrat

1. Is Bishoftu pickups are available in this area?

   ☑ yes ☐ no

2. At what age range bishoftu pickup drivers (users) are?

   20 - 35

3. What type of job do expect that mostly the pickup drivers (users) do?

   Tele Communication Drivers (government sector)

4. Have you seen bishoftu pickup caused accident before?

   ☑ yes ☐ no

5. If your answer is yes, how frequently accidents occur on the pickups?

   With in a month

6. What are the opposing materials that collides with this pickup?

   Mostly to Other Vehicle.

7. What type of severity appear to the occupant?

   Mild enjury to sever injury.

8. What do you think about the causes of the accident?

   above speed limmit.

9. What type of collision did frequently occur on the pickup?

   Mostly Head On collision.

10. During what type of collision, occupant severity increases?

    frontal Collision.

11. What do you think about minimization of occupant injury?

    - maintaining the gap b/n front vehicle.
    - give opportonities to pedestrian.

Questions for pilot study

Location: Addis Ababa, kolfe keraneo Subcity

1. Is Bishoftu pickups are available in this area?

   ☑ yes ☐ no

2. At what age range bishoftu pickup drivers (users) are?

   between 27 - 35

3. What type of job do expect that mostly the pickup drivers (users) do?

   Self business owners.

4. Have you seen bishoftu pickup caused accident before?

   ☑ yes ☐ no

5. If your answer is yes, how frequently accidents occur on the pickups?

   with in 10 days

6. What are the opposing materials that collides with this pickup?

   Poles (Guard rails)

7. What type of severity appear to the occupant?

   mild to sever injury.

8. What do you think about the causes of the accident?

   driving speed.

9. What type of collision did frequently occur on the pickup?

   mostly on front side part

10. During what type of collision, occupant severity increases?

    Rollover accident.

11. What do you think about minimization of occupant injury?

    minimizing speed.

Appendix – D

Data collected from Federal Transport Minister and Federal Police Commission

From Information Communication Technology Directorate

Type of Vehicles and Number in the Regions (up to Sene 2009) Registration												
Description	**AA**	**AM**	**AF**	**BN**	**DD**	**SO**	**TG**	**GM**	**HA**	**SN**	**OR**	**Total**
Ambulance	180	0	34	27	9	2	69	0	4	7	165	**497**
Automobile	171523	1485	55	34	1967	558	927	228	1275	51	6376	**184479**
Bajaj	0	2132	2302	0	0	0		0	536	4671	5152	**14793**
Tri Cyle	0	40	0	0	0	0	0	0	0	27	16861	**16928**
Bus(< 12 Seats)	25929	7146	442	260	1376	755	2799	0	0	50	126	**38883**
Bus(> 11 Seats)	14524	9747	372	229	457	537	1521	1375	357	178	2126	**31423**
Combiner	10	17	0	0	1	2	8	0	357	0	6322	**6717**
Dozer	0	0	3	0	0	1	5	0	20	0	252	**281**
Dry Cargo(<=10 Quintals)	34446	1602	273	94	847	953	733	0	176	95	1067	**40286**
Dry Cargo(>10 Quintals)	105150	4099	224	92	3916	2152	4372	0	2	15	527	**120549**
Dual Purpose Vehicle	43253	3443	339	255	1104	515	1665	0	36	21	131	**50762**
Field Vehicle	43681	1590	298	138	426	912	1034	0	445	16	7168	**55708**
Grader	5	2	0	0	1	1		0	3	0	17517	**17529**
Forklift	145	0	3	0	6	0	2	0	317	0	19880	**20353**
Not Specified	18370	8121	25	16	214	263	187		0	50762	13480	**91438**
Gotach	5178	0	0	0	57	0	308	0	1699	0	1305	**8547**
Liquid Cargo	5057	272	34	2	203	114	621	0	7	65	358	**6733**
Liquid Trailer	0	11	0	0	0	0		0	336	0	2189	**2536**
Motor Bicycle	21509	26442	1048	3237	5761	1157	5705	2166	0	4	642	**67671**
Other	9766	442	35	1	89	33	524	1353	72	22	3	**12340**
Three wheel dry load	8	0	0	6	2	166	65	0	1	0	263	**511**
Three wheel public load	506	0	0	1508	299	5145	5046	0	0	0	7	**12511**
Tractor	1027	281	46	124	20	0	184	0	0	1	239	**1922**
Trailer	23810	292	8	1	379	1	2485	0	0	0	13	**26989**
Vehicle with Machinery	367	135	14	1	109	27	62	0	0	0	164	**879**
Total	**524444**	**67299**	**5555**	**6025**	**17243**	**13294**	**28322**	**5122**	**5643**	**55985**	**102333**	**831265**

From Information Communication Technology Directorate

Type of Vehicles and Number in the Regions (up to Sene 30.2010) Registration												
Description	**AA**	**AM**	**AF**	**BN**	**DD**	**SO**	**TG**	**GM**	**HA**	**SN**	**OR**	**Total**
Ambulance	198	0	37	35	9	2	91	0	4	25	238	639
Automobile	184227	1485	59	49	2057	558	1421	228	1275	16162	4796	212317
Bajaj	0	2132	2644	0	289	0	0	0	536	8721	34339	48661
Tri Cyle	0	40	0	0	0	0	0	0	0	27	0	67
Bus(< 12 Seats)	26408	7146	448	324	1468	755	4768	0	0	709	14174	56200
Bus(> 11 Seats)	15242	9747	449	325	514	537	3335	1375	357	1144	22772	55797
Combiner	20	17	0	0	1	2	5	0	357	0	75	477
Dozer	16	0	3	3	0	1	5	0	20	0	0	48
Dry Cargo(<=10 Quintals)	37384	1602	289	101	890	953	1069	0	176	3070	7063	52597
Dry Cargo(>10 Quintals)	109952	4099	229	98	4089	2152	4886	0	2	1195	1810	128512
Dual Purpose Vehicle	44954	3443	348	301	1157	515	2063	0	36	1435	372	54624
Field Vehicle	45081	1590	303	148	447	912	1185	0	445	117	5421	55649
Grader	7	2	0	0	1	1	4	0	3	0	1	19
Forklift	188	0	4	1	6	0	13	0	317	0	2	531
Not Specified	18154	8121	32	25	222	263	602	0	0	1534	6020	34973
Gotach	5598	0	0	0	59	0	572	0	1699	0	0	7928
Liquid Cargo	6341	272	35	2	206	114	645	0	7	65	189	7876
Liquid Trailer	0	11	0	0	0	0	0	0	336	0	117	464
Motor Bicycle	22931	26442	1152	4129	5891	1157	10744	2166	0	49409	29378	153399
Other	9912	442	36	1	88	33	494	1353	72	36	1763	14230
Three wheel dry load	12	0	0	24	2	166	888	0	1	0	4	1097
Three wheel public load	375	0	0	1909	0	5145	9962	0	0	0	0	17391
Tractor	1059	281	46	134	21	0	265	0	0	7	503	2316
Trailer	25336	292	8	1	394	1	2793	0	0	0	302	29127
Vehicle with Machinery	543	135	15	1	113	27	115	0	0	0	0	949
Total	**553938**	**67299**	**6137**	**7611**	**17924**	**13294**	**45925**	**5122**	**5643**	**83656**	**129339**	**935888**

From Information Communication Technology Directorate

Type of Vehicles and Number in the Regions (up to Sene 30.2011) Registration												
Description	**AA**	**AM**	**AF**	**BN**	**DD**	**SO**	**TG**	**GM**	**HA**	**SN**	**OR**	**Total**
Ambulance	253	0	38	44	7	14	164	0	4	28	365	917
Automobile	205773	1701	66	49	2246	609	1660	228	1275	80	6012	219699
Bajaj	0	4722	2889	0	2318	0	0	0	536	9307	48822	68594
Tri Cyle	0	37	0	0	0	0	0	0	0	27	0	64
Bus(< 12 Seats)	27357	8805	465	347	1607	837	5201	0	0	12503	3024	60146
Bus(> 11 Seats)	16698	12840	532	378	681	677	3886	1375	357	10029	38439	85892
Combiner	23	53	0	0	1	2	5	0	357	0	78	519
Dozer	17	0	3	3	0	1	5	0	20	0	0	49
Dry Cargo(<=10 Quintals)	41333	2396	301	102	993	1036	1163	0	176	102	1868	49470
Dry Cargo(>10 Quintals)	115023	4591	240	103	4313	2348	5030	0	2	153	7188	138991
Dual Purpose Vehicle	47278	3907	380	310	1370	684	2188	0	36	1438	97	57688
Field Vehicle	47059	1767	318	153	487	1037	1228	0	445	123	3299	55916
Grader	6	2	0	0	2	1	4	0	3	0	2	20
Forklift	237	0	4	1	8	0	18	0	317	0	2	587
Not Specified	18943	1462	34	48	248	0	396	436	1179	3118	7929	33793
Gotach	5756	0	0	0	67	2	613	0	1699	0	0	8137
Liquid Cargo	6703	318	35	2	226	148	650	0	7	65	437	8591
Liquid Trailer	0	14	0	0	0	0	0	0	336	0	187	537
Motor Bicycle	24700	40229	1181	4865	6689	1366	12358	2166	1178	54084	49903	198719
Other	10279	643	36	1	105	33	485	1353	72	38	2905	15950
Three wheel dry load	15	9625	0	39	7	233	1417	0	1	0	4	11341
Three wheel public load	368	0	0	2259	0	6106	12953	0	0	0	0	21686
Tractor	1199	392	51	136	21	0	304	0	0	10	530	2643
Trailer	26326	349	8	1	417	1	2891	0	0	0	217	30210
Vehicle with Machinery	738	148	17	1	125	25	132	0	0	0	0	1186
Total	**596084**	**94001**	**6598**	**8842**	**21938**	**15160**	**52751**	**5558**	**8000**	**91105**	**171308**	**1071345**

From Information Communication Technology Directorate

Type of Vehicles and Number in the Regions (up to sene 30.2012) Registration

Description	AA	AM	AF	BN	DD	SO	TG	GM	HA	SN	OR	Total
Ambulance	303	0	82	55	6	45	187	0	4	58	438	1178
Automobile	222683	1786	83	53	2360	648	1994	322	1303	98	5258	236588
Bajaj	0	9308	3925	0	3086	0	0	0	4909	11325	55462	88015
Tri Cyle	0	0	0	0	0	0	0	0	0	0	0	0
Bus(< 12 Seats)	28432	9197	493	375	1656	979	5656	2125	80	13300	27315	89608
Bus(> 11 Seats)	17707	13953	678	467	786	871	4473	859	3000	9617	32289	84700
Combiner	27	54	0	0	1	1	5	0	0	0	79	167
Dozer	16	0	3	3	0	1	4	0	0	0	0	27
Dry Cargo(<=10 Quintals)	44898	3597	338	105	1041	1104	1298	0	0	1577	1839	55797
Dry Cargo(>10 Quintals)	119032	3653	259	108	4522	2604	5148	0	0	3612	7325	146263
Dual Purpose Vehicle	49234	4068	461	330	1569	989	2266	0	56	1701	2889	63563
Field Vehicle	48837	1835	371	160	507	1148	1282	330	300	149	3037	57956
Grader	5	2	0	0	2	1	4	0	0	0	2	16
Forklift	281	0	4	1	9	1	18	0	0	0	2	316
Not Specified	19955	1532	71	56	283	511	397	231	0	295	1650	24981
Gotach	5854	0	0	0	66	5	624	0	0	0	0	6549
Liquid Cargo	6866	313	37	2	241	186	658	0	0	67	181	8551
Liquid Trailer	0	14	0	0	0	0	0	0	0	0	171	185
Motor Bicycle	25726	45137	1355	6108	7656	1651	14405	2370	1076	76565	61386	243435
Other	10786	718	35	30	124	33	485	0	0	43	3796	16050
Three wheel dry load	16	42	0	50	9	250	1874	0	0	0	4	2245
Three wheel public load	356	10311	0	2612	0	8523	16647	0	0	0	0	38449
Tractor	1325	401	54	138	21	0	317	0	0	16	526	2798
Trailer	27266	360	8	1	431	1	2913	0	0	1	377	31358
Vehicle with Machinery	835	153	20	1	134	27	145	0	0	0	0	1315
Total	**630440**	**106434**	**8277**	**10655**	**24510**	**19579**	**60800**	**6237**	**10728**	**118424**	**204026**	**1200110**

From Information Communication Technology Directorate

Type of Vehicles and Number in the Regions (up to sene 30.2013) Registration												
Description	**AA**	**AM**	**AF**	**BN**	**DD**	**SO**	**TG**	**GM**	**HA**	**SN**	**OR**	**Total**
Ambulance	322	0	90	56	6	45	187	0	4	65	590	1365
Automobile	255793	1834	86	56	2413	648	1994	0	1303	104	5758	269989
Bajaj	0	11381	4608	0	3302	0	0	1439	4909	12901	65218	103758
Tri Cyle	0	0	0	0	0	0	0	0	0	0	0	0
Bus(< 12 Seats)	31330	9787	494	393	1666	979	5656	2125	80	13874	29068	95452
Bus(> 11 Seats)	19206	14802	713	526	860	871	4473	859	3000	12579	39631	97520
Combiner	106	61	0	0	2	1	5	0	0	0	78	253
Dozer	16	1	3	3	0	1	4	0	0	0	0	28
Dry Cargo(<=10 Quintals)	52338	3825	351	109	1083	1104	1298	0	0	176	2187	62471
Dry Cargo(>10 Quintals)	139376	3767	267	117	4670	2604	5148	0	0	233	8201	164383
Dual Purpose Vehicle	56063	4258	486	343	1704	989	2266	0	56	1712	3028	70905
Field Vehicle	53233	2066	389	164	524	1148	1282	0	300	206	3266	62578
Grader	6	2	0	0	2	1	4	0	0	0	2	17
Forklift	351	0	4	1	10	1	18	0	0	0	2	387
Not Specified	21185	1621	72	57	327	511	397	0	0	2540	2293	29003
Gotach	7235	0	0	0	67	5	624	0	0	0	0	7931
Liquid Cargo	8307	331	39	2	244	186	658	0	0	67	184	10018
Liquid Trailer	0	14	0	0	0	0	0	0	0	0	0	14
Motor Bicycle	28235	48997	1454	7385	8111	1651	14405	2643	1076	80466	63359	257782
Other	12526	778	35	39	137	33	485	0	0	44	4304	18381
Three wheel dry load	17	281	0	56	10	250	1874	0	0	0	9	2497
Three wheel public load	350	13807	0	3111	0	8523	16647	0	0	0	0	42438
Tractor	1505	415	54	146	21	0	317	0	0	33	1015	3506
Trailer	32676	381	8	1	450	1	2913	0	0	1	408	36839
Vehicle with Machinery	1004	158	21	1	134	27	145	0	0	0	0	1490
Total	**721180**	**118567**	**9174**	**12566**	**25743**	**19579**	**60800**	**7066**	**10728**	**125001**	**228601**	**1339005**

ማሳሰቢያ፡- የአዲስ አበባ ተሽከርካሪ ከሁሉም ክፍለከተሞች የተሰበሰበው መረጃ መርጅ በሚደረግበት ጊዜ ካለፈው ቁጥር ጋር ሲነፃፀር ዝቅ በማለቱ ከ6ወር በፊት በተሰጠው መረጃ መሰረት እንዲሆን እንገልፃለን፡፡

ተራ ቁጥር	ተጎጂዎች	ዕድሜ	ሞት		ከባድ የአካል ጉዳት		ቀላል የአካል ጉዳት		ድምር
			ወንድ	ሴት	ወንድ	ሴት	ወንድ	ሴት	
1	አሽከርካሪ	ከ18 ዓመት በታች	9	2	44	2	27	1	85
		ከ18-30 ዓመት	473	9	386	2	207	74	1151
		ከ31-50 ዓመት	195	4	252	11	207	105	774
		ከ51 ዓመት በላይ	56	3	137	5	189	34	424
		ድ ም ር	733	18	819	20	630	214	2434
2	እግረ	ከ7 ዓመት በታች	64	35	58	26	30	15	228
		ከ7-13 ዓመት	116	38	163	49	76	43	485
		ከ14-17 ዓመት	99	40	196	42	169	45	591
		ከ18-30 ዓመት	384	104	855	265	603	179	2390
		ከ31-50 ዓመት	367	121	701	159	387	155	1890
		ከ51 ዓመት በላይ	262	88	244	83	143	48	868
		ድ ም ር	1292	426	2217	624	1408	485	6452
3	ተሳፋሪ	ከ7 ዓመት በታች	40	26	32	23	60	27	208
		ከ7-13 ዓመት	69	29	108	40	148	44	438
		ከ14-17 ዓመት	330	72	171	73	329	203	1178
		ከ18-30 ዓመት	781	303	1182	505	1005	665	4441
		ከ31-50 ዓመት	439	235	853	349	1004	486	3366
		ከ51 ዓመት በላይ	221	104	478	260	779	288	2130
		ድ ም ር	1880	769	2824	1250	3325	1713	11761
		ጠቅላላ ድምር	3,905	1,213	5,860	1,894	5,363	2,412	20,647

2010 ዓ/ም አሽከርካሪውን ለአደጋ ያበቁ ምክንያቶች

ተራ ቁጥር	ምክንያቶች	አደጋው ያስከተለው ጉዳት				ድምር
		ሞት	ከባድ የአካል ጉዳት	ቀላል የአካል ጉዳት	የንብረት ጉዳት	
1.	ሰክሮ መንዳት	6	26	10	123	165
2.	በእጽ ደንዝዞ መንዳት	1	5	2	66	74
3.	ቀኙን ለቆ መንዳት	181	172	101	749	1203
4.	ለተሽከርካሪ ቅድሚያ ባለመስጠት	86	185	101	6,274	6,646
5.	ለእግረኛ ቅድሚያ ባለመስጠት	997	1,955	1,310	251	4,513
6.	ርቀት ጠብቆ አለመከተል	365	200	237	7,954	8,756
7.	ኩርባና ሜዳ ላይ በመቅደም	1	8	1	121	131
8.	ጠምዛዛ (ከርቭ) መንገድ ላይ በመቅደም	4	3	3	227	237
9.	ከተደመ በኋላ ድንገት ታጥፎ በመግባት	24	18	15	1,232	1,289
10.	ከተወሰነ ፍጥነት በላይ በመንዳት	787	869	426	3,506	5,588
11.	አላግባብ በመቅደም	195	175	74	1970	2,414
12.	አላግባብ በመታጠፍ	63	34	36	1,381	1,514
13.	የትራፊክ ፖሊስ ትዕዛዝ በመጣስ	2	4	3	317	326
14.	የትራፊክ መብራት በመጣስ	3	29	7	197	236
15.	የቁም ምልክት በመጣስ	1	4	2	163	170
16.	ቅድሚያ ስጥ የሚል ምልክት በመጣስ	6	43	11	1,031	1091
17.	ከቆመበት አላግባብ በመነሳት	7	16	22	784	829
18.	አላግባብ በማቆም	11	11	12	434	468
19.	በድካም ወይም በመተኛት	4	10	14	19	47
20.	በሐሳብ በመዋጥ	74	6	6	61	147
21.	አላግባብ በማብራት	22	2	3	8	35
22.	አላግባብ በመጫን	52	146	119	183	500
23.	የፍሬን ጉድለት	122	125	109	367	723
24.	የጎማ መውለቅ	165	98	76	777	1116
25.	የጎማ መፈንዳት	11	10	8	17	46
26.	የመሪ ጉድለት	176	96	92	364	728
27.	የመንገድ ጉድለት	13	21	27	41	102
28.	የእግረኛ ጉድለት	55	63	27	93	238
29.	ሌላ	227	256	132	308	923
30.	ያልታወቀ	159	150	87	347	743
	ድ ም ር	3820	4,740	3,073	29,365	40,998

ተራ ቁጥር	ተጎጂዎች	ዕድሜ	ሞት		ከባድ የአካል ጉዳት		ቀላል የአካል ጉዳት		ድምር
			ወንድ	ሴት	ወንድ	ሴት	ወንድ	ሴት	
1	አሽከርካሪ	ከ18 ዓመት በታች	25	-	26	4	10	-	65
		ከ18-30 ዓመት	444	8	374	4	166	8	1,004
		ከ31-50 ዓመት	169	2	250	4	163	2	590
		ከ51 ዓመት በላይ	61	3	121	3	153	1	342
		ድ ም ር	699	13	771	15	492	11	2,001
2	እግረኛ	ከ7 ዓመት በታች	61	23	44	26	19	7	180
		ከ7-13 ዓመት	94	30	105	50	57	26	362
		ከ14-17 ዓመት	102	37	171	58	81	53	502
		ከ18-30 ዓመት	324	114	888	303	586	165	2,380
		ከ31-50 ዓመት	365	104	576	166	318	121	1,650
		ከ51 ዓመት በላይ	179	80	231	116	152	75	833
		ድ ም ር	1,125	388	2,015	719	1,213	447	5,907
3	ተሳፋሪ	ከ7 ዓመት በታች	23	13	140	37	66	26	305
		ከ7-13 ዓመት	101	5	93	20	288	36	543
		ከ14-17 ዓመት	164	63	216	124	278	176	1,021
		ከ18-30 ዓመት	596	281	1,195	426	965	489	3,952
		ከ31-50 ዓመት	457	199	747	303	649	361	2,716
		ከ51 ዓመት በላይ	367	103	390	196	368	84	1,508
		ድ ም ር	1,708	664	2,781	1,106	2,614	1,172	10,045
		ጠቅላላ ድምር	3,532	1,065	5,567	1,840	4,319	1,630	17,953

Table title: 2011ዓ/ም በትራፊክ አደጋ ምክንያት ጉዳት የደረሰባቸው ሰዎች ብዛት

2011ዓ/ም አሽከርካሪውን ለአደጋ ያበቁ ምክንያቶች

ተራ ቁጥር	ምክንያቶች	አደጋው ያስከተለው ጉዳት				ድምር
		ሞት	ከባድ የአካል ጉዳት	ቀላል የአካል ጉዳት	የንብረት ጉዳት	
1	ሰክሮ መንዳት	3	1	-	90	94
2	በእጽ ደንዝዞ መንዳት	-	-	1	46	47
3	ቀኙን ለቆ መንዳት	188	166	74	1,380	1,808
4	ለተሽከርካሪ ቅድሚያ ባለመስጠት	100	239	154	7,259	7,752
5	ለእግረ ቅድሚያ ባለመስጠት	1,112	1,970	1,086	574	4,742
6	ርቀት ጠብቆ አለመከተል	362	171	183	8,074	8,790
7	ኮረብታ ጫፍ ላይ በመቅደም	17	15	2	22	56
8	ጠምዛዛ (ከርቭ) መንገድ ላይ በመቅደም	3	4	3	43	53
9	ከቀደመ በኋላ ድንገት ታጥፎ በመግባት	9	25	9	1,091	1,134
10	ከተ ሰነ ፍጥነት በላይ በመንዳት	702	671	344	2,974	4,691
11	አላግባብ በመቅደም	150	158	25	2,350	2,683
12	አላግባብ በመታጠፍ	35	30	20	2,229	2,314
13	የትራፊክ ፖሊስ ትዕዛዝ በመጣስ	1	-	-	74	75
14	የትራፊክ መብራት በመጣስ	-	1	-	206	207
15	የትራፊክ መብራት በመጣስ	1	1	-	78	80
15	የቁም ምልክት በመጣስ					
16	ቅድሚያ ስጥ የሚል ምልክት በመጣስ	1	42	3	840	886
17	ከቆመበት አላግባብ በመነሳት	13	13	6	342	374
18	አላግባብ በማቆም	8	3	4	281	296
19	በድካም ወይም በመተኛት	3	3	3	17	26
20	በሐሳብ በመዋጥ	1	10	7	1	19
21	አላግባብ በማብራት	2	2	2	1	7
22	አላግባብ በመጫን	44	113	114	259	530
23	የፍሬን ጉድለት	194	85	90	219	588
24	የጎማ መ ለቅ	172	86	76	304	638
25	የጎማ መፈንዳት	8	15	10	9	42
26	የመሪ ጉድለት	173	99	95	300	667
27	የመንገድ ጉድለት	13	7	8	15	43
28	የእግረኛ ጉድለት	53	24	40	32	149
29	ሌላ	148	218	160	722	1,248
30	ያልታወቀ	222	152	68	390	832
	ድ ም ር	3,738	4,324	2,587	30,222	40,871

ተራ ቁጥር	ተጎጂዎች	ዕድሜ	ሞት		ከባድ የአካል ጉዳት		ቀላል የአካል ጉዳት		ድምር
			ወንድ	ሴት	ወንድ	ሴት	ወንድ	ሴት	
2012 ዓ/ም በትራፊክ አደጋ ምክንያት ጉዳት የደረሰባቸው ሰዎች ብዛት									
1	አሽከርካሪ	ከ18 ዓመት በታች	19	9	51	12	22	21	134
		ከ18-30 ዓመት	256	45	377	93	240	34	1,045
		ከ31-50 ዓመት	227	28	310	42	265	31	903
		ከ51 ዓመት በላይ	64	10	34	11	74	7	200
		ድ ም ር	566	92	772	158	601	93	2,282
2	እግረኛ	ከ7 ዓመት በታች	49	30	47	22	120	5	273
		ከ7-13 ዓመት	43	28	107	141	53	16	388
		ከ14-17 ዓመት	79	32	143	177	176	50	657
		ከ18-30 ዓመት	388	100	801	282	216	132	1,919
		ከ31-50 ዓመት	338	83	405	191	102	94	1,213
		ከ51 ዓመት በላይ	172	57	255	120	115	37	756
		ድ ም ር	1,069	330	1,758	933	782	334	5,206
3	ተሳፋሪ	ከ7 ዓመት በታች	53	17	59	30	28	22	209
		ከ7-13 ዓመት	24	49	68	50	84	36	311
		ከ14-17 ዓመት	249	57	141	77	614	379	1,517
		ከ18-30 ዓመት	610	157	1,584	150	655	337	3,493
		ከ31-50 ዓመት	300	160	482	332	602	341	2,217
		ከ51 ዓመት በላይ	300	100	200	135	175	164	1,074
ድ ም ር			1,536	540	2,534	774	2,158	1,279	8,821
ጠቅላላ ድምር			3,171	962	5,064	1,865	3,541	1,706	16,309

2012 ዓ/ም ዓ/ምአሽከርካሪውን ለአደጋ ያበቁ ምክንያቶች

ተራ ቁጥር	ምክንያቶች	አደጋው ያስከተለው ጉዳት				ድምር
		ሞት	ከባድ የአካል ጉዳት	ቀላል የአካል ጉዳት	የንብረት ጉዳት	
1	ስክር መንዳት	24	11	11	46	92
2	በእጽ ደንዝዞ መንዳት	5	8	1	9	23
3	ቀኙን ለቆ መንዳት	140	239	100	1,299	1,778
4	ለተሽከርካሪ ቅድሚያ ባለመስጠት	101	210	112	8,212	8,635
5	ለእግረ ቅድሚያ ባለመስጠት	958	1,847	1,015	1,097	4,917
6	ርቀት ጠብቆ አለመከተል	248	209	186	7,912	8,555
7	ከረብታ ጫፍ ላይ በመቅደም	3	11	3	692	709
8	ጠምዛዛ (ከርቭ) መንገድ ላይ በመቅደም	17	15	4	261	297
9	ከቀደመ በኋላ ድንገት ታጥፎ በመግባት	13	13	5	792	823
10	ከተ ሰነ ፍጥነት በላይ በመንዳት	854	807	338	1,517	3,516
11	አላግባብ በመቅደም	57	93	34	1,635	1,819
12	አላግባብ በመቃጠፍ	37	31	13	2,254	2,335
13	የትራፊክ ፖሊስ ትዕዛዝ በመጣስ	8	2	3	500	513
14	የትራፊክ መብራት በመጣስ	2	2	-	362	366
15	የትራፊክ መብራት በመጣስ	1	9	10	123	143
15	የቁም ምልክት በመጣስ					
16	ቅድሚያ ስጥ የሚል ምልክት በመጣስ	2	3	-	407	412
17	ከቆመበት አላግባብ በመነሳት	13	16	13	358	400
18	አላግባብ በማቆም	12	7	2	246	267
19	በድካም ወይም በመተኛት	10	5	1	31	47
20	በሐሳብ በመዋጥ	8	3	3	28	42
21	አላግባብ በማብራት	3	20	-	1	24
22	አላግባብ በመጫን	53	90	8	100	251
23	የፍሬን ጉድለት	182	128	58	345	713
24	የጎማ መ ለቅ	125	8	60	188	381
25	የጎማ መፈንዳት	9	76	7	3	95
26	የመሪ ጉድለት	222	6	50	160	438
27	የመንገድ ጉድለት	14	7	3	13	37
28	የእግረኛ ጉድለት	30	29	12	-	71
29	ሌላ	163	182	122	753	1,220
30	ያልታወቀ	262	199	73	363	897
ድ ም ር		3,576	4,286	2,247	29,707	39,816

2010ዓ/ም. የተሽከርካሪ - ዓይነት

	አደጋ - ያስከተለ - ጉዳት	1	2	3	4	5	6	7	8	9	10	11	12	13	14	15	16	17	18	19	ድምር
										ቦቴ							ጋሪ	ባቡር	ሌላ	ያልታወቀ	
1	ሞት	19	201	182	129	269	370	434	195	123	266	536	625	103	24	19	35	0	148	142	3820
2	ከባድ የአካል ጉዳት	25	482	501	251	478	376	253	90	30	868	573	433	48	25	18	11	1	149	128	4740
3	ቀላል የአካል ጉዳት	26	215	220	156	282	227	157	63	45	663	357	176	80	17	16	22	0	254	97	3073
4	የንብረት ጉዳት	43	773	5798	1839	4756	2314	1646	825	54	4679	3236	2015	436	105	38	103	1	411	293	29365
	ድምር	113	1671	6701	2375	5785	3287	2490	1173	252	6476	4702	3249	667	171	91	171	2	962	660	40998

2011ዓ/ም የተሽከርካሪው ዓይነት

ተራ ቁጥር	አደጋው ያስከተለው ጉዳት	1	2	3	4	5	6	7	8	9	10	11	12	13	14	15	16	17	18	19	20	ድምር
										ቦቴ							ጋሪ	ባቡር	ባጃጅ	ሌላ	ያልታወቀ	
1	ሞት	28	238	136	104	256	348	402	161	121	358	599	532	193	22	14	32	1	-	81	112	3,738
2	ከባድ የአካል ጉዳት	34	378	500	240	468	320	238	112	25	768	646	246	64	17	10	15	-	-	105	138	4,324
3	ቀላል የአካል ጉዳት	12	143	375	202	220	158	140	40	23	517	305	129	62	16	13	17	-	-	155	60	2,587
4	የንብረት ጉዳት	48	552	6,288	2,055	3,984	1,919	1,727	599	134	6,641	3,532	1,360	647	74	48	68	-	-	192	354	30,22[illegible]
	ድምር	122	1,311	7,299	2,601	4,928	2,745	2,507	912	303	8,284	5,082	2,267	966	129	85	132	1	-	533	664	40,87[illegible]

2012 ዓ/ም የተሽከርካሪው ዓይነት

ተራ ቁጥር	አደጋው ያስከተለው ጉዳት	1	2	3	4	5	6	7	8	9	10	11	12	13	14	15	16	17	18	19	20	ድምር
										ቦቴ							ጋሪ	ባቡር	ባጃጅ	ሌላ	ያልታወቀ	
1	ሞት	63	265	126	123	177	227	397	146	143	438	542	289	158	54	46	81	3	49	84	166	3,577
2	ከባድ የአካል ጉዳት	33	398	553	238	301	376	285	82	23	588	739	165	76	28	20	20	-	54	111	196	4,286
3	ቀላል የአካል ጉዳት	22	180	339	123	161	131	75	38	16	379	273	157	70	23	23	17	-	42	130	48	2,247
4	የንብረት ጉዳት	76	303	7,934	2,065	3,160	1,981	1,456	403	198	5,267	3,895	1,134	1,041	106	73	62	-	45	166	342	29,707
	ድምር	194	1,146	8,952	2,549	3,799	2,715	2,213	669	380	6,672	5,449	1,745	1,345	211	162	180	3	190	491	752	39,817

Appendix – E

Publication

LAME 2022

3rd Biennial International Conference

on

"Future Learning Aspects of Mechanical Engineering"

FLAME 2022

Organized By

Department of Mechanical Engineering

Amity School of Engineering and Technology

Amity University Uttar Pradesh, Noida

August 3rd -5th 2022

Venue: Amity University, Sector-125, Noida, Uttar Pradesh

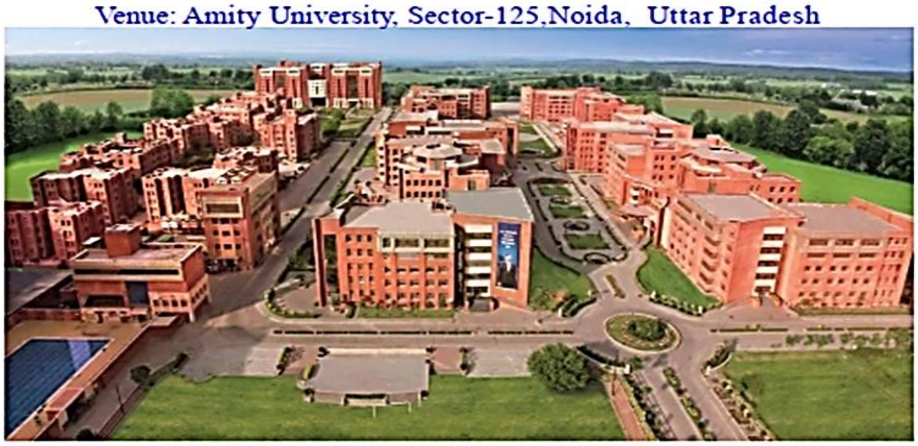

AMITY UNIVERSITY UTTAR PRADESH, NOIDA CAMPUS

In Association with

Springer

ELSEVIER

Department of Sciences & Technology Government of India

UNIVERSITY OF LEICESTER

SIEMENS

Ingenuity for life

- All the accepted papers will be indexed in the **SCOPUS** database.
- Selected and extended versions of papers will be published as Special Issue in Scopus/SCI/ESCI Indexed international journal of repute.

Conference website: *https://www.amity.edu/flame2022/*

FLAME 2022 Notification for Paper Submission Number 327 Inbox x

FLAME-2022 <flame2022@easychair.org>

9:24 AM (54 minutes ago)

to me

Dear Adane Gashu,

Submission Number 327
Title: Analysis of crashworthiness of Bishoftu pickup Vehicle Structure during Side Pole Crash

We would like to inform you that your manuscript has been reviewed and the reviewer's comments are appended at the bottom of this e-mail.

Based on the reviews received, your manuscript has been PROVISIONALLY accepted for presentation and publication in FLAME-2022. Please incorporate the reviewer's stated concerns and highlight the changes with RED in color and update the revised manuscript.

You are requested to send the following documents in the attachment to flame@amity.edu in a Zipped file (Paper Submission Number as a file name).

1. Revised Paper with Highlighted Changes in RED Colour (word file). File Name: Paper Submission Number _Draft.doc
2. Receipt of Registration Fee paid. File Name: (Paper Submission Number _Fee receipt.pdf).
3. Response to Reviewers (word file). File Name: Paper Submission Number _response.doc
4. Folder with all the figures (in TIFF format numbered as Fig.1, Fig.2, etc): Folder Name: Figures_ paper submission number
5. Camera Ready Paper (pdf and word, both files). File Name: Paper Submission Number _camera.doc and Paper Submission Number _camera.pdf
6. Permission request form. Ensure that all permissions have been obtained for any material within the manuscript which is not your original work, or (in most cases) is your own work but which you have previously published. File Name: Paper Submission Number _Permission

Kindly follow the submission guidelines while preparing the Camera-Ready paper mentioned on the conference website. https://www.amity.edu/flame2022/call-for-paper.asp

Please note that the registration fee is only accepted through the payment gateway.
Registration Link: https://amity.edu/nspg/FLAME2022/

The due date to submit the required documents and registration is 13th June 2022.

Analysis of crashworthiness of Bishoftu pickup Vehicle Structure during Side Pole Crash

Adane Gashu [1*], Ramesh Babu Nallamothu [2]

[1*] *Department of Mechanical Engineering, SoMCME, Adama Science and Technology University, Adama, Ethiopia*

[2] *Department of Mechanical Engineering, Amity University, Uttar Pradesh, India.*

rbnallamothu@gmail.com [2], ade.gashu06@gmail.com [1*]

ABSTRACT

Now a day's, vehicle accident is becoming a critical issue all over the world specially in Ethiopia that demands engineers endeavor to find ways to minimize the injury occurrence. So, preservation of occupant compartment space during vehicle collision is the most significant thing. Stiffness, Crash speed, mass and geometric interaction have their own influence on the intrusion of the occupant compartment during vehicle impact. In this study, the dynamic characteristics of Bishoftu pickup vehicle (BPV) during side pole collision were studied using finite element method (FEM). The BPV model used here was modelled using CATIA v5 and simulated using LS-DYNA which is widely used by the automotive industry to analyse vehicle design and predict a car's behavior in a collision. After modeling and analysis is end up, based on the output value there will be modification on the weak parts that is expected to achieve improvement on the energy absorption, strength and weight reduction. Then the modified BPV was analysed under the same condition as the existing one. The result of the simulations shows that with the modification, 78mm more living space, 1000 N reduction of impact force, and 1.1 kJ of additional energy is absorbed. So with the modified model, the safety and crashworthiness of the BPV were greatly improved during side collision without affecting the appearance and weight of the existing models.

Keywords: FEM, LS-DYNA, CATIA V5, Side pole collision, Stiffness

1. Introduction

According to the WHO Global Status Report on Road Safety 2018, 1.35 million people died in 2016 due to road accidents worldwide. Road injuries are the eighth leading cause of death worldwide with 18.2 deaths per 100,000 people, and are the leading cause of death among children and adolescents aged 5-29 years. Road deaths and injuries are evenly distributed throughout the world, with 93% of deaths occurring in low- and middle-income countries comprising 41% of global vehicles. About 29% of these deaths are fourwheel drive, 23% pedestrian, and 3% cycling [1].

Car side collisions in all countries are marked as high. Protecting passengers is very difficult in a collision due to the lack of adequate space for large deformation so, side impact are very dangerous. In collision-related vehicles, in terms of fatal causes, side impact collisions remain in second place immediately after frontal collisions in the USA [2]. A car crash on the side with a pole or tree is always the most dangerous collision. From 2004 to 2009, the death toll rose to 52% in the track side against a strong pole as per statistical data. In that case, the proportion of side effects is more than 60% [3].

Issues related to the lateral structure of car energy absorption and human responses in the event of a side impact are extensively investigated to quantify side impacts [4]. This paper focuses on the dynamic characteristics of the Bishoftu pickup vehicle which is produced in Bishoftu, Ethiopia during side pole collision using finite element method. A Bishoftu pickup vehicle (BPV) is shown in Figure 1. They are generally a double cap with four wheels (two on the front and two on the rear). It contains five occupants, the driver generally sits front left side of the cabin, one on the right and three occupants on the rear part of the cabin and also it has a luggage part on the rear part of the vehicle. It has a maximum velocity of 120 km/hr and gross weight (weght including vehicle and occupant) of the vehicle is around 2495 kg.